NOTE TO USERS

This reproduction is the best copy available.

uOttawa

L'Université canadienne
Canada's university

FACULTÉ DES ÉTUDES SUPÉRIEURES ET POSTDOCTORALES

uOttawa

L'Université canadienne
Canada's university

FACULTY OF GRADUATE AND POSTDOCTORAL STUDIES

Mélanie St-Jean
AUTEUR DE LA THÈSE / AUTHOR OF THESIS

M.Sc. (Geography)
GRADE / DEGREE

Department of Geography
FACULTÉ, ÉCOLE, DÉPARTEMENT / FACULTY, SCHOOL, DEPARTMENT

Nature and Origin of Massive Ground Ice Bodies, Yukon Territory and Alaska
TITRE DE LA THÈSE / TITLE OF THESIS

B. Lauriol
DIRECTEUR (DIRECTRICE) DE LA THÈSE / THESIS SUPERVISOR

I. Clark
CO-DIRECTEUR (CO-DIRECTRICE) DE LA THÈSE / THESIS CO-SUPERVISOR

EXAMINATEURS (EXAMINATRICES) DE LA THÈSE / THESIS EXAMINERS

A. Lewkowicz

C. Zdanowicz

Gary W. Slater
Le Doyen de la Faculté des études supérieures et postdoctorales / Dean of the Faculty of Graduate and Postdoctoral Studies

NATURE AND ORIGIN OF MASSIVE GROUND ICE BODIES, YUKON TERRITORY AND ALASKA

A thesis submitted to
The school of Graduate Studies and Research
In partial fulfillment of the requirements
For the degree Master of Science

Mélanie St-Jean

Department of Geography
University of Ottawa
Ottawa, Canada
May 2009

Your file Votre référence
ISBN: 978-0-494-59454-4
Our file Notre référence
ISBN: 978-0-494-59454-4

Table of Contents

List of figures and tables

Chapter 1-3

Chapter 4: Manuscript 1

Chapter 5: Manuscript 2

ABSTRACT

Gas bubbles in ice hold relevant information on the origin and process of formation, distinguishing between an atmospheric and dissolved origin. Using ice crystallography, stable O-H isotopes and gas composition, this thesis provides new clues to the understanding of ice wedge formation and filling process in the Yukon Territory and Alaska. An improved extraction line and mass spectrometry technique were used to analyze the gas composition of ice bubbles (O_2, N_2 and Ar). Conclusions from this study infer that climatic conditions may influence the source of infilling during ice wedge growth. Wet and dry environments have result in two different signatures in ice wedges. The Vault Creek tunnel ice wedges in Alaska, dated to the late Pleistocene, a cold and dry period, preserve stable O-H isotope and gas compositions similar to those expected for ice formed by snow densification. On the other hand, ice wedges from the Old Crow region, dated to the late Holocene, preserved isotopic and gas compositions more similar to those expected for ice formed by the freezing of liquid water. In some cases, the results from the occluded gases (O_2, N_2 and Ar) showed low oxygen concentration and high $\delta^{18}O$ values, indicating respiration prior to formation. These results are significant to palaeoclimatic interpretation of ice wedges in permafrost areas.

ATTESTATION
INTELLECTUAL CONTRIBUTION

The main focus of the thesis is on the analysis of the gas composition within massive ground ice bodies using the wet extraction technique. In terms of laboratory work, I personally devoted most of my time to improvement of the wet extraction line and on the analysis of the gas composition (O_2, N_2 and Ar) of air trapped in the ice coming from the all the sites presented in the thesis. Crystallographic analyses were also done entirely by myself, with great assistance from Pierre Bertrand, the professional photographer of the University of Ottawa. I participated in some of the other laboratory work, such as the stable O-H isotopes analyses of the ice and the sediment grain size analyses.

Other researchers contributed to the different case studies presented in the last three manuscripts. Denis Lacelle contributed to part of the stable O-H isotopes analyses, and to the interpretation of air in ice bubbles. Bernard Lauriol provided his expertise for the sediment geochemical analyses, the description of the stratigraphy and the Quaternary history related to the sites.

The first three chapters of this thesis were written by me, with minor modifications by different reviewers and supervisors. The first manuscript, concerning the description of the wet extraction line, was entirely written by me. Paul Middlestead provided technical assistance for the modifications made on the wet extraction line.

The second manuscript, concerning the filling process in ice wedges, was mostly written by me, with contributions from other authors in their field of expertise.

ACKNOWLEDGMENTS

I would like to express my appreciation to my supervisors, Bernard Lauriol, Department of Geography, University of Ottawa, and Ian D. Clark, Department of Earth Sciences, University of Ottawa, for their guidance and support during all phases of this research. I would like to thank my committee members, C. Zdanovicz and A. Lewkowicz, for their helpful comments and advice.

I would also like to acknowledge the contribution of D. Lacelle from the Canadian Scace Agency for his helpful comments and advice on many occasions during my research program.

I warmly thank P. Middlestead, W. Abdi and G. St-Jean (G.G. Hatch Isotope Laboratory, University of Ottawa) for their technical assistance in the improvement of the gas extraction wet line and the mass spectrometry method.

Special thanks to Ruth Gotthardt, for logistical support in Whitehorse, to Kenji Yoshikawa, for the logistical support at the Vault Creek tunnel sampling in Fairbanks, and to Hanno Meyer, for the exchange of ideas and data. J. Clark, I. Clark, J.-F. Dion, M. Fortin-McCuaig provided valuable field support, while L. Tellier and J. Bjornson provided valuable laboratory assistance.

This thesis was funded by Natural Sciences and Engineering Research Council of Canada (NSERC) discovery grants to I.D. Clark and B. Lauriol, and by the Northern Scientific Training Program (NSTP) and the Natural Sciences and Engineering Research Council (NSERC) scholarship grants to Mélanie St-Jean.

Finally, I would like to warmly thank my parents, my brother and my friends, for constant encouragement, companionship and understanding.

Chapter 1: Introduction

In terrestrial polar regions, polygonal terrain is often associated with the presence of subsurface massive ground ice, the most common form being ice wedges. The process of ice wedge crack formation has been studied for decades and is well understood (Shumski, 1964; Mackay, 1974; 1990; 1992; 2000; Mackay and Burn, 2002; French, 2007). However, uncertainties remain about the infilling process (by hoar frost, snow, snow meltwater or rainfall), and this has significant implications for paleoclimatic and paleoenvironmental reconstructions (Michel, 1982; Mackay 1983; Meyer *et al.*, 2002; Schirrmeister *et al.*, 2002; Popp *et al.*, 2006). Ice wedge cracks form by thermal contraction of the ground during the cold winter months, usually following a rapid and sustained drop in air temperature (Lachenbruch, 1966; Mackay, 1974; 1992; Allard and Kasper, 1998; Christiansen, 2005; Fortier and Allard, 2005). In the spring, snow meltwater can infiltrate these cracks, and provided that the ground temperature is $< 0°C$, it can freeze inside (Washburn, 1980; Lauriol *et al.* 1995). This repeated process builds up ice wedges, the youngest ice being near the center. However, other studies suggest that ice wedges may also grow by the freezing of water vapour, by hoar-frost accretion, or by snow infilling (Shumski, 1964; Tormirdiaro, 1996; French and Guglielmin, 2000). These processes may govern ice wedge growth in modern or ancient cold and dry environments such as Siberia, Antarctica or Beringia.

Several methods have been used to investigate the origin of massive ground ice (French and Pollard, 1986; Mackay 1989; Murton and French, 1994; French, 1998; Kotler and Burn, 2000; Cardyn *et al.*, 2007; Lacelle *et al.*, 2007), but some of these methods have never been applied to ice wedges. The process of ice wedge filling can potentially be inferred from the characteristics of the ice, including its crystallography, bubble content, the stable isotope ratios of O and H, and

the composition of occluded air. For example, ice wedges formed by the freezing of liquid water tends to contain elongated bubbles distributed vertically, whereas in ice wedges filled by snow (or hoar), the bubbles are more spherical (French, 2007). The stable isotope ratios of O and H in ice ($\delta^{18}O_{ice}$ and δD_{ice}) can also help to determine its origin (Michel and Fritz, 1982; Jouzel and Souchez, 1982; Lorrain and Demeur, 1985; Mackay and Dallimore, 1992; Lacelle *et al.*, 2004). In particular, the slope of the linear regression of δD_{ice} against $\delta^{18}O_{ice}$ may differ between ice formed by snow (or hoar) densification and ice formed by freezing water. Recently, a method was developed using the molar gas ratios in occluded air to differentiate between ground ice formed by snow (or hoar) densification and by freezing water (Cardyn *et al.*, 2007; Lacelle *et al.*, 2008). In the former case, the occluded gases in the ice (O_2, N_2, Ar) should preserve their atmospheric mixing ratios, whereas in ice formed by freezing water the ratios will depart from the atmosphere's, owing to the respective solubility of different gases in water. Several processes, however, can later modify the gas ratios of air entrapped in the ice. Some of these processes can be identified from the stable isotope ratios of oxygen and nitrogen gases (O_2 and N_2; Cardyn *et al.*, 2007).

The main goal of this study is to investigate the filling process in ice wedges of various ages (modern to Pleistocene) preserved in Yukon and Alaska. This was accomplished using a variety of parameters, including ice crystallography, the determination of $\delta^{18}O_{ice}$ and δD_{ice}, the molar ratios of occluded gases (O_2/Ar and N_2/Ar), and the stable isotope composition of O_2 ($\delta^{18}O_{O2}$) and N_2 ($\delta^{15}N_{N2}$) gases.

The thesis is organized in six chapters. In chapter 2, a literature review covers current understanding of permafrost and ground ice, as well as identification methods and approaches. The third chapter contains detailed methodology followed during the field investigations and the laboratory work. The fourth chapter describes in detail the gas extraction and analysis protocol. In the fifth chapter, a manuscript article on the ice wedges filling process is presented. Finally, chapter 6 concludes the thesis, and is followed by appendices containing raw data and results.

Chapter 2: Literature Review

Permafrost and Ground Ice

According to the Associate Committee on Geotechnical Researc (ACGR) (1988), massive ground ice consists of large tabular ice bodies whose volumetric ice content exceeds 95 %, whereas icy sediments contain excess ice and have a volumetric ice content in the 50 to 95 % range.

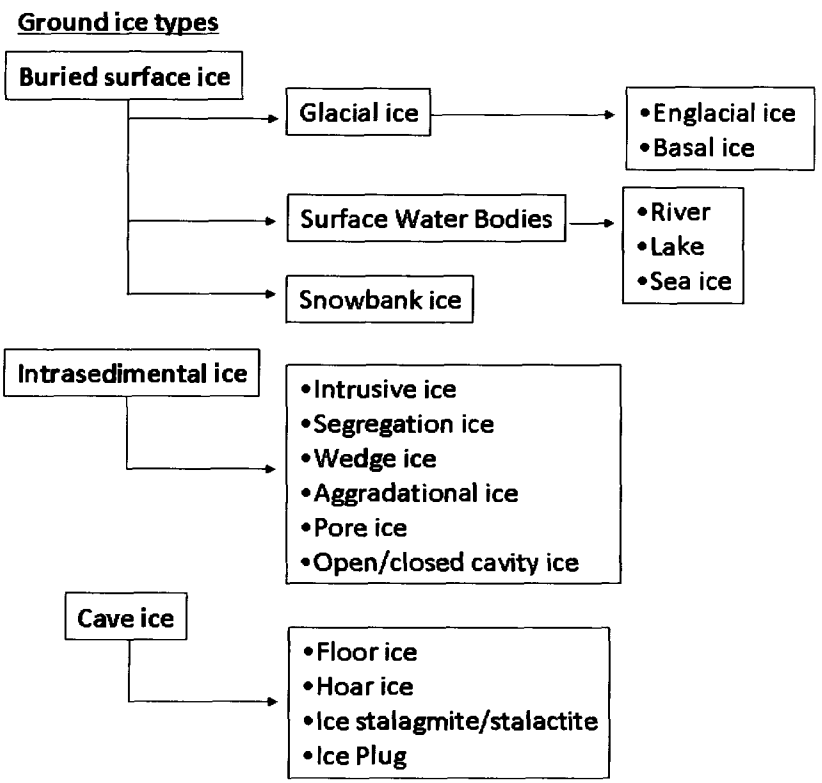

Figure 1: A general classification of massive ground ice types
Source: Adapted from Lacelle et al., 2008 (modified from Mackay, 1972; 1989; French 2007)

Several attempts have been made to classify massive ground ice by type. Most massive ice bodies can be divided to three mains types: buried ice, intrasedimental ice and cave ice (see Figure 1). In Figure 2, a genetic classification of intrasedimental ice based on the water source

and process of formation is presented. For this project, we focus on two main ice types, buried ice and intrasedimental ice, which will be described in more detail in the next paragraphs.

Buried Ice

Buried ice can be river, lake, sea, snowbank or glacier ice. Most of the buried massive tabular ground ice bodies in the western Canadian Arctic and in northwestern Siberia occur near the limits of known glaciations (French, 2007). Their preservation in permafrost probably results from burial under glacigenic material, which prevented complete thaw when the thickness of the debris covering the ice exceeded the active layer thickness, There is an ongoing debate over the existence of such buried glacier bodies. Many Siberian geocryologists, mostly using geochemical methods, deny the possibility of a glacial origin (e.g. Lazudov, 1972; Ansimova and Kritsuk, 1983; Dubikov, 1983; Dubikov and Ivanova, 1988; Kritsuk and Ansimova, 1985; Kritsuk and Chervova, 1985; Leibman 1996; Michel, 1998; Leibman et al., 2000, 2001; in Ingolson and Lokrantz, 2003). On the other hand, many Quaternary geologists, who use mostly stratigraphic and sedimentological arguments, support the existence of buried glacier ice (e.g. Lorrain and Demeur, 1985; Astakhov et al, 1996; French and Harry, 1990; St-Onge and McMartin, 1995; Dyke and Savelle, 2000; Lacelle et al., 2007).

Intrasedimental Ice

The most easily recognizable intrasedimental ice are ice wedges, which will be described in detail in the next section. Other main types of intrasedimental ice are segregated ice, intrusive ice, segregated-intrusive ice, injection ice and aggradational ice.

Massive segregated ice is formed by *in situ* freezing of water within sediments (Mackay, 1989). Segregated ice is a general term for soil with high ice content (French, 2007). Segregated ice is

formed by cryosuction of water towards the freezing front to form stratified ice lenses (French, 2007). French (2007) stated that segregated ice may be distinguished from intrusive ice by the stratified character and the presence of soil particles in the ice. However, in practice, the two types are often difficult to distinguish.

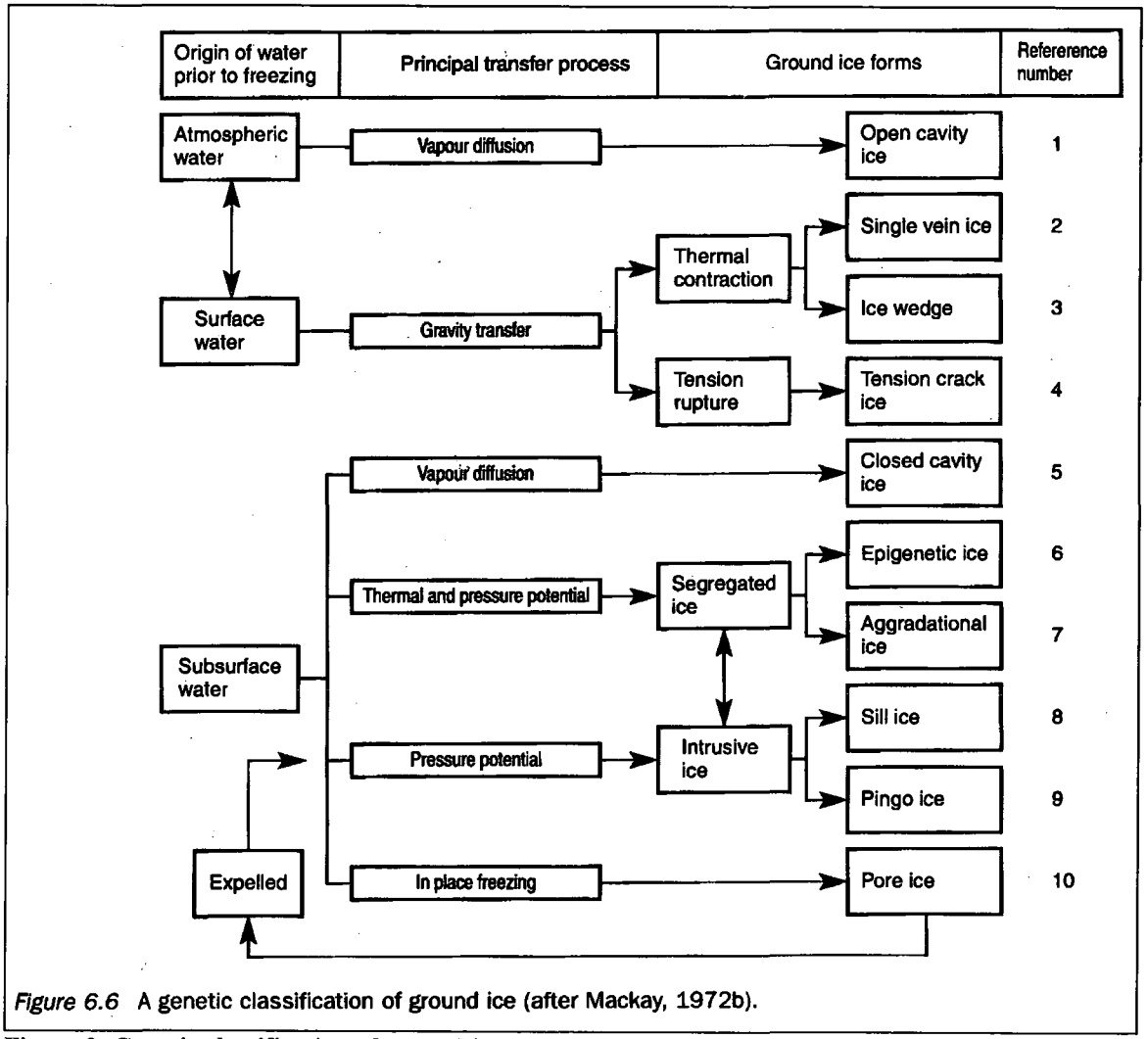

Figure 6.6 A genetic classification of ground ice (after Mackay, 1972b).

Figure 2: Genetic classification of ground ice
Source: French (2007)

Intrusive ice is formed when bulk water is intruded under pressure in the ground and then freezes (Mackay, 1989). When the water pressure gradient fluctuates between low and high, a mix of segregated and intrusive ice is formed (Mackay, 1989). Deformation of the overlying sediments is a typical characteristic of intrusive ice (French and Pollard, 1986). Sill and pingo ice are the

two most common types of intrusive ice. Pingo ice form in open-system or close-system conditions, and are common geomorphic features in permafrost areas (Hughes, 1969). They are ice-cored hills created by the intrusion and freezing of water under pressure (Pissart, 1987). Seasonal frost mounds are also another surface features which contain intrusive ice. These mounds are characterized by a core of pure ice, composed of large elongated crystals which grow parallel to the freezing direction (Pollard and French, 1984; 1985). These frost mounds should not be confused with palsas, which are large masses of segregated ice formed within peat or mineral soil in discontinuous permafrost (Pollard and French, 1984). Gases trapped in intrusive ice formed in frozen sedimentary rocks and kimberlite as a result of the injection of ground water enriched with gases yields molar gas ratios fairly close to atmospheric values, albeit with a slightly lower O_2/Ar ratio (Alexeev and Alexeeva, 2002).

Aggradational ice forms when the upper part of permafrost rises over a period of years by the addition of sediment to the surface or by a decrease in the thickness of the active layer (Mackay, 1972). The latter that new segregated ice is formed at the base of the active layer, at the top of permafrost.

Ice Wedge Ice

Ice wedges form in permafrost areas only where the mean annual temperature is below -6°C (Kasper and Allard, 2001). The wedges commonly join together to form polygons that are commonly observed in these areas. Mackay (1990) classified them into three categories: epigenetic wedges that are younger than the enclosing materials, syngenetic wedges that develop at the same time as the enclosing material, and anti-syngenetic wedges that grow downwards on hillslopes during removal of surface material.

Wedge ice is easily identified in natural exposures by its V-shape, truncated top, and the vertically irregular stratified structure of the ice. However, in some cases, wedge ice is irregularly shaped (i.e. , in long section or when post-depositional deformation occurs in relict wedge ice). They range in width from a few cm beneath small polygonal cracks, to as much as a few m beneath large troughs (Corte, 1963). However, with syngenetic growth ice wedges can grow up to 6-8 m wide and 20-30 m deep (Shumski, 1984). The most important characteristic of ice wedges is the vertical irregularly stratified structure of the ice, which is due to the alternation of ice layers with differing amounts of mineral and air inclusions (Corte, 1963). These inclusions give, in most cases, a yellowish color to the ice veins. Wedge ice contains the greatest concentration of air bubbles compare to other ground ice types, and is readily identifiable by this characteristic (Corte, 1963). The air bubbles contain a large amount of exogeneous air (up to 60% in volume), which comes from the pores of depth hoar (Shumski, 1964). The air in ice wedges is typically a nearly oxygen-free mixture of inert and biogenic gases produced by the oxidation of plant remains (Shumski, 1964).

The origin of ice wedge origin has been a subject of controversy mostly because of their complex shape and composition. The history of research on ice wedges is a long one. The first scientist to suggest that ice wedges might be caused by the accumulation of ice in frost cracks was Figurin in 1823. Several 19th century Russians researchers were in favor of a glacial or nival origin (Tol'1897; Tolmachev, 1903, Tolmachev, 1903; Grigor'ev, 1932 and 1946; cited in Shumski, 1964). The most accepted process today to explain ice wedge growth in the science community is that water is the material which fills the frost cracks. Some researchers have argued that the primary source of water for ice wedge growth is snow meltwater (Washburn, 1980; Lauriol et al.,

1995). Other researchers suggest that in some cases, ice wedge growth occurs by hoar-frost accretion rather than by water trickling into the wedge during spring thaw and subsequently refreezing. In fact, Shumski (1964) observed that in some cases, ice veins formed without liquid water nourishment, but by depth hoar filling. This process was also observed for Antarctic ice wedges by French and Guglielmin (2000). Ice wedges observed in Antarctica had distinctive characteristics such as a milky white colour, abundant small gas inclusions, low sediment content, and little or no foliation (French and Guglielmin, 2000). Environments where hoar-frost accretion filling has been observed are usually very cold and dry with a very thin snow cover.

Mackay (1974) observed 1-3 mm ice veinlets within a larger wedge at Garry Island, NWT, Canada. However, ice veinlets as thick as 2 cm have been observed in Siberian syngenetic ice wedges (Shumski, 1964). In Barrow, Alaska, the average increment of ice veinlets was estimated at 2 mm (Black, 1974), in Antarctica, measurements suggested accretion rates of 0.5-3.8 mm/yr (Berg and Black, 1966), and on Ellesmere Island, measurements showed accreation rates between 4-25 mm/yr (Lewkowicz, 1994). In contrast, at Illisarvik, the growth rates for ice veinlets during the first 10 years of active cracking were 1-3 cm/a (Mackay and Burn, 2002). The vastly different growth rates suggest considerable spatial variability, possibly due to different environmental conditions. Under the present conditions, the maximum depth of cracking is 5-7 m, but during the Pleistocene, it was 9-15 m (Shumski, 1964). Frost cracks tend to open between mid-January and mid-March, but preferentially in late winter when air and ground temperatures drop rapidly (Mackay, 1974).

Mackay (1992) found that frost crack frequencies are highly variable, and the correlation between crack frequency and air temperature is poor. However, Christiansen's (2005) suggested

that a long period of cooling, with ground temperatures below -15°C at the top of the permafrost table are required for cracking to occur. Lachenbruch's (1966) also showed that for thermal-contraction cracking to occur, air temperatures need to fall to between -20°C and -30°C, and temperatures at the top of the permafrost to at least -15°C. This was confirmed by Allard and Kasper (1998). Fortier and Allard (2005) showed that cracks opened after a drop in air temperature of about 7.9°C over a mean period of 18 hours, with a mean thermal gradient in the active layer at the time of cracking of -10.9°C /m. These studies were done in different locations around the world, indicating that varying environmental conditions may influence the timing of frost cracking as well as the ice wedge filling process.

The frequency of cracking is related inversely to snow depth (Mackay and Black, 1973). However, Christiansen (2005) observed thermal-contraction cracking even below a 30 cm deep, snow-filled ice wedge trough. She explained that cooling of the ground in that case can be done mainly through the more or less snow-free ramparts, which experience both the lowest temperatures and most rapid drops in temperature, while the ice-wedge troughs are partly insulated with snow. If we take those facts into consideration, the use of mean ice-wedge growth rates for estimating the age of ice wedges, or theirs casts, for paleoenvironmental reconstruction may be misleading or inaccurate (Mackay, 1992).

As described in the preceding paragraphs, several types of ground ice and permafrost features exist, which have different characteristics depending mainly on the growth processes. However, it is often difficult to differentiate between ground ice types because of shared characteristics. For example, both massive tabular segregated ice and buried glacier ice display ice stratification.

Different methods and approaches have been attempted to differentiate these ice types. More details about these methods and approaches, which can also be used to understand the filling process in ice wedges, are described in the next section.

Identification Methods and Approaches

In Canada, the discussion concerning the origin of massive ground ice bodies has mostly focused on whether such ice are remnants of the Laurentide ice sheet, or whether they formed by segregation/injection processes (Lacelle, 2002). Determining the origin of tabular massive ground ice bodies is of interest because unlike other ground ice types, their origin has so far remained obscure. A number of approaches have been used to investigate the origin of massive ground ice. Cryostratigraphy was the first approach used in massive ground ice identification (Mackay 1971; French and Harry, 1988; Murton and French, 1994; French, 1998; Kotler and Burn, 2000). Later, ice crystallography led to a better understanding of the process that lead to the formation of massive ground ice (Pollard and French, 1984; French and Pollard, 1986; Pollard and Dallimore, 1988). In recent times, the stable O-H isotope composition of massive ground ice bodies has been studied and proved to be very helpful in understanding massive ground ice genesis (Michel and Fritz, 1982; Jouzel and Souchez, 1982; Lorrain and Demeur, 1985; Mackay and Dallimore, 1992; Lacelle et al., 2007).

Recently, attempts have been made to study the origin of ground ice using the gas content in air bubbles. Methane (CH_4) concentration and ^{14}C concentration have been measured in ground ice, following methods developed for glaciers. The concentration of methane in air bubbles in ice wedges and frozen soils of Siberia has also been measured by Brouchkov and Fukuda (2002).

They found that methane content in air bubbles of ice wedges was lower than in frozen soil, but larger than the present day atmospheric concentrations. Another finding was that older permafrost had higher concentrations of methane than younger permafrost.

Radiocarbon (^{14}C) was measured in massive ground ice bodies from the Canadian north (Moorman et al., 1996) and more recently on the Antarctica EPICA Dronning Maud Land glacial ice core (Van de Wal et al., 2007). Moorman et al. (1996) found that ^{14}C ages obtained from the massive ground ice bodies gave younger ages for the ice previously speculated. However, the issue with measuring ^{14}C in ice bubbles is its source. It can either come from atmospheric gases trapped during the accumulation in the glacier or through *in situ* ^{14}C production by cosmic rays. Another issue is that trapped atmospheric $^{14}CO_2$ offers the possibility of dating, but fast neutrons and muons can modify the ^{14}C signature of CO_2 in snow and ice. Val de Wal et al. (2007) produced a model to correct for *in situ* production of $^{14}CO_2$. However, the validity of this model remains to be tested by measurements on other ice cores and ground ice, since it has been done only on 17 samples of glacier ice.

A new approach developed by Sowers et al. (1997), and modified by Cardyn et al. (2007), focuses on the determination of gas ratios in ice bubbles. Since these gas ratios vary depending on the genesis of the ice, it may be a powerful technique to differentiate between buried glacier ice and intrasedimental ice. Few studies combine stratigraphical-sedimentological-structural and geochemical-petrographical techniques. Our own study follows the advice of Mackay (1989) and French and Harry (1990) that it is crucial to use a combination of methods to attempt a genetic interpretation of a massive ice body. The focus in this study will be on analyzing stable isotope ratios of gases in the ice bubbles, but other parameters such as stable O-H isotope ratios of the ice

and ice crystallography will be explored as well. Principles and theories behind these methods and techniques are described below.

Petrographic Analysis

Petrographic analysis, also called ice crystallography, is useful for descriptive purposes as well as a mean to know more about ice growth processes and conditions (French, 2007). Petrographic analysis is carried out using a four-axis universal stage instrument, which is used for accurate and rapid determination of the optical properties and orientation of crystal plates or fragments. In order to examine the crystal size and c-axis orientation, thin sections are prepared from ice samples (Langway, 1958). The desired thickness, between 0.3 and 0.5 mm, is obtained by careful melting, and surface of the ice is made as flat as possible (Östrem, 1963). Thin sections are photographed between crossed polarizing filters to measure crystal size. The direction and speed of the freezing process can be inferred from the different characteristics of the crystals such as size, shape, boundary characteristics and c-axis orientation (French, 2007). Ice crystals normally grow at right angles to the direction of freezing and there is an inverse relationship between crystal size and the rate of freezing (French, 2007).

In terms of c-axis orientation, it was described in the literature that there is a gradual transition in crystal orientation from the upper end to the deeper part of an ice wedge. Main axes are vertically oriented at the upper end; they are randomly oriented in the transitional zone (or middle zone), and horizontally oriented in the deeper zone (Corte, 1963; Shumski, 1964). This grain reorientation happens because of the horizontal stress involved in wedge growth that causes a recrystallization (Corte, 1963). According to Shumski (1964), horizontal orientation

occurs when the temperature of ice during crystallization is low, and random orientation occurs when the temperature is close to zero (Shumski, 1964). However, the picture may be complicated considerably by the influence of depth-hoar crystals, which act as centres of crystallization for the water which fills the cracks in the event of incomplete remelting and usually this makes the crystal orientation more random (Shumski, 1964). Future work on ice wedges should take this fact into consideration, and care should be taken to relate the position of the sample and the ice wedge type (epigenetic, syngenetic or anti-syngenetic).

Crystallography in ice wedges has been explored by Corte (1963) and Shumski (1964). In their studies, they found that crystals are limited horizontally by the width of the cracks. Often the crystals are somewhat larger vertically than horizontally in vein profile, giving the impression of a column. Furthermore, crystal size varies with the timing of formation in ice wedges. The smaller grains are those formed recently in a thermal contraction crack, while those at each side are older grains formed by recrystallization from small ones (Corte, 1963). Younger crystals range from 1 to 3 mm^2 in area compare to older crystals ranging from 0.5 to 3 cm^2 (Corte, 1963).

Östrem (1963) found that crystals are small in buried glacier ice. Pollard (1990) found similar patterns, finding usually small anhedral equigranular crystals with a high concentration of vertically oriented bubbles trains and tubular bubbles. It was also shown that generally, glacier ice exhibits three to four preferred orientations of crystals, a pattern that is most pronounced near the glacier tongue (Östrem, 1963). A uniform freezing condition is implied if the crystal and orientation are typical of the entire ice body (French and Pollard, 1986). In intrusive ice, Pollard and French (1985) found that crystals are oriented towards the freezing direction. According to

Pollard (1990), segregated ice tends to be composed of large equigranular anhydral crystals whose c-axis is oriented to the plane of the ice layers. However, unambiguous identification of ice types cannot be made solely by crystallography (French, 2007).

Stable O-H Isotopes

Isotopes are atoms of the same element that have the same numbers of protons and electrons but different numbers of neutrons. The difference in the number of neutrons between the various isotopes of an element means that the various isotopes have similar charges but different masses. For example, normal water, $^{1}H_2{}^{16}O$, has a molar mass of 18 compared to heavy water, $^{2}H_2{}^{16}O$, which has a molar mass of 20.

The most common isotopes within water are ^{16}O (99.63%) and ^{1}H (99.98%). Four other isotopes (^{18}O, ^{17}O, ^{3}H, and D or ^{2}H) exist but are much less abundant. Stable environmental isotopes are measured as the ratio of the two most abundant isotopes of a given element (Clark and Fritz, 1997). The abundance of oxygen and hydrogen isotopes are expressed as the parts per thousand of difference between the sample and the reference, VSMOW (Vienna Standard Mean Ocean Water), whereby

$$\delta = ((R_{sample} - R_{standard}) \times 1000) / R_{standard}$$

Where R is the isotope ratio: $^{18}O/^{16}O$ or D/H

These changes in abundance are referred to as delta-values expressed as parts per thousand differences between the sample and the reference. It means that a sample value of -10‰ has 10‰ less ^{18}O than the reference, or is 10‰ depleted. Surface air temperature is the most important control on the isotopic composition of water (Craig, 1961).

The Global Meteoric Water Line (Figure 3) characterized the relation between $\delta^{18}O$ and δD in most global precipitation and is expressed as:

$$\delta D = 8\ \delta^{18}O + 10‰ \text{ (Craig, 1961)}$$

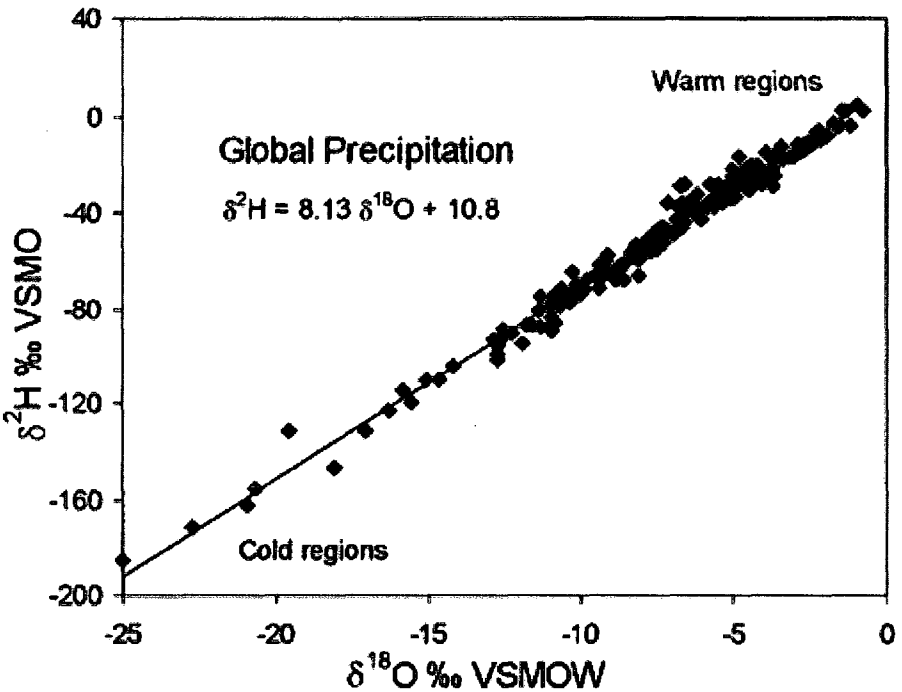

Figure 3: Global Meteoric Water Line
Source: Clark and Fritz (1997)

However, the slope and intercept of any "Local Meteoric Water Line" (LMWL), which is the line derived from precipitation collected from a single site or set of "local" sites, can be significantly different from the GMWL. For example, the Canadian meteoric line is,

$$\delta D = 7.75\ \delta^{18}O + 9.83 \text{ (Clark and Fritz, 1997)}$$

And, the LMWL for Inuvik published by Vardy et al. (1998) is

$$\delta D = 7\ \delta^{18}O - 12.02$$

Variations in isotopes are linearly related to the temperature variations (Dansgaard, 1964):

$$\delta^{18}O = 0.695T - 13.6‰$$

Where, T is the mean annual air temperature at the ground surface and $\delta^{18}O$ represents the mean annual value at that site. This relationship exists because that precipitation and rainout are driven by decreasing temperature. Evaporation and condensation will also have a fractionation effect on the isotope values (Clark and Fritz, 1997) (see Figure 4). If water vapour evaporates from the ocean and travels towards higher latitudes, it is cooled and the vapour becomes progressively depleted in heavy isotopes according to a Raleigh-type distillation process. This means that lower latitude precipitation will be enriched in heavier isotopes, and higher latitude precipitation will be significantly depleted.

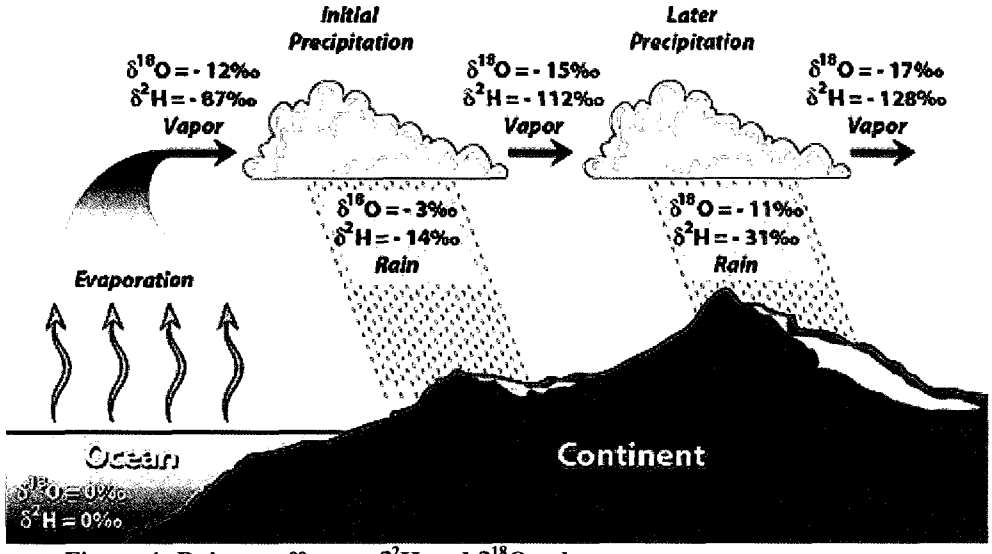

Figure 4: Rainout effect on δ^2H and $\delta^{18}O$ values
Source: Based on Hoefs (1997) and Coplen et al. (2000)

The isotopic composition of water provides a tool to distinguish between waters of different origins. Murton (2005) and French (2007) defines it as a major component of cryostratigraphy, since it is helpful in estimating paleaoclimatic conditions during the formation of ground ice, even though it may be derived from precipitation whose $\delta^{18}O$ may vary considerably seasonally and annually. Stable isotope analyses of ground ice is a useful tool for the interpretation of

permafrost stability and history where the identification of isotopic discontinuities (thaw unconformities), caused by changing climate, may be revealed within the frozen sediments (Murton and French, 1994). It is generally agreed that co-isotope slopes greater than about 7.2 are associated with atmospheric sources, such as glacier ice, whereas co-isotope slopes below 6 are to be expected for groundwater derived intrasedimental ice formed during the later stages of closed-system freezing (Jouzel and Souchez, 1982; Mackay and Dallimore, 1992; Lacelle et al., 2004). However, it was shown that the slope may not always be related to the water origin (French and Harry, 1990). In fact, injection ice (pingo ice) has exhibited a slope of 7.2. Overall, the use of isotopic analysis of water is certainly a valuable method giving relevant information on the source of water and the freeze-thaw processes.

Molar Gas Ratios

The concentration and ratios of O_2, N_2 and Ar gases entrapped in the ice, offer an innovative tool that assist in the differentiation between ground ice of glacial (firnified glacier ice), non-glacial intrasedimental and surface origin. The principle behind this technique is that the gas ratios (O_2/Ar and N_2/Ar) entrapped in glacier ice tend to preserve an atmospheric signature modified by firn diffusion and gravitational settling, whereas the gas ratios of segregated-intrusive ice are significantly different from those found in the atmosphere and glacier ice due to the different solubilities of the gases in water (Lacelle et al., 2007; Cardyn et al., 2007).

Gas entrapped in glacier ice

The gas composition of the atmosphere is dominated by N_2 (78.08%), followed by O_2 (20.94%) and Ar (0.93 %). This leads to O_2/Ar and N_2/Ar ratios of 22.42 and 83.60 respectively, with little change over time (Cardyn et al., 2007). Firn densification and occlusion of porosity are the processes that trapped the atmospheric gases in glacier ice (Craig et al, 1988; Sowers et al., 1992; Schwander, 1996). Several years are required for a complete occlusion of air in the ice; this means that gases trapped in the ice can be younger than the ice itself (Barnola et al., 1991; Arnaud et al., 2000; Clark et al., 2007). The abundance of gases (O_2, N_2, Ar and $\delta^{18}O_{O2}$ and $\delta^{15}N_{N2}$) can be slightly modified from the initial atmospheric values during the occlusion of the gases in the firn layer. This is due to several influencing factors such as gravitational fractionation, presence of micro-fissures in the ice and thermo-fractionation (Cardyn et al., 2007). Gravitational fractionation of heavy gases, such as Ar, during occlusion of gases in the firn can lead to a decrease in the O_2/Ar and N_2/Ar ratios. Several factors determine the magnitude of this fractionation: structure of the firn, which is influenced by temperature, wind speed and snow accumulation at the depositional site (Hattori, 1983; Mariotti, 1983; Sowers and Bender, 1989; Caillon et al., 2003; Landais et al., 2006; Petrenki et al., 2006). Micro-fractures can also affect the molar gas ratios because smaller atoms like Ar will diffuse faster than the molecules of O_2 and N_2, with larger cross-sectional diameter (Craig et al., 1988). Another process that influences the molar gas ratios is thermo-fractionation. The $\delta^{18}O_{O2}$ is influenced by changes in global temperatures and ice volume (Bender et al., 1994). In other words, it can provide an indication of rapid temperatures changes such as the change cause by the disappearance of the Laurentide and Eurasian ice sheets (Bender et al., 1994). In fact, $\delta^{18}O_{O2}$ has progressively decreased from about -0.2 to 1.3 ‰ since the Late Pleistocene (Bender et al., 1994).

Gases entrapped in intrasedimental ice

Due to the different solubilities of the gases in water, the gas ratios in intrasedimental ice formations (pore, wedge, segregated and intrusive ice) are expected to be different from atmospheric ratios of gases in occluded firn ice. Elements and explanations in the next paragraph are from Cardyn et al. (2007). Gases dissolve in water under equilibrium conditions according to their Henry's Law solubility constant, K_H:

$$K_{Hgas} = m_{gas} / P_{gas}$$

Where m_{gas} represents the dissolved concentration in moles per kg of water, and P_{gas} represents the partial pressure of the gas (atm). The partial pressure of a gas is its fractional contribution to the total gas pressure P_{total} and is calculated as its molar fraction multiplied by the total gas pressure:

$$P_{gas} = \frac{\text{mols}_{gas}}{\text{mols}_{total}} \times P_{total}\,(\text{atm})$$

To be consistent with the analytical method used, the concentration of dissolved gas in water is often expressed volumetrically. The units are the cc $_{gas\text{-}STP}$/ccwater, where cc $_{gas\text{-}STP}$ is the cubic centimeter volume occupied by the moles of the gas at standard temperature and pressure (STP = 273.16 K and 1 atmosphere). The proportionality constant for gas solubility expressed as a volume at STP rather than as mole fraction, is the Bunsen coefficient B_o, which is equal to K_H RT_k.

Calculations of the equilibrium gas concentration in water at STP have been made using the Bunsen coefficient (Benson and Krause, 1980; 1984) and Henry's constant for O_2, N_2 and Ar

(CRC, 1988; Andrews, 1992). The higher solubility of argon in water results in O_2/Ar and N_2/Ar ratios of 20.83 and 35.50 respectively, which are lower than for atmospheric ratios. The isotopic composition of N_2 and O_2 dissolved in fresh water also differs from their values in air. Kendall and Aravena (2000) showed that $\delta^{15}N$ of dissolved N_2 is 1 ‰, and that $\delta^{18}O$ of dissolved O_2 is 0.7‰. Consequently, relative abundance of O_2, N_2 and Ar are expected to be different in intrasedimental ice and firnified glacier ice, but deltas ($\delta^{18}O_{O2}$ and $\delta^{15}N_{N2}$) should be similar since fractionation is not greatly affected by dissolution.

The analysis of gases in ice is the main technique used in this study. The gas extraction procedure followed in this study have been improved from the original procedures developed by Sowers et al. (1997) and modified by Cardyn et al. (2007), in order to minimize possible contamination. Chapter 4 is dedicated to the description of the gas extraction improved procedure. The next chapter (Chapter 3) presents the detailed methodology of this study in relation to field investigations and laboratory work.

Chapter 3: Methods and Techniques

Field Investigation

The first field investigation on ice wedges and massive ground ice bodies was undertaken between June 6th and June 28th 2006 along the Eagle, Bell and Porcupine River, Northern Yukon (figure 5). More than one hundred samples were collected from the ice wedges along the three rivers for the determination of $^{18}O/^{16}O$ and D/H ratios of melted ice samples. Peat and wood samples were collected from above the ice wedges at several locations for radiocarbon dating. Three ice wedges located on the Porcupine River, within 10 km of Old Crow, were sampled for gas composition. Ice blocks were taken in the middle section of the ice wedges, at middle height.

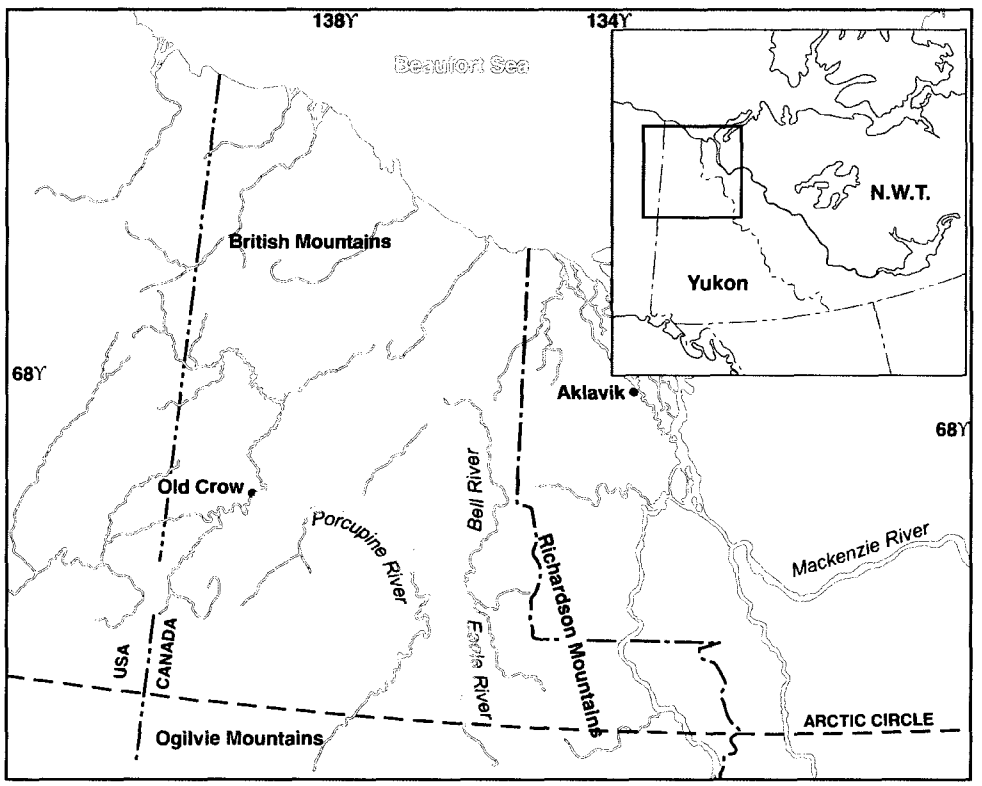

Figure 5: Study area for summer 2006

A second field investigation was undertaken between June 25th and July 18th 2007 along the Demspter Highway (Yukon). An ice block was sampled on the side of an ice wedge at the Moose Lake site (Figure 6). Fieldwork was also undertaken in Alaska during that summer, between

July 3rd and July 8th 2007, to sample older ice wedges in the Vault Creek tunnel in Fairbanks (Figure 6). Vault Creek ice wedges were sampled in the lower part of the wedge, in the middle, but these ice wedges were strongly deformed.

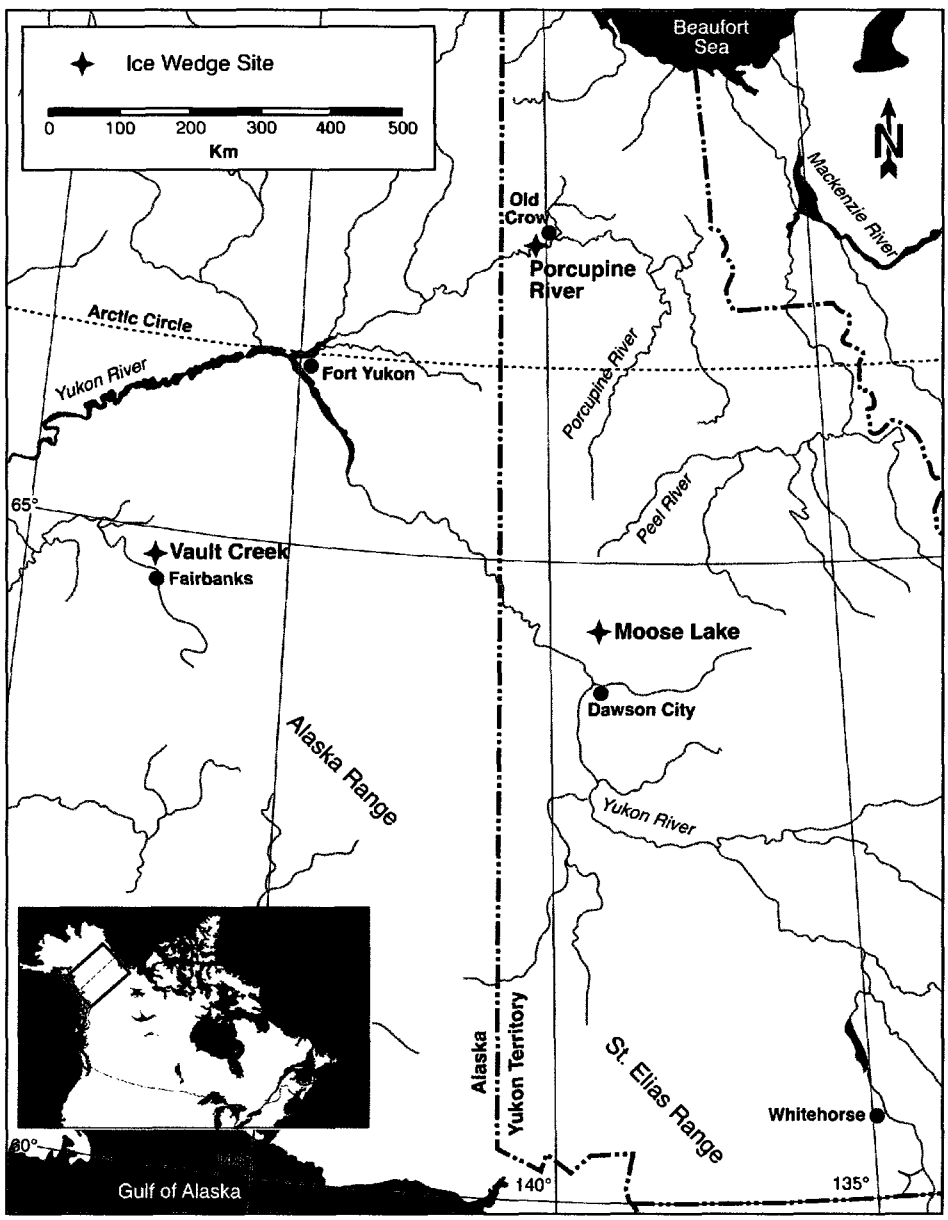

Figure 6: Map of Yukon and Alaska showing location of the three ice wedge sites mentioned in the thesis

Further field investigations were undertaken in summer 2008. An ice block was sampled on the side of an ice wedge at the Moose Lake site. Also, a vertical transect of melted ice samples was

collected on the side of this ice wedge. Finally, an organic silt sample was taken at Moose Lake site, at the bottom side of the ice wedge.

The sampling of the ice was done with an ice axe for the first two years, and with a chain-saw in 2008. The collected ice was put in portable coolers, which can keep ice frozen for 5 days. By experience, we know that additional wrapping can preserve the ice for a week. We spent a several days in each selected area to collect the ice and, afterwards, we stored the ice in freezers at –30 °C in Dawson, Engineering Creek, Old Crow, Fairbanks and Eagle Plains before sending it to Whitehorse and then to Ottawa. Ice samples were shipped to Ottawa as frozen cargo with WestJet Company, taking the route of Whitehorse to Vancouver and Vancouver to Ottawa. In order to avoid contamination, 1-2 cm of ice surface was cut from all ice samples before cutting for analyses.

Laboratory Methods and Techniques

Petrographic Analysis

Crystallographic examination of the ice block samples was carried out at the Geological Survey of Canada's Snow and Ice Core Laboratory (Ottawa, ON). The blocks were trimmed and cut into 5 mm thick slices to examine structure and gas inclusion patterns under plain light. Thin sections (0.4 mm) were then prepared for examination on a four-axis universal stage following methods described in Langway (1958). The thin sections were photographed between crossed polarizing filters to measure crystal size and shape. Crystal c-axis orientations were not analyzed because the ice blocks were not spatially orientated. Moreover, most of our samples were taken in the middle of the ice wedges, in the transition zone, where crystals are expected to be randomly oriented (Corte, 1963; Shumski, 1964). Preliminary analyses showed random

orientations, and we decided not to undertake the c-axis analysis knowing that almost all our samples would be randomly oriented. Instead, crystal size and shape were measured from the images we photographed under crossed polarization. Two major steps were undertaken with different software. First, crystal boundaries were delineated manually using CorelDraw software. This step was done manually because the software could not properly delineate crystal boundaries because of the Newton rings and other inclusions in the ice that were misinterpreted. Then, an image analysis of crystals was undertaken using the software "Clemex Application Suite". Lliboutry (1964) stated that to have good statistical representation, about 100 crystals should be measured. Several vertical and horizontal thin sections were chosen for each ice site based on the criteria of image quality and the number of crystal counted in vertical and horizontal axes. Details about number of thin sections and number of crystals are presented in Table 1.

Table 1: Thin section analysis details

Site	# thin sections (total)	# vertical thin sections	# horizontal thin sections	# crystals measured on vertical thin sections	# crystals measured on horizontal thin sections	# crystals measured (total)
Old Crow area	4	1	3	752	1351	2103
Moose Lake	2	1	1	170	118	288
Vault Creek	3	3	0	363	0	363

Stable O-H Isotopes

The $^{18}O/^{16}O$ and D/H ratios of melted ice samples were determined using two instruments. The first instrument consists of a field portable liquid water analyzer (Los Gatos Research Liquid water analyzer model 908-0008). The liquid water analyzer is based on off-axis integrated cavity output spectroscopy, and was coupled to a CTC LC-PAL autosampler for simultaneous $^{18}O/^{16}O$ and D/H ratios measurements of H_2O. The samples measured with this instrument came from

Moose Lake ice wedges, collected during summer 2008. All measured water samples were calibrated and normalized to internal laboratory water standards that were previously calibrated relative to VSMOW using conventional IRMS systems. Consequently, results are presented using the δ-notation ($\delta^{18}O$ and δD), where δ represents the parts per thousand differences for $^{18}O/^{16}O$ or D/H in a sample with respect to Vienna Standard Mean Ocean Water (VSMOW). Analytical reproducibility for $\delta^{18}O$ and δD is ± 0.3‰ and ± 1‰, respectively. The complete measurement procedure and performance of the liquid water analyzer is described in Lis et al. (2008).

The second instrument is a Finnigan MAT Delta plus XP + Gasbench, operated in the G.G. Hatch Laboratory (University of Ottawa; Department of Earth Sciences). The samples measured with this instrument came from the Old Crow area ice wedges, sampled in summer 2006 and 2007. Water samples were analysed for both deuterium/hydrogen and 18/16 oxygen ratios. To determine ^{18}O and ^{2}H contents, copper and coal were added to avoid organic contamination of the samples. Hokko beads were added to Exetainer vials containing 0.2 to 0.6 mL of water. The vials were flushed and filled with a gas mixture of 2% hydrogen in helium off-line. The H_2 gas was analysed automatically in continuous flow. The results was normalized to VSMOW. The routine precision (2 sigma) of the analysis is +/-1.5 ‰. The oxygen isotopic composition of water was determined in a similar manner by CO_2-water equilibration at 25°C using 0.2 to 0.6mL of water without the Hokko beads, and a gas mixture of 2% CO_2 in helium. The CO_2 was analysed on the same Finnigan MAT Delta plus XP + Gasbench. The CO_2-water fractionation factor used at 25°C is 1.0412 (Friedman & O'Neil, 1977). The routine precision (2 sigma) of the analyses is +/-0.10 ‰. Both isotopes can be determined from a single aliquot of water. In this

case, the oxygen was run first, the vial caps was changed, then the hydrogen was run with the hokko beads.

Soil and Organic Samples

Soil and organic matter adjacent to the massive ice bodies were sampled for stratigraphic analyses and carbon dating. The particle size distribution, mineralogy and chemical composition of the sediment samples was determined to assess its origin, and several radiocarbon dates were measured in the organic samples to know more about the context and age of the massive ice bodies.

Particle size distribution was determined by laser light scattering using a Microtrac S3500 particle size analyzer. Six duplicates of each sample were measured in order to have reliable results that represent the entire sample. Sample preparation involved the destruction of the organic matter with hydrogen peroxide and dispersion with sodium hexametaphosphate. Sediment samples (50-100g) were first immersed to saturation in deonized water. Then, 50 ml of a solution of hydrogen peroxide (35%) was added three times in order to destroy the organic matter. Afterwards, the mixture was boiled in order to evaporate the hydrogen peroxide. Finally, sodium hexametaphosphate was added to saturation to initiate dispersion of the sediments.

The mineralogy of the loess was determined by XRD analysis. The chemical composition of the sediment samples was determined from x-ray fluorescence measurements on fused samples using a Philips PW-2400 spectrometer. The mineralogy of the soil samples was determined by powder x-ray diffraction. The XRD analysis was performed on powdered samples that were mixed with acetone, spread over a glass slide and analyzed with a Siemens D5000 x-ray

diffractometer with a step size of 0.02 and scanning speed of 0.4 sec. per step to record the spectra.

Several organic samples have radiocarbon dated by accelerator mass spectrometry at Beta Analytical (Florida, USA). The samples were pre-cleaned in a weak acid (2% hydrochloride) to remove undesirable carbonate residues and then rinsed in distilled water, air dried and crushed for the measurement. The radiocarbon age is presented as conventional ^{14}C years BP using Libby's half-life of 5568 years.

Gas Composition

For the determination of the concentration and isotopes of O_2, N_2 and Ar gases in ice wedges, three ice wedges from each site were sampled and 3 samples from each ice block were analyzed in order to have confidence in our results. Unfortunately, there were exceptions to that chosen number of samples per sites for several reasons. Two sites had less than 3 ice wedges sampled: Vault Creek and Moose Lake. For the Vault Creek site, only two samples taken from the second ice wedge were qualified for the bubbles analysis because part of the block experienced melting and refreezing during transportation. For Moose Lake, since this is a site of relict ice wedges that had experience melting, only two ice wedges were accessible for sampling and not too affected by melting. Another exception is one of the Old Crow ice wedges (OC-144), where just one sample was retrieved from the ice wedge because of the limited amount available for this analysis.

A wet extraction technique was used to measure the concentration of O_2, N_2 and Ar gases trapped in the massive ground ice. Approximately 50 g of ice was placed inside a glass vessel

and immersed in a cold ethanol bath (–20°C). The ice samples were first sublimated under vacuum conditions for 30 min to remove possible contamination, and then melted by submerging the glass vessel in warm water to release the gases trapped in it. The ice was then frozen from the bottom, forcing the dissolved gas out of the water. The released gases were then condensed into a glass septum vial containing 5A molecular sieves, which was immersed in liquid nitrogen. After a second melt/freeze condensation cycle, the glass septum vial was filled with ultrapure He gas in order to have a pressure of 1 atmosphere in the vial. When filled, the vial was removed from the line, brought to room temperature, and analyzed for the concentration of O_2, N_2 and Ar through a GasBench II interfaced to a Finnigan Mat Delta^{plus} XP isotope ratio mass spectrometer equipped with a special eight-collector assembly. Air collected outside the laboratory building was used as the standard reference gas and yielded average O_2/Ar and N_2/Ar ratios of 22.43 ± 0.13 and 83.58 ± 0.64 respectively, similar to the theoretical atmospheric composition. More detail descriptions about this wet extraction technique are presented in Chapter 4.

Chapter 4:

An improved method for measurement of isotopic and gas ratios (O_2/Ar, N_2/Ar, $\delta^{18}O$, $\delta^{15}N$ and $\delta^{40}Ar$ of air entrapped in ground ice

Mélanie St-Jean[1], Paul Middlestead[2], Ian D. Clark[2], Bernard Lauriol[1]

[1]Department of Geography, University of Ottawa, Ottawa, ON, K1N 6N5, Canada

[2]Department of Earth Sciences, University of Ottawa, Ottawa, ON, K1N 6N5, Canada

Manuscript

Abstract

We present a modified wet extraction technique for measuring the concentration, ratios and isotopes of O_2, N_2 and Ar gases entrapped in ice. The extraction technique analytical reproducibility was checked through air standard measurements, which yielded average O_2/Ar and N_2/Ar ratios of 22.43±0.13 and 83.58±0.64, respectively. The $\delta^{18}O$, $\delta^{15}N$ and $\delta^{40}Ar$ values of air standards averaged respectively -0.03±0.33, -0.0007±0.22, and -0.0001±2.75. Applications in permafrost areas for this modified wet extraction technique comprised the possible identification of massive ground ice types and differentiation between filling processes in ice wedges. Several modifications were made to the original extraction technique that was implemented by Cardyn (2002), including (1) the replacement of the stainless steel tube by a glass tube containing 5A molecular sieve, with a Vacutainer red cap, which is connected to the line through a needle that is coming out of the line; (2) the elimination of the transfer loop step, which was replaced by an ultrapure helium source directly connected to the extraction line; (3) the removal of the peak jump during the analysis on the mass spectrometer, which was replaced by doing two separate runs, one analyzing O_2 and Ar and the other one analyzing N_2; (4) the creation of software which can generate real Amperage based data, removing the major need for data corrections. These modifications improved the precision of the technique, and the standard deviation for the N_2/Ar ratios, which was 7.87 before, decreased to 0.64.

Introduction

Measurements of stable isotopes of gases trapped in air bubbles in ice cores have been used to infer ancient environmental conditions, in ice sheet (e.g. Sowers et al., 1989, 1992, 1997; Craig and Wiens, 1996; Severinghaus et al., 1998; Severinghaus et al, 2003), and more recently in massive ground ice (Moorman and al., 1996; Cardyn et al., 2007; Lacelle et al., 2007). Massive ground ice and icy sediment bodies are commonly observed in formerly glaciated and unglaciated areas in permafrost areas. There is a growing interest in these ground ice exposures because of their implications for Pleistocene ice sheet dynamics and geomorphology (Rampton, 1974, 1988; French and Harry, 1990; Lantuit and Pollard, 2008) and for paleoclimatic and paleoenvironmental reconstructions (St-Onge and McMartin, 1995; Dredge et al., 1999; Dyke et Savelle, 2000; Lacelle et al., 2004; Murton et al., 2005; Lacelle et al., 2007). The nature and origin of massive ground ice bodies have been investigated using textural, morphological and stratigraphic criteria, ice crystallography and stable oxygen and hydrogen isotope ratios. To these conventional techniques, the measurement of the concentration and isotopes of O_2, N_2 and Ar gases entrapped in the ice offers an innovative tool that allows differentiation between ground ice of glacial (firnified glacier ice), non-glacial intrasedimental, and superficial origin. The principle behind this technique is that the gas ratios (O_2/Ar and N_2/Ar) entrapped in glacier ice tend to preserve an atmospheric signature slightly modified by firn diffusion and gravitational settling, whereas the gas ratios of segregated-intrusive ice are significantly different from those found in the atmosphere and glacier ice due to the different solubilities of the gases in water (Lacelle et al., 2007; Cardyn et al., 2007).

More recently, gas compositions in ice has been used to understand the filling process in ice wedges (St-Jean et al, manuscript). The formation of ice wedges is typically caused by the infiltration of melted snow in thermal contraction cracks during the spring (Washburn, 1980; Lauriol et al. 1995). Given that the ground's temperature is below 0°C, the snow meltwater freezes in the crack as a single ice vein. This repeated process creates multi-vein ice wedges, the youngest ice being near the centre. However, other researchers have suggested that the thermal cracks could be filled, in some cases, by hoar frost accretion (Shumski, 1964; French and Guglielmin, 2000). These different hypotheses can be tested with the measurement of ice bubble gas composition. For example, if the filling process involves hoar-frost accretion or snow infill, the gases entrapped in ice will preserve an atmospheric composition, whereas the gas ratios

resulting from snow meltwater freezing in the thermal cracks in the spring will have a distinctive composition due to the different solubilities of gases in water.

The measurement of the concentration and isotopes of O_2, N_2 and Ar gases entrapped in the ice was achieved through a modified wet extraction technique first developed by Sowers et al. (1997) and previously modified by Cardyn et al. (2007). Background information and theory on the origin of gases entrapped in ice was well described by Cardyn and al. (2007). However, several modifications to the extraction technique used by Cardyn and al. (2007) have been made in the past two years in order to improve the analysis precision and to reduce possible contamination. This paper describes the new procedures for the analysis of gas entrapped in ice.

Methodology

The analysis of the gas entrapped in the ice samples involves three main steps. First, the ice samples need to be cut to remove possible contamination on the outer surface and to be able to fit in the extraction vessel. Secondly, the gases are extracted from the ice and transferred into a glass tube. Finally, the extracted gas samples are analyzed by mass spectrometry.

Cutting and Storage

The ice is selected for cutting based on its bubble content. Certain types of ice are bubble-rich and therefore pose no problem. On the other hand, ground ice can be bubble-poor and has to be carefully examined to ensure that the ice analyzed will in fact contain gas. Depending on the bubble dimensions and amount, 2 to 5 pieces of ice are used for an extraction. Ice samples weight approximately 50 g. A band saw in a walk-in freezer maintained at -10°C is used to cut the samples and trim all faces, removing 1-2 cm of ice to expose fresh surfaces. Dimensions of the pieces are ~ 2.5 cm x 2.5 cm x 4.5 cm. The samples are then individually wrapped in foil and place in aseptized Nasco Whirl-pak® bags, stored in a freezer until analysis. Each sample was analyzed within a week of cutting.

Extraction

The line has the usual rotary pump, but is supplemented with a turbo pump (Fig 1.). Approximately 50 g of ice is introduced with metal tweezers in a glass vessel (H) and immersed in a cold ethanol bath (–20°C), which is poored in a dewar flask that is place under the glass

vessel. The ice samples are first sublimated under vacuum conditions for 30 min to remove possible contamination. Sublimation cleans the surface of the ice sample of any absorbed air.

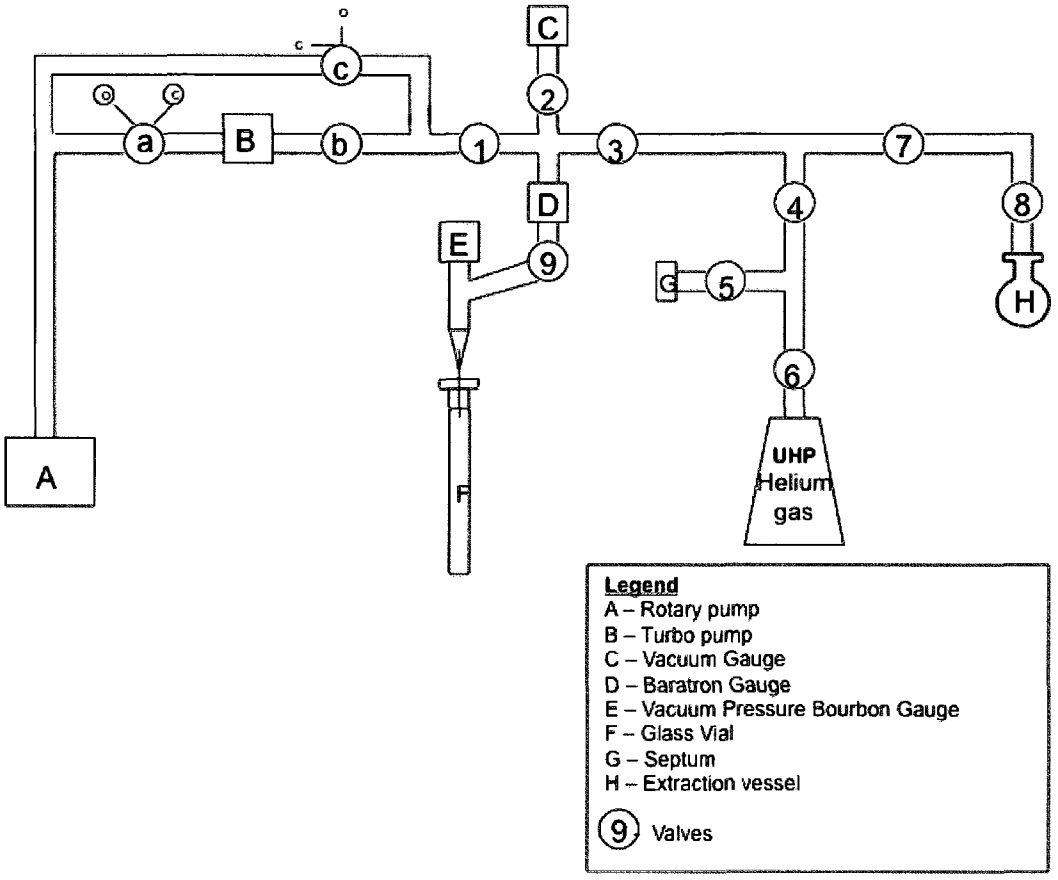

Figure 1: Wet extraction line

Care is taken to ensure that the temperatures of the dewar flask stays below -20 °C. After this sublimation, ice is melted by submerging the glass vessel (H) in warm tap water to release the entrapped gases. The sample is then frozen from the bottom by the immersion of the glass vessel in a cold ethanol bath (-75°C), forcing the dissolved gas out of the water. When the ice is frozen all the way to the top, the ethanol is cooled to -100°C and the bath level is then raised until the part containing the ice is completely immersed. Care is taken to ensure that the temperatures of the dewar stays between -90°C and -100°C for at least 15 minutes, in order to avoid the presence of water vapour in the vessel. The released gases are then condensed into a glass septum vial (F) containing 5A molecular sieves, which is immersed in liquid nitrogen for a 15 minutes transfer. By observing the pressure gauges (C), we are able to confirm that the gas sample has been

transferred into the glass tube when pressure returns to pre-expansion values. High residual pressure can indicate incomplete transfer and is used as a basis for rejection of a sample. After a second melt/freeze condensation cycle, the glass septum vial is filled with ultrapure He gas in order to have a pressure of 1 atmosphere in the vial. When filled, the vial is removed from the line, brought to room temperature, and analyzed for the ratios and deltas of O_2, N_2 and Ar. The complete description of the step-by-step procedures is presented in Appendix 1.

Mass Spectrometry Analysis

Samples are analyzed on a Thermo Finnigan DeltaPlusXP for continuous flow isotope ratio mass spectrometry with an eight collector assembly coupled with a GasBench II with Restek model RT-Msieve 5A (30m length, 0.32mm internal diameter) for sample transfer. Gas samples are introduced into the GasBench by helium transport. They initially go through a process of water removal before entering the Restek column. An aliquot of the sample is taken and then transferred into the gas chromatograph (GC) column where the gases are separated depending on their polarity.

All the gases have a unique retention time and therefore exit this column at different periods allowing the mass spectrometer to analyze one gas at a time. The gases then go through another phase of water removal before entering the ion source where all the particles are ionized. Following this step the ionized particles enter the magnetic field where they will be separated by mass, into different collectors. Three references gases are also measured every time for Ar, N_2 and O_2 for isotopic ratios measurement. Analytical reproducibility of the mass spectrometer for $d^{18}O$ and $d^{15}N$ is $\pm$ 0.1‰.

Verification of Method

Several steps are undertaken in the technique to verify the reliability and accuracy of the method. Leak checks and blank tests are performed routinely on the extraction line, as well as air standards and fabricated ice standards.

Leak checks are performed several times per day routinely by closing the valve connecting the manifold to the pump and verifying that the vacuum gauge remained constant. A slight increase is always observed due to degassing but it stabilizes at approximately 10^{-3}mTorr.

A blank test to verify background level of gases is performed daily on the extraction line. To accomplish this test, the line is isolated from the pump for 15 minutes, and residual gases (if any were present) where transferred into the glass vial for measurement on the mass spectrometer. This way, we know immediately if there is a leak or contamination in the line. Results from these tests indicate that no measurable background gases accumulate in the line.

The atmosphere is the ultimate standard gas to which all our measurements are referred. Air collected outside the laboratory building is used as the standard reference gas. The extraction technique analytical reproducibility is checked through these air standard measurements. Standard air samples are collected outside the laboratory with a 1 ml gas tight syringe, made by Hamilton. The needle is inserted in the line with the syringe closed, to test for leaks in the syringe. This is done regularly. Standard samples are injected into the ice extraction line and run through roughly the same procedure as the ice sample, mimicking as closely as possible the path taken by ice core samples (see Appendix 1 for more details). In table 1 and figure 2, 3 and 4, results from 46 aliquots of 0.6 ml (STP) measured over five periods of analysis are presented. These air standards yield average O_2/Ar and N_2/Ar ratios of 22.43±0.13 and 83.58±0.64, respectively, similar to the theoretical atmospheric composition (22.43 and 83.6, respectively). The stable isotope results are presented using the δ-notation representing the parts per thousand differences for $^{18}O/^{16}O$, $^{15}N/^{14}N$ or $^{40}Ar/^{36}Ar$ from the standard reference gas. The $\delta^{18}O$, $\delta^{15}N$ and $\delta^{40}Ar$ standard values averaged respectively -0.03±0.33, -0.0007±0.22, and -0.0001±2.75.

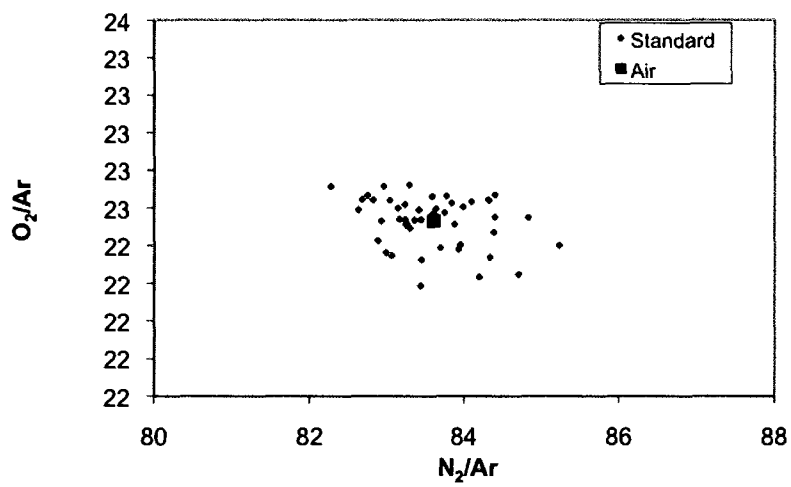

Figure 2: Comparison of the gas ratios (O_2/Ar and N_2/Ar) of the working standard with the atmospheric values

Table 1. Air standard measurements

Standard	O_2/Ar	N_2/Ar	$\delta^{18}O$(‰)	$\delta^{15}N$(‰)	$\delta^{40}Ar$(‰)
1	22.37	84.39	-0.11	0.16	-0.91
2	22.47	83.74	-0.30	0.03	-0.98
3	22.52	83.84	-0.37	0.06	-0.98
4	22.50	83.99	0.21	-0.06	-1.07
5	22.25	83.06	-0.15	0.03	-0.70
6	22.56	83.77	0.25	0.25	-0.10
7	22.43	83.36	0.05	-0.05	-0.12
8	22.28	83.93	0.38	0.07	0.93
9	22.26	82.98	0.10	-0.02	1.00
10	22.61	82.95	-0.16	-0.17	1.13
11	22.49	83.63	0.00	-0.15	1.79
12	22.54	83.03	-0.04	0.04	-1.74
13	22.24	84.33	0.51	0.20	0.89
14	22.45	84.40	0.57	0.43	0.43
15	22.41	83.25	-0.80	-0.36	-0.16
16	22.41	83.88	0.06	0.21	0.43
17	22.57	84.40	0.37	0.48	1.17
18	22.52	83.23	-0.39	-0.12	-0.22
19	22.61	82.27	-0.20	-0.34	-0.45
20	22.13	84.20	0.02	0.12	0.59
21	22.49	82.63	-0.45	-0.31	-0.22
22	22.33	82.88	-0.73	-0.55	-0.72
23	22.54	84.31	0.04	0.12	-0.69
24	22.09	83.43	0.25	-0.07	-0.82
25	22.15	84.71	0.55	0.28	0.06
26	22.47	83.59	-0.17	-0.11	-0.71
27	22.29	83.69	-0.33	-0.17	-1.02
28	22.22	83.44	-0.04	-0.20	-0.50
29	22.43	82.92	-0.03	0.00	-0.21
30	22.54	82.82	-0.07	-0.07	0.01
31	22.54	82.67	-0.16	-0.14	-0.08
32	22.62	83.28	-0.20	0.00	0.37
33	22.56	83.58	-0.13	0.04	0.57
34	22.54	84.32	0.26	0.22	1.62
35	22.53	84.10	0.04	0.12	1.40
36	22.39	83.30	-0.01	0.24	-5.02
37	22.44	83.16	-0.09	0.01	-4.60
39	22.50	83.14	-0.18	-0.10	-4.17
39	22.56	82.75	-0.03	0.12	-2.01
40	22.30	83.95	-0.52	-0.48	-9.20
41	22.44	83.23	-0.21	-0.20	-0.22
42	22.49	83.41	-0.13	-0.13	1.33
43	22.42	83.25	-0.12	-0.13	3.29
44	22.45	84.83	0.47	0.29	5.26
45	22.44	83.44	-0.03	-0.08	6.07
46	22.30	85.23	0.85	0.48	9.27
Average	22.43	83.58	-0.03	0.00	0.00
Standard deviation	0.13	0.64	0.33	0.23	2.75

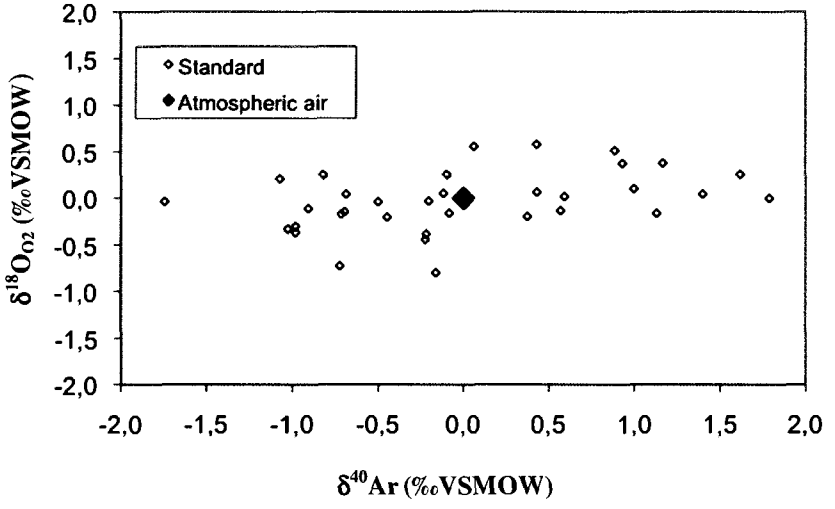

Figure 3: Co-isotopes diagram ($\delta^{18}O$/ $\delta^{40}Ar$) of the working standard, compared with the atmospheric values

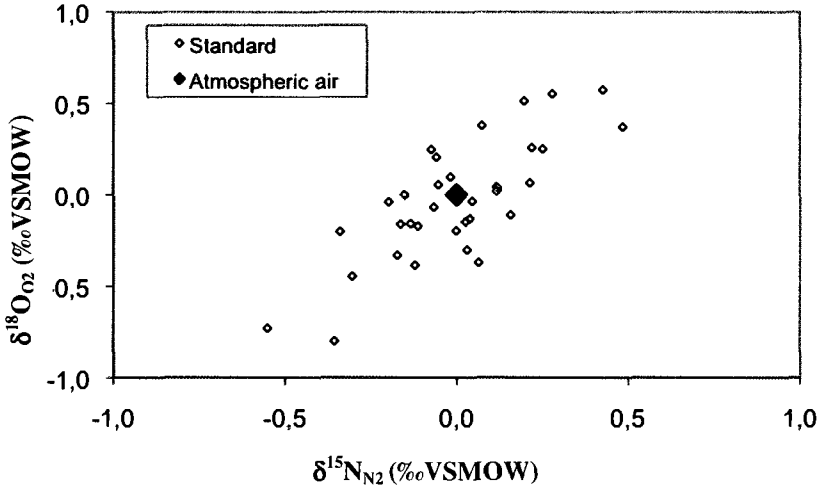

Figure 4: Co-isotopes diagram (δ¨O/δ¨N) of the working standard, compared with the atmospheric values

Discussion

Modifications to the Extraction Technique

Several modifications were made to the original extraction technique that was implemented by Cardyn (2002). The first modification involved the removal of the stainless steel tube in which gases were transferred. This tube was replaced by a glass vial containing 5A molecular sieves, with a Vacutainer red cap, which is connected to the line through a needle that comes out of the line (Fig. 1). The previous stainless steel tube was immersed in liquid helium, which was expensive and inconvenient since a tank lasted only for 1-2 weeks. The 5A molecular

sieves introduced in the glass vial allow the use of liquid nitrogen to condense the gases, which is much less expensive and more convenient in terms of availability.

The second modification involves the elimination of the transfer loop step. The problem was that only an aliquot of the sample was taken and mixed with ultrapure helium with the older line (transfer line). To replace the transfer loop, an ultrapure helium source was connected directly to the line with a valve to control the helium flow (Fig. 1). The replacement of the stainless steel tube for the glass vial is also connected to the elimination of the transfer loop. The transfer loop was a way to move the sample from the tube that did not had a septum, which is needed to connect the sample with the mass spectrometer. The elimination of the transfer step minimizes possible contamination of the sample and allows extraction of smaller samples for the same amount of gas actually analyzed by the mass spectrometer.

The third modification involved the removal of the peak jump during the analysis on the mass spectrometer, since it was causing many problems. To avoid this peak jump, two separate runs are done, following each other, resulting in two different chromatograms. The first run analyzes O_2 and Ar and the second run analyzes N_2.

The fourth modification involved units of measurement on the software. Major data corrections were required before as data was coming out in mV and not in amps. A special software version was created that gave real Amperage based measurements. No more corrections are required to get basic data.

The precision has been improved dramatically from Cardyn and al. (2007) study, where standard reference gas yielded average O_2/Ar and N_2/Ar ratios of 22.43 ± 0.58 and 83.60 ± 7.87, while our standard reference gas yielded average O_2/Ar and N_2/Ar ratios of 22.43 ± 0.13 and 83.58 ± 0.64 respectively. The standard deviation for the N_2/Ar ratios, which was 7.87 before, decreased to 0.64.

Reproducibility of Ice Measurements (variability)

Because we run all samples in duplicate or triplicate, the standard deviation of the replicates gives information about reproducibility. Some ice blocks are within the analytical precision of the extraction technique, but most of the blocks have a higher standard deviation than the standards (Table 2). This heterogeneity does not come from the mass spectrometer or the extraction technique, since they both proved to be precise through the air standard

measurements. Therefore, the heterogeneity is mostly due to the variability within the ice itself. Ice samples analyzed for this project are coming from two ground ice types: ice wedge ice, and massive ground ice.

Table 2: Standard deviation for each ice block

Ice blocks	# replicates	O_2/Ar	N_2/Ar	$\delta^{18}O$(‰)	$\delta^{15}N$(‰)	$\delta^{40}Ar$(‰)
Ice wedges						
OC-143	3	0.57	1.90	5.06	1.05	6.87
OC-INC	3	0.67	1.67	3.82	0.09	1.13
VC1	3	2.27	0.77	0.68	0.29	1.21
VC2	2	0.49	0.75	0.29	0.16	0.75
ML2007	3	0.65	0.58	1.01	0.22	0.54
ML2008	4	3.02	0.99	0.89	0.13	2.64
Massive Ground Ice Bodies						
RC1	3	3.26	0.34	6.90	0.77	3.65
RC2	4	1.67	0.46	1.27	0.17	4.11
ET-SA	3	0.58	7.78	1.33	0.7	2.47
ET-TM	3	0.11	1.85	0.56	0.39	1.11
CL-2007	3	0.52	0.2	0.62	0.22	0.79
ER-1	2	0.26	0.11	0.60	0.33	0.57
ER-2	4	0.66	0.33	5.56	0.15	1.16
ER-3	3	1.17	1.53	3.22	0.47	4.61
Air standard	46	0.13	0.64	0.33	0.23	2.75

Ice wedge ice is made of several ice veinlets, ranging from 1 mm to 3 cm width depending on the location and age of the ice wedges, each of which represents different years (i.e., Shumski, 1964; Berg and Black, 1966; Black, 1974; Mackay, 1974; Mackay and Burn, 2002). Due to the size of individual samples, each sample represents a composite of several discrete near vertical layers of wedge ice that represent different years. Therefore, the gas ratios and deltas reported are averages for the entire sample and may not reflect the full range of values that may be found in an analysis of each individual layer. Also, massive ground ice bodies and ice wedges can be heterogeneous in terms of gas inclusions present within the ice. Ground ice is not as pure as ice cores coming from glaciers and often contains sediments and organic matter. The higher standard deviation can then possibly be explained by variations in sediment and organic content in the ice. The oxidation of plant remains and the respiration from microbial activity is responsible for lowering the oxygen concentration in ice bubbles and has been

observed in ice wedges (Shumski, 1964). In fact, Clein and Schimel (1995) indicated that microbial activity occurred at temperatures down to -5°C in tundra and taiga soils. Furthermore, the variation is sediment and organic content can affect the gas composition since we can have more organic inclusions in a particular ice veinlet within the same ice block. Other processes can affect the gas ratios and isotopic values, and they are described in the next section.

Even if the ice types that we are analyzing are heterogeneous, the standard deviation from each ice block is fairly low compared to the difference between the theoretical dissolved and atmospheric ratios. The theoretical atmospheric values for O_2/Ar and N_2/Ar ratios are 22.42 and 83.60 respectively, and the theoretical dissolved gases ratios for O_2/Ar and N_2/Ar ratios are 20.83 and 35.50. Even with a higher standard deviations, the results from the ice blocks can still give relevant information on how the ice was formed (see Appendix 2: Gas composition results from all the sites).

Summary and Conclusion

We presented a modified wet extraction technique for measuring the concentration, ratios and isotopes of O_2, N_2 and Ar gases entrapped in ice. The extraction technique analytical reproducibility is checked through air standard measurements, which yielded average O_2/Ar and N_2/Ar ratios of 22.43±0.13 and 83.58±0.64, respectively. The $\delta^{18}O$, $\delta^{15}N$ and $\delta^{40}Ar$ values of air standards averaged respectively -0.03±0.33, -0.0007±0.22, and -0.0001±2.75. Applications in permafrost areas for this modified wet extraction technique comprised the identification of massive ground ice types and the differentiation between filling processes in ice wedges. Several modifications have been made to the original extraction technique that was implemented by Cardyn (2002). These modifications improved the precision of the technique, standard deviation for the N_2/Ar ratios, which was 7.87 before, decreased to less than 1, with a value of 0.64. However, in some cases, the results from the occluded gases (O_2, N_2 and Ar) did not give clear differentiation between sources of infill or between massive ground ice types, since the ratios were modified by biological and chemical processes such as microbial respiration. Consequently, additional gases that could be used in the identification of ground ice type and that would provide a better discrimination in case where biological processes affect the molar gas ratios are the noble gases Kr and Xe. These gases have very large solubility differences, and together with Ar, are not modified by chemical or biological reactions, and would therefore be

very useful in situations where such reactions would produce a similar signature. However, extracting and measuring these noble gases with high precision and reproducibility is currently a technical challenge.

References

Benson, B.B., Krause, D.Jr., 1980. The concentration and isotopic fractionation of oxygen dissolved in freshwater and seawater in equilibrium with the atmosphere, *Limnology and Oceanography 25: 662-671.*

Berg, T.E. and Black, R.F. 1966. Preliminary measurements of growth of nonsorted polygons, Victoria Land, Antarctica, American Geophysical Union, *Antarctic Research Series 8:* 61-108.

Black, R.F. 1974. Ice-wedge polygons of northern Alaska. *In* Glacial geomorphology. Edited by D.R. Coates. State University of New York, Binghamton, N.Y. Publications in Geomorphology, pp.247-275.

Cardyn, R. 2002. Analysis of gases in ice from regions of northern Canada. Thesis (M.Sc.), University of Ottawa, Ottawa, 79 pages.

Cardyn, R., Clark, I.D., Lacelle, D., Lauriol, B., Zdanowicz, C., and Calmels, F. 2007. Molar gas ratios of air entrapped in ice: A new tool to determine the nature and origin of relict massive ground ice bodies in permafrost, *Quaternary Research 68 (2):* 239-248.

Clark, I. and Fritz, P. 1997 "Environmental Isotopes in Hydrogeology" CRC Press, Lewis Publishers, USA. pp.328.

Clein JS and Schimel JP. 1995. Microbial activity of tundra and taiga soils at sub-zero temperatures. *Soil Biol. Biochem* **27**(9): 1231-1234

Craig, H., Wiens,R.C. 1996. Gravitational Enrichment of $^{84}Kr/^{36}Ar$ Ratios in Polar Ice Caps: A Measure of Firn Thickness and Accumulation Temperature, *Science* 22(271): 1708-1710. DOI:10.1126/science.271.5256.1708

Dredge, L.A., Kerr, D.E., Wolfe, S.A. 1999. Surficial materials and related ground ice conditions, Slave Province, NWT, Canada. *Canadian Journal of Earth Sciences* 36: 1227-1238.

Dyke, A.S, Savelle, J.M. 2000. Major end moraines of Younger Dryas age on Wollaston Peninsula, Victoria Island, Canadian Arctic: implications for paleoclimate and for formation of hummocky moraine. *Canadian Journal of Earth Sciences 37*: 601-619.

French, H.M. and Guglielmin, M., 2000. Frozen ground phenomena in the vicinity of Terra Nova Bay, Northern Victoria Land, Antarctica : A preliminary report, *Geografiska Annaler 82A(4):* 513-526.

French, H.M. and Harry, D.G. 1990. Observations on buried glacier ice and massive segregated ice, western Arctic coast, Canada. *Permafrost and Periglacial Processes* 1, 31-43.

Grew KE, Ibbs, TL. 1972. Thermal Diffusion if Gases. Cambridge University Press, New York.

Heaton, T.H.E., Vogel JC. 1981. "Excess air" in groundwater. *Journal of Hydrology* **50**: 2011-216.

Ikeda-Fukazawa T, Fukumizu K, Kawamura K, Aoki S, Nakazawa T, Hondoh T. 2005. Effects of molecular diffusion on trapped gas composition in polar ice cores. *Earth and Planetary Science Letters* **229***:* 183-192.

Lacelle , D., Bjornson, J., Lauriol,. B., Clark, I.D., Troutet, Y. 2004. Segregated-intrusive ice of subglacial meltwater origin in retrogressive thaw flow headwalls, Richardson Mountains, NWT, Canada, *Quaternary Science Reviews 23 (5-6):* 681-696.

Lacelle, D., Lauriol, B., Clark, I.D., Cardyn, R., Zdanovicz, C. 2007. Middle Pleistocene-age glacier ice exposed in the headwall of a retrogressive thaw flow near Chapman Lake, central Yukon Territory, Canada. *Quaternary Research 68(2):*249-260.

Lantuit, H., Pollard, W. H.2008. Fifty years of coastal erosion and retrogressive thaw slump activity on Herschel Island, southern Beaufort Sea, Yukon Territory, Canada. *Geomorphology* 95(1-2):84-102. doi:10.1016/j.geomorph.2006.07.040

Lauriol, B., Duchesne, C. and Clark, I.D. 1995. Systématique du remplissage en eau des fentes de gel: les résultats d'une étude oxygène-18 et deutérium. *Permafrost and Periglacial Processes* 16: 47-55.

Llund, L.J., Horne, A.J., Williams, A.E. 2000. Estimating denitrification in a large constructed wetland using stable nitrogen isotope ratios. *Ecological engineering* 14: 68-76.

Mackay, J.R. 1974. Ice wedge cracks, Garry Island, NWT. *Canadian Journal of Earth Sciences* 11: 1366-1383.

Mackay and Burn, 2002. The first 20 years (1978-1979 to 1998-1999) of ice-wedge growth at the Illisarvik experimental drained lake site, western Arctic coast, Canada, *Canadian Journal of Earth Sciences 39:* 95-111.

Moorman, B.J., F.A. Michel and A. Wilson, 1996. ^{14}C dating of trapped gases in massive ground ice, Western Canadian Arctic. *Permafrost and Periglacial Processes* 7 :257-266.

Murton, J.B., Whiteman, C.A., Waller, R.I., Pollard, W. H., Clark, I.D., Dallimore, S.R. 2005. Basal ice facies and supraglacial melt-out till of the Laurentide ice sheet, Tuktoyaktuk Coastlands, western Arctic Canada. Quaternary Science Reviews 24, 681-708.

Quay, P.D. Wilbur, D.O. Richey, J.E. Devol, A.H. Benner, R., Forsberg, B.R. 1995. The $^{18}O/^{16}O$ of dissolved oxygen in rivers and lakes in the Amazon Basin: Determining the ratio of respiration to photosynthesis rates in freshwaters, Limnol. Oceanogr. 40(4): 718-729.

Rampton, V.N. 1974. The influence of ground ice and thermokarst upon the geomorphology of the Mackenzie-Beaufort region. *In:* Alpine Geomorphology, Proceedings of the Third Guelph Symposium on Geomorphology. Geo-Abstracts, Norwich, pp. 43-59.

Rampton, V.N. 1988. Origin of massive ground ice on Tuktoyaktuk Peninsula, Northwest Territories, Canada: a review of stratigraphic and geomorphic evidence. *In*: Fifth International Conference, Proceedings, vol.1. Tapir, Trondheim, pp.850-855.

Severinghaus, J.P., Brook, E.J. 1999. Abrupt climate change at the end of the last glacial period inferred from trapped air in polar ice. *Science* 286: 930-934.

Severinghaus, J.P., Grachev, A., and Caillon, N. 2003. A method for precise measurement of argon 40/36 and krypton/argon ratios in trapped air in polar ice with applications to past firn thickness and abrupt climate change in Greeland and at Siple Dome, Antarctica, *Geochemica et Cosmochimica Acta 67(3):* 325-343.

Severinghaus, J.P. Sowers, T., Brook, E.J, Alley, R.B., Bender, M.L. 1998. Timing of abrupt climate change at the end of the Younger Dryas period from thermally fractionated gases in polar ice. *Nature* 391: 141-146.

Shumskii, P.A. 1964. Principles of Structural Glaciology, Dover Publications, Inc. New York, 497 pages.

Sowers, T., Bender, M. 1989. Elemental and isotopic composition of occluded O_2 and N_2 in polar ice, *Journal of Geophysical Research 94*: 5137-5150.

Sowers, Bender, M., Raynaud, D., Korotkevich, Y.S. 1992. $\delta^{15}N$ of N_2 in air trapped in polar ice: a tracer of gas transport in the firn and a possible constraint on ice-age gas differences, *Journal of Geophysical Research 97*: 15,683-15,697.

Sowers, T., Brook, E., Etheridge, D., Blunier, T., Fuchs, A., Leuenberger, M., Chappellaz, J., Barnola, J.M., Wahlen, M., Deck, B., Weyhenmeyer, C. 1997. An interlaboratory comparison

of techniques for extracting and analyzing trapped gases in ice cores. *Journal of Geophysical Research 102:* 26,527-26,538.

St-Onge, D.A. MacMartin, I. 1995. The Bluenose Lake Moraine, a moraine with a glacier core. *Géographie Physique et Quaternaire 53*: 287-295.

Washburn, A.L. 1980. Geocryology: a survey of periglacial processes and environments, Wiler, New York, 406 p.

Wilson, G.B., McNeill, G.W. 1997. Noble gas recharge temperatures and the excess air component. *Applied Geochemistry* 12 (6): 747-762.

Zheng J, Kudi A, Fisher DA, Blake EW, Gerasimoff, M. 1998. Solid electrical conductivity (ECM) from four Agassiz ice cores, Ellesmere Island NWT, Canada; high-resolution signal and noise over the last millenium and low resolution over the Holocene, *The Holocene* **8**(4): 413-421.

Chapter 5:

Investigation on the Source of Infill of Ice Wedges Using Crystallography, Stable O-H Isotopes of Ice, and Elemental - Isotopic composition of occluded O_2, N_2 and Ar gases

Mélanie St-Jean[1], Bernard Lauriol[1], Ian D. Clark[2], Denis Lacelle[3]

[1]Department of Geography, University of Ottawa, Ottawa, ON, K1N 6N5, Canada

[2]Department of Earth Sciences, University of Ottawa, Ottawa, ON, K1N 6N5, Canada

[3]Planetary Exploration and Space Astronomy, Canadian Space Agency, St-Hubert, QC, J3Y 8Y9, Canada

Corresponding authors:
melanie.stjean@gmail.com (M. St-Jean); idclark@uottawa.ca (I. Clark); blauriol@uottawa.ca (B. Lauriol); denis.lacelle@asc-csa.gc.ca (D. Lacelle)

Manuscript: Permafrost and Periglacial Processes
Special issue: Isotope and Geochemistry of Permafrost

ABSTRACT

This study investigates the source and mechanism of infill in ice wedges of various ages (modern to Pleistocene age) collected in the western Arctic. This objective was accomplished by using a variety of techniques, including ice crystallography, geochemical and stable O-H isotopes analyses of the ice, and gas composition (O_2, N_2 and Ar) of air entrapped in the ice. Collectively, the results indicate that climatic conditions may influence the source of infilling during the ice wedge growth, so that wet and dry environments result in two different signatures in ice wedges. For example, Vault Creek tunnel ice wedges, dated to the late Pleistocene, a cold and dry period, preserved stable O-H isotope and gas compositions similar to those expected for ice formed by snow densification, while ice wedges from the Old Crow region, dated to the late Holocene, preserved isotopic and gas compositions more similar to what is expected for ice formed by the freezing of liquid water. The O_2/Ar ratios appeared to be much lower than both dissolved and atmospheric ratios, which could be explained by respiration of microorganisms living within the ice bubbles or interstitial water at the grain boundaries.

Keywords: ice wedge, ice crystallography, isotopic and gas composition, Yukon, Alaska

INTRODUCTION

In terrestrial polar regions, polygonal terrain is often associated with the presence of subsurface massive ground ice, the most common being wedge ice. The process of ice wedge formation has been studied for many decades and is well known (e.g., Shumski, 1964; Mackay, 1974; 1990; 1992; 2000; Mackay and Burn, 2002; French, 2007). However, there still remain uncertainties regarding the infilling material resulting in wedge ice (i.e., hoar frost, snow, snow meltwater, rainfall), and these have significant implication regarding the use of wedge ice for paleoclimatic and paleoenvironment reconstruction studies (e.g., Michel, 1982; Mackay 1983; Meyer *et al.*, 2002; Schirrmeister *et al.*, 2002; Popp *et al.*, 2006). In the North American literature, the commonly accepted process for the formation for ice wedges is through thermal contraction cracking of the ground during the cold winter months following a rapid and sustained drop in air temperature (e.g., Lachenbruch, 1966; Mackay, 1974; 1992; Allard and Kasper, 1998; Christiansen, 2005; Fortier and Allard, 2005). In the spring, snow meltwater can infiltrate the thermal contraction cracks, and given that the ground's temperature is below 0°C, the snow meltwater freezes in the crack as an ice vein (Washburn, 1980; Lauriol *et al.* 1995). This repeated process creates multiple vein wedge ice, the youngest ice being near the center. However, studies by Shumski (1964), Tormirdiaro (1996) and French and Guglielmin (2000) have suggested that ice wedges in some cases, grow by water vapour condensation, hoar-frost accretion or snow infilling the thermal crack. For example, in the Yukatia Peninsula (Siberia), Shumski (1964) observed the growth of ice veins without water replenishment and suggested that the thermal contraction cracks could be infilled in some cases by hoar-frost accretion. A similar filling process was also observed in Antarctic ice wedges by French and Guglielmin (2000). Therefore, these distinct hypotheses of ice wedge growth could in part be attributed to the climate regime under which the ice wedge grow, as Siberia and Antarctica examples are documenting wedge ice that grew under a cold and dry climate, whereas North American examples are derived from wedge ice that grew under a cold and wetter climate.

A number of approaches have been used to investigate the origin of massive ground ice (e.g. French and Pollard, 1986; Mackay 1989; Murton and French, 1994; French, 1998; Kotler and Burn, 2000; Cardyn *et al.*, 2007; Lacelle *et al.*, 2007), but these have yet to been applied to ice wedges. Wedge ice is easily identified in natural exposures by its V-shape, truncated top, and the vertically irregular stratified structure of the ice. However, in some cases, wedge ice is

irregularly shaped (i.e. , in long section or when post-depositional deformation occurs in relict wedge ice). The source and mechanism of infill in wedge ice can be examined by combining several techniques, including ice petrography, stable O-H isotope composition and gas composition of air entrapped in the ice. Stable O-H isotope ratios in massive ground ice bodies have proved to be useful in determining the origin of the ice (e.g., Michel and Fritz, 1982; Jouzel and Souchez, 1982; Lorrain and Demeur, 1985; Mackay and Dallimore, 1992; Lacelle *et al.*, 2004). The slope of the regression between the δD and $\delta^{18}O$ composition of ground ice provides clues about its origin because ice formed by firn (snow) densification will plot along a regression slope similar to the global meteoric water line (GMWL: $\delta D = 8\ \delta^{18}O + 10$; Craig, 1961), whereas ground ice formed by freezing of liquid water plots along a much lower regression slope. More recently, the analysis of elemental composition of gases entrapped in ground ice allows differentiation between ground ice formed by snow densification and liquid water (Cardyn *et al.*, 2007; Lacelle *et al.*, 2008). For example, if the filling process involves hoar-frost accretion or snow infill, the gases entrapped in ice (CO_2, O_2, N_2, Ar) should preserve an atmospheric composition, whereas gases trapped in ice resulting from snow meltwater freezing in the thermal cracks in the spring will have highly distinct composition due to the different solubilities of gases in water (Henry's Law constant), assuming that the ice has not subsequently exchanged with atmosphere due to subsequent cracking. Several physico-chemical and biological processes, however, can modify the N_2/Ar and O_2/Ar ratios preserved in ice wedges (Cardyn *et al.*, 2007).

The objective of this study is to investigate the source and mechanism of infill in ice wedges of various ages (modern to Pleistocene age) preserved in Yukon and Alaska, western Arctic (Fig. 1). This objective is accomplished by using a variety of techniques, including ice crystallography, stable O-H isotopes analyses of the ice and elemental and isotopic composition of gases (O_2, N_2 and Ar) entrapped in the ice.

SITE DESCRIPTIONS

In this study, samples of wedge ice were collected from the Old Crow region in northern Yukon, near Moose Lake in central Yukon, and in the Vault Creek tunnel, central Alaska (Fig. 1). The wedge ice collected from these three sites are of modern, Holocene and Pleistocene age.

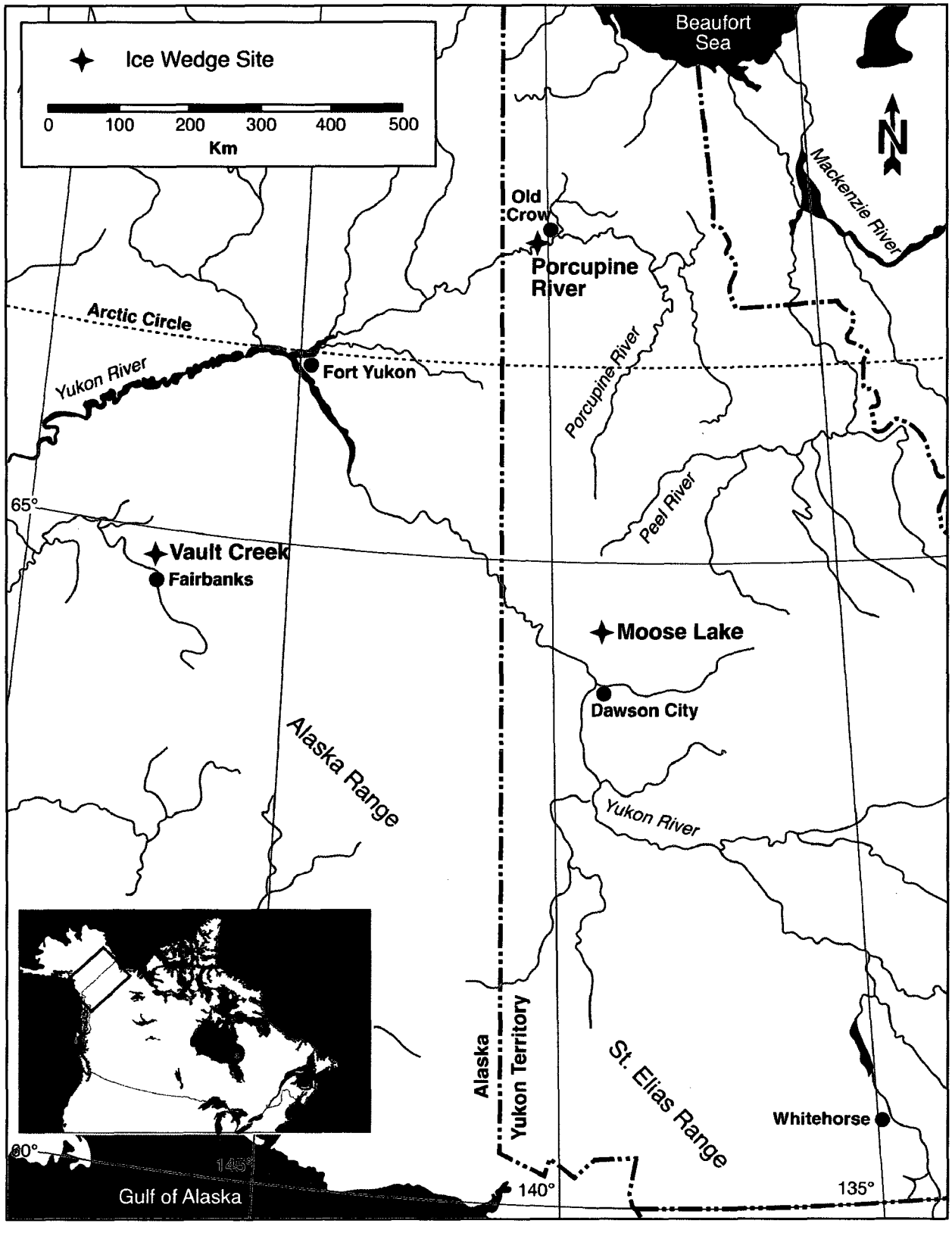

Figure 1: A) Map of Yukon and Alaska showing location of the three ice wedge sites mentioned in this study.

Old Crow region, northern Yukon Territory

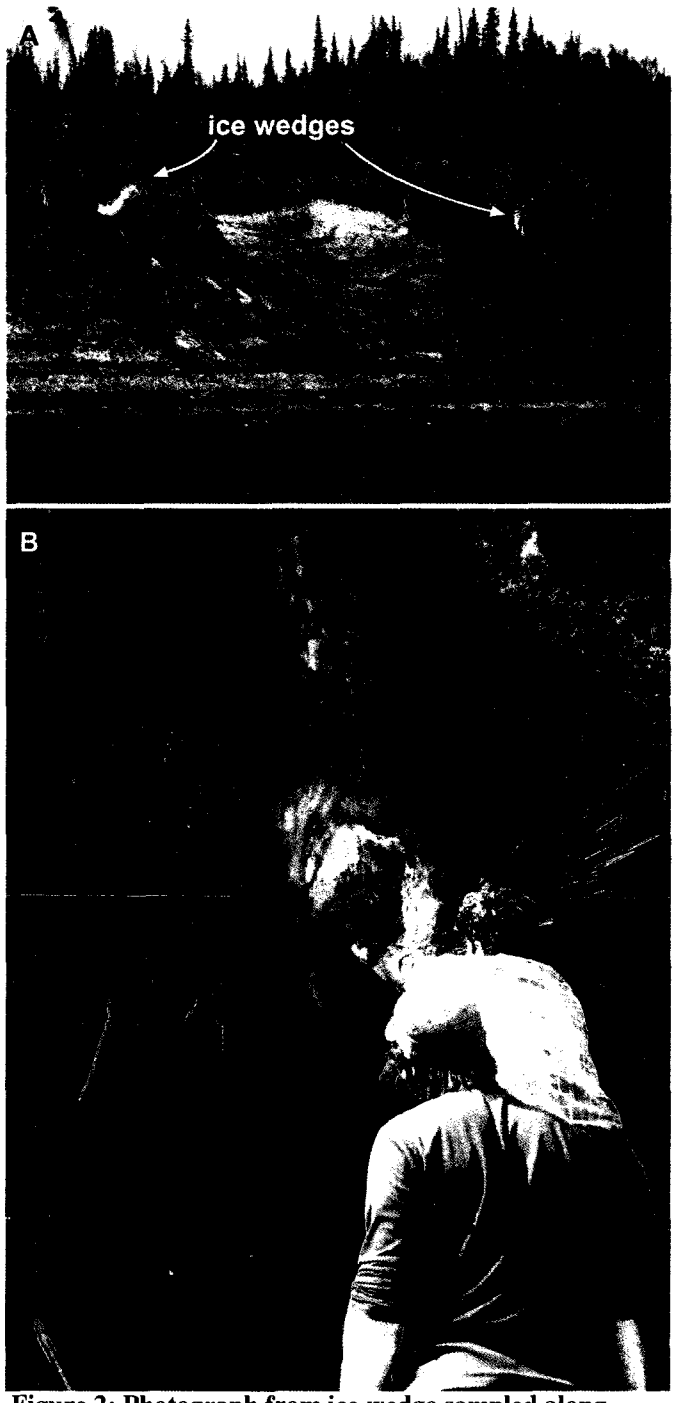

Figure 2: Photograph from ice wedge sampled along the Eagle, Bell and Porcupine Rivers, taken in July 2006.

Ice wedges were sampled on the terraces of the Eagle, Bell and Porcupine rivers (northern Yukon). This region is currently characterized by long cold winters (January temperature: –31.1 ± 4.8°C), short cool summers (July temperature: 14.6 ± 1.4°C) and relatively low precipitation (total annual precipitation 265 mm) (1970-2000 climate data from Old Crow meteorological station; Environment Canada, 2004). These climatic conditions ensure the presence of continuous permafrost in the area, except beneath deep water bodies.

A series of epigenetic ice wedges were sampled in 2006 on the lower Holocene-age terraces of the Eagle, Bell and Porcupine rivers, northern Yukon (Fig. 2). The general stratigraphic sequence of the terraces presents a bottom unit of coarse sand deposits overlain by a silt unit, in which the ice wedges are found, and which is covered by peat. Two conventional ^{14}C ages obtained from the peat covering the ice-rich silt unit, gave the same age of 1660 ± 80 years ^{14}C BP (UL-23254; UL-23255), whereas ten wood pieces collected in the ice-rich silt unit provided ^{14}C ages of 7500 ± 2000 ^{14}C BP (Lauriol *et al.*, 1995).

The chronostratigraphy of the terraces shows that the ice wedges started to grow during the middle Holocene and are still active today.

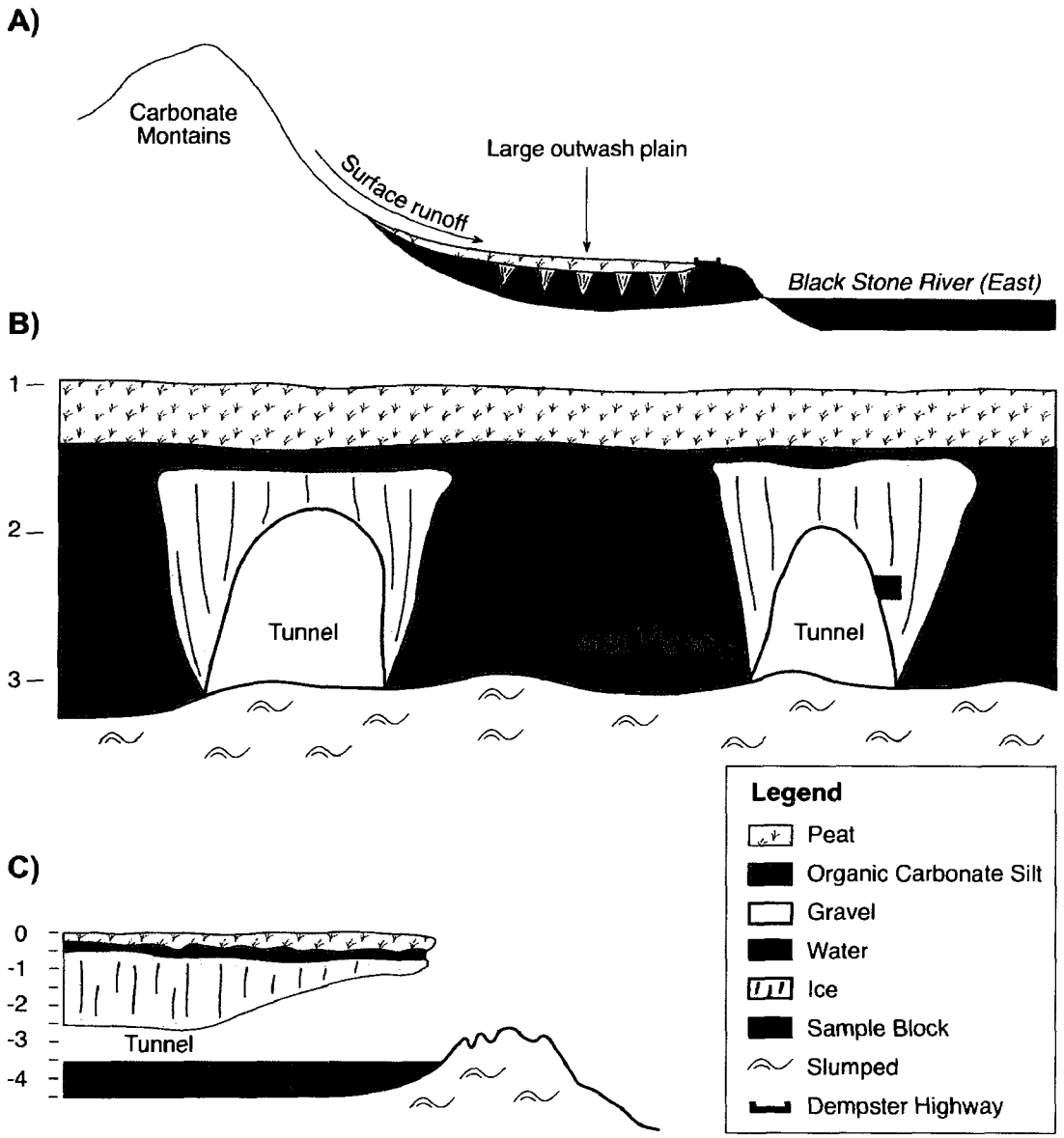

Figure 3: Schematic diagrams of Moose Lake ice wedge site in 2007-2008. A) Large scale view of the area. B) Cross-section front view of the ice wedges. C) Cross-section side view of the ice wedges.

Moose Lake, central Yukon Territory

Epigenetic ice wedges were sampled in 2007 from a large glacial outwash plain (1100 m a.s.l.) located about 15 km north of North Fork Pass (Ogilvie Mountains, central Yukon). This region has a continental sub-Arctic climate regime, with long cold winters (January temperature:

–26.7 ± 6.7°C), short mild summers (July temperature: 15.6 ± 0.8°C) and relatively low precipitation (total annual precipitation 321 mm) (1970-2000 climate data from Dawson City meteorological station; Environment Canada, 2004).

The most common stratigraphic sequence in the Moose Lake area shows an organic ice-rich silt unit covered by peat (Fig. 3). In 2007 and 2008, a subterranean drainage network was observed along ice wedge polygons which led to a thermokarst landscape (Fig. 4). This network, observed on the 1953 aerial photo, was probably initiated by the perturbation of the soil during the construction of the Dempster Highway in the early 1950's. The perturbation has induced a surface runoff that subsequently evolved into the formation of underground tunnels through the ice wedge polygonal network. This type of hydro-thermal erosion of ice wedge has been described on Bylot Island by Fortier *et al.* (2007). Two wedge ice samples were collected in the tunnels. A single conventional ^{14}C date was measured in the organic ice rich silt at 2.5 m below the surface, provided an age of 4130 ± 40 ^{14}C years BP (Beta 251190). This strongly suggests that the ice wedges formed in the silt unit are also of Holocene age.

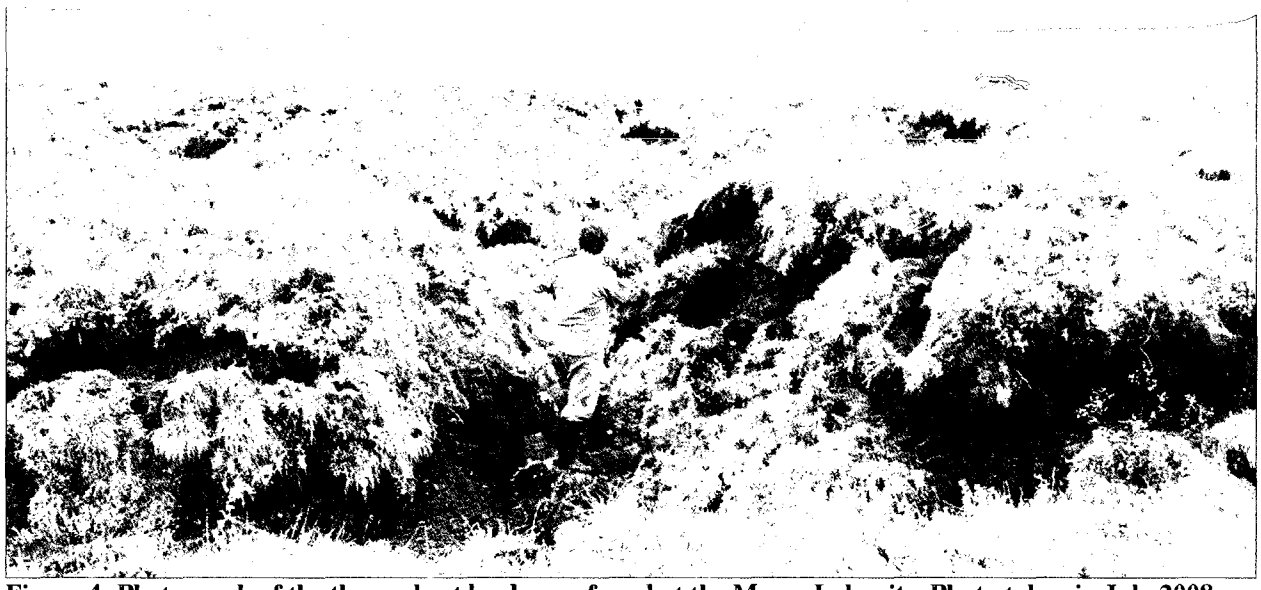

Figure 4: Photograph of the thermokart landscape found at the Moose Lake site. Photo taken in July 2008

Vault Creek tunnel, central Alaska

Relict Pleistocene-age ice wedges were sampled in the Vault Creek tunnel, central Alaska, in 2007. The Vault Creek tunnel is located on a north-facing slope about 40 km north of

Fairbanks, Alaska (Fig. 5). The region is currently characterized by a continental climate regime with a mean annual air temperature of –3°C and total precipitation of 263 mm (climate data recorded at Fairbanks airport over the 1971-2000 period; Meyer *et al.* 2008). These climatic conditions result in the presence of discontinuous permafrost in the region.

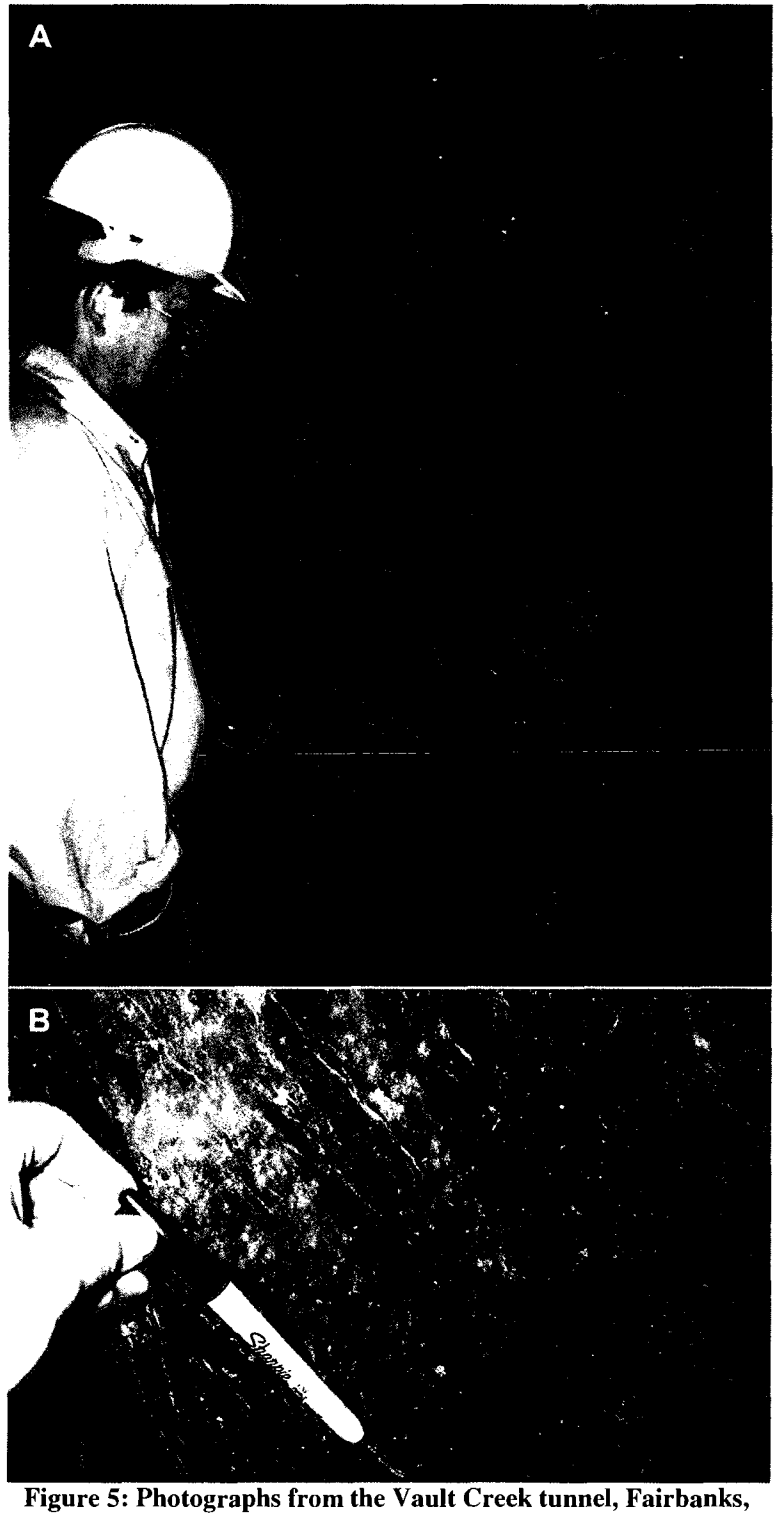

Figure 5: Photographs from the Vault Creek tunnel, Fairbanks, showing: A) Structure of the wedge ice; and B) Example of a sampled ice wedge. Photos taken in July 2007

A study by Meyer *et al.* (2008) reconstructed the environmental history of the tunnel, and examined the stable O-H isotope composition of the ice wedges. According to Meyer *et al.* (2008), the stratigraphy of the tunnel consists of a lower unit consisting of 17.5 m thick ice-bonded fluvial gravel and an upper 3 m thick unit of ice-rich silty sediments in which large ice wedges are found. In between these two units is a 7.5 m thick transition unit consisting of fluvial gravels interbedding the ice-rich silt. This unit contains small ice wedges. Seven radiocarbon measurements from the silt unit provided ages > 40,000 ^{14}C years BP, whereas organic matter in one wedge ice yielded an age of 34,400 ± 4390 ^{14}C years BP (Meyer *et al.*, 2008). Two wedge ice samples were collected in the ice-rich silty sediments section of the tunnel.

SAMPLING AND ANALYTICAL METHODS

According to Mackay (1989) and French and Harry (1990), combining a variety of analytical techniques can provide better information regarding the source and mechanism of infilling of wedge ice than a single approach. The methods used include the analysis of the gas composition of air entrapped in the ice, in addition to the more traditional crystallographic and stable O-H isotopes analyses. For crystallographic and gas analyses, 0.125 m^3 ice blocks were extracted from the exposed ice surface using a chain-saw or an ice axe, and the ice samples were kept frozen in a thermally insulated box maintained at or below –15°C. Ice samples for stable O-H isotope ratios were collected with an ice axe, melted in the field in sealed plastic bags and then poured in 20 ml polyethylene bottles prior to shipment back to Ottawa. As sampling took place during the thaw season, at least 5 cm of ice was removed from the surface to minimize possible mixing with liquid or refrozen runoff prior to sampling.

Ice crystallography

Crystallographic examination of ground ice can provide information regarding crystal growth (French and Pollard, 1986), and was carried out at the Geological Survey of Canada's Snow and Ice Core Laboratory (Ottawa, ON). The blocks were trimmed and cut into 5 mm thick slices to examine structure and gas inclusion patterns under plain light. Thin sections (0.4 mm) were then prepared for examination on a four-axis universal stage following methods described in Langway (1958). The thin sections were photographed between crossed polarizing filters to measure crystal size and shape. Crystal c-axis orientations were not analyzed because the ice blocks were not spatially oriented and most of our samples were taken in the middle section of the ice wedges, in the transition zone, where the ice is presumably younger and crystals are expected to be randomly oriented (Corte, 1963; Shumski, 1964).

Stable O-H isotope composition

The $^{18}O/^{16}O$ ratio of melted water samples was determined on CO_2 isotopically equilibrated with 0.2 ml of water at 25°C (analytical reproducibility of ± 0.1‰). The D/H ratio was measured on H_2 isotopically equilibrated with water at 25°C using a Pt based catalyst (analytical

reproducibility of ± 1.5‰). Both stable isotope measurements were made on the same sample using a Gas Bench II interfaced with a Finnigan Mat Delta XL mass spectrometer. Results are presented using the δ-notation ($\delta^{18}O$ and δD), where δ represents the parts per thousand differences for $^{18}O/^{16}O$ or D/H in a sample with respect to Vienna Standard Mean Ocean Water (VSMOW).

Gas composition

For the measurement of the elemental and isotopic composition of O_2, N_2 and Ar gases trapped in the wedge ice, approximately 50 g of ice was placed inside a glass vessel and immersed in a cold ethanol bath (–20°C). The ice samples were first sublimated under vacuum conditions for 30 min to remove possible contamination, and then melted by submerging the glass vessel in warm water to release the gases trapped in it. The ice was then frozen from the bottom, forcing the dissolved gas out of the water. The released gases were then condensed into a glass septum vial containing 5A molecular sieves, which was immersed in liquid nitrogen. After a second melt/freeze condensation cycle, the glass septum vial was filled with ultrapure He gas to reach a partial pressure of 1 atmosphere inside the vial. When filled, the vial was removed from the line, brought to room temperature, and analyzed for the concentration and isotope compositionof O_2, N_2 and Ar through a GasBench II interfaced to a Finnigan Mat Delta^{plus} XP isotope ratio mass spectrometer equipped with a special eight-collector assembly.

Following the nomenclature of molar ratios of gases occluded in glacier ice (e.g., Sowers et al., 1989), the O_2 and N_2 concentration of trapped air in the ice are expressed by first normalizing the data to the inert gas Ar and then presented in the parts per hundred differences with respect to the O_2/Ar (22.43) and N_2/Ar (83.60) ratios of present-day air. Forty-six analysis of the standard reference gas (air collected outside the laboratory) yielded average O_2/Ar and N_2/Ar ratios of –0.00 ± 0.59% and –0.02 ± 0.76%, respectively, similar to the general present-day atmospheric composition. The $^{18}O/^{16}O$ ratio of O_2 entrapped in the ice is presented using the δ-notation ($\delta^{18}O_{O2}$), where δ represents the parts per thousand differences for $^{18}O/^{16}O$ in the sample with respect to air collected outside the laboratory. Analytical reproducibility is ± 0.32‰

RESULTS

Old Crow region, northern Yukon

The ice wedges collected in the Old Crow region contained spherical and elongated gas inclusions. The diameter of the spherical bubbles ranges from 0.5 to 1 mm, whereas that of the elongated bubbles ranges from 0.5 to 5 mm (Fig. 6A). The ice crystal area for horizontal and vertical thin sections average 2.38 ± 2.79 mm^2 and 1.58 ± 1.94 mm^2, respectively (Figs. 6B-6C).

Stable O-H isotopes from four ice wedges in the Old Crow region (sampled in the banks of the Eagle and Porcupine Rivers) show homogeneity between ice wedges centers and exteriors, indicating climatic stability over the period of growth. The $\delta^{18}O$ values of wedge ice range from –27 to –24‰, which is within the range of winter precipitation recorded at Inuvik (NWT) and of other Holocene-age ice wedges in the Old Crow area (–27 to –23‰; Lauriol *et al.*, 1995). In a δD-$\delta^{18}O$ diagram (Fig. 7), samples from the four ice wedges collected along the Porcupine River plot along individual regression slopes of 5.5, 6.4, 8.7 and 4.5), whereas samples from the ice wedge collected along the Eagle River plot along a slope of 9.6, although with a much lower correlation coefficient.

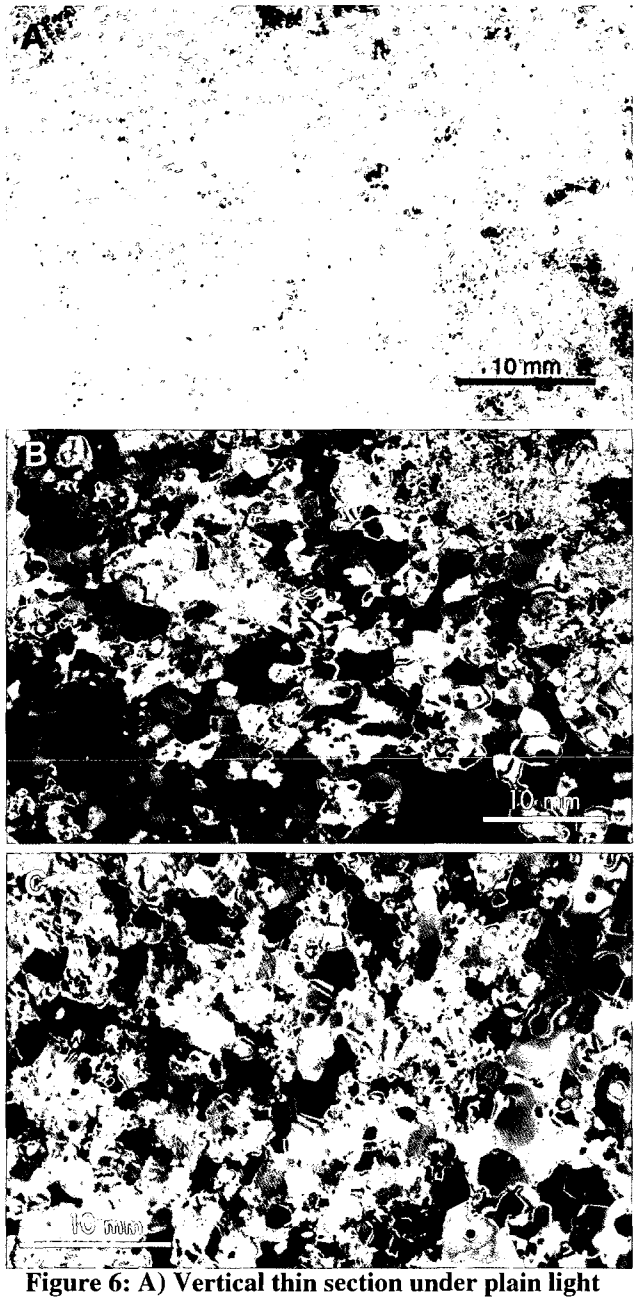

Figure 6: A) Vertical thin section under plain light showing ice bubbles; B) Horizontal thin section under crossed polarizing filters; and C) Vertical thin section under crossed polaroids, of wedge ice from the Old Crow area, northern Yukon.

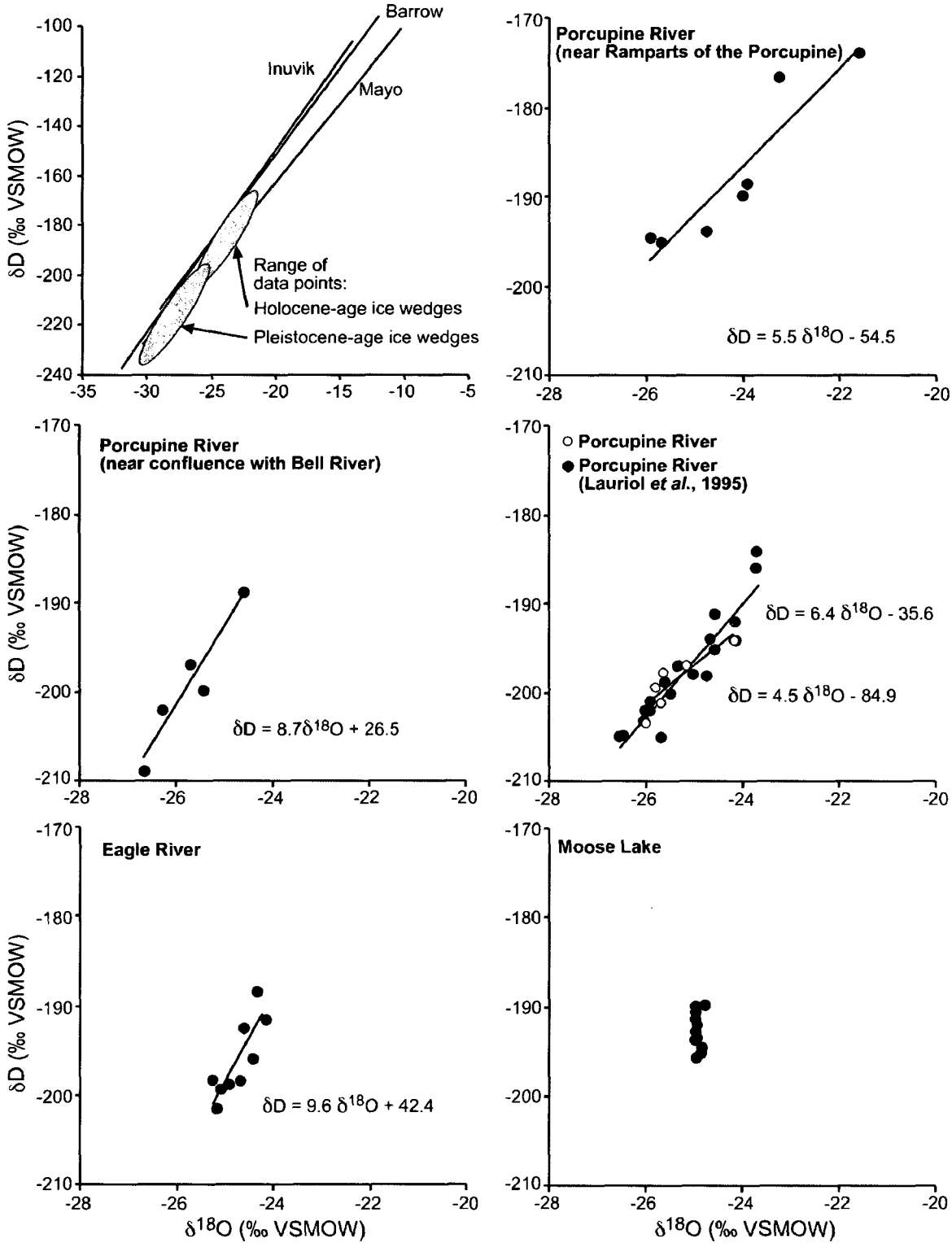

Figure 7: Stable O-H isotope composition of the ice wedges in the Old Crow area and Moose Lake region.

The molar ratios (O_2/Ar and N_2/Ar) of gases entrapped in three ice wedges collected along the Porcupine River average –86.4 ± 7.9% and –15.3 ± 5.7%, respectively (Fig. 8A). The N_2/Ar

ratio falls between the atmospheric and dissolved gases ratios, whereas the O_2/Ar ratios are lower than both the atmospheric and theoretical dissolved ratios. The $\delta^{18}O_{O2}$, and $\delta^{15}N_{N2}$ values of the occluded gases in the Porcupine River samples average 7.7 ± 5.8‰ and –0.6 ± 0.7‰, respectively. The $\delta^{15}N_{N2}$ values are similar to the atmospheric values, whereas the $\delta^{18}O_{O2}$ values are much higher that the atmospheric values.

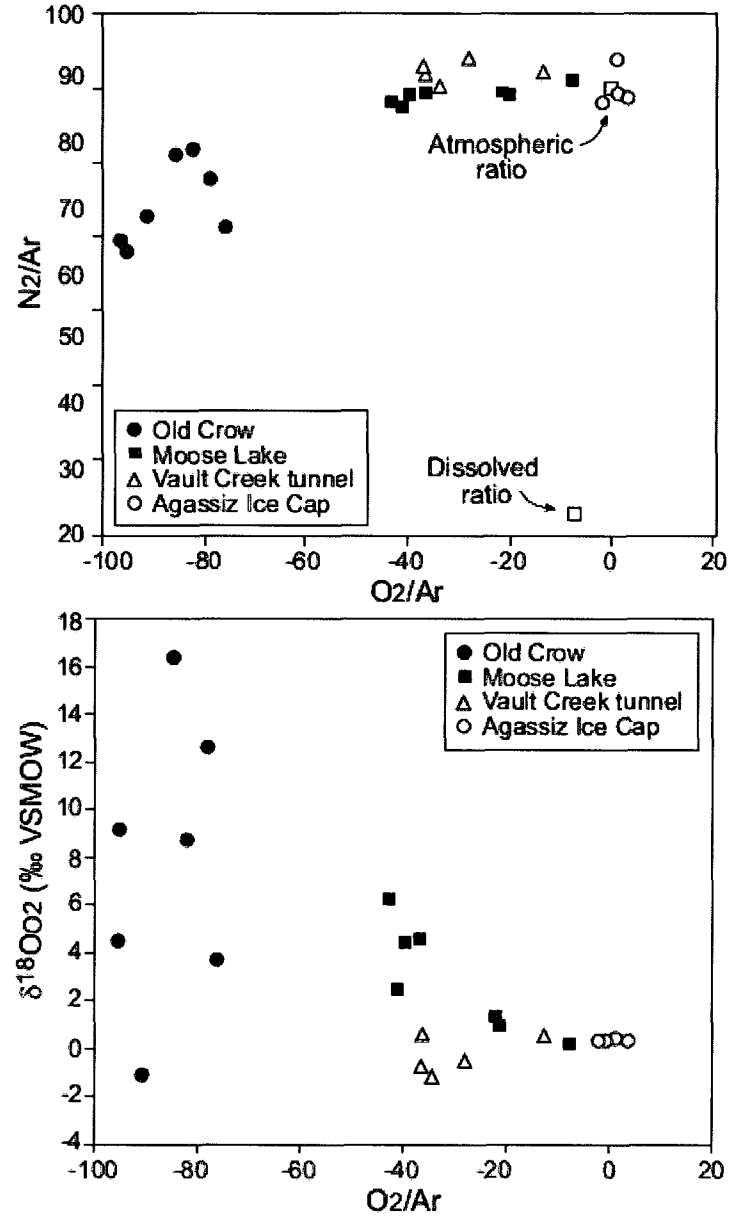

Figure 8: A) Molar gas ratios (N_2/Ar and O_2/Ar) in the wedge ice samples collected from the Old Crow region in northern Yukon, near Moose Lake in central Yukon, and in the Vault Creek tunnel, central Alaska. B) $\delta^{18}O_{O2}$ and O_2/Ar composition of gases entrapped in the wedge ice samples collected from the Old Crow region in northern Yukon, near Moose Lake in central Yukon, and in the Vault Creek tunnel, central Alaska

Moose Lake, central Yukon

Examination of trimmed ice blocks from the Moose Lake ice wedges under plain light revealed numerous mm-scale elongated gas inclusions. Gas inclusions form two distinct patterns: i) a dominant pattern involving very elongated and vertically distributed bubbles (5-12 mm long); and ii) a few small spherical bubbles (1-3 mm in diameter), more or less dispersed throughout the ice. Crystallographic analyses showed small subhedral to euhedral ice crystals with area averaging 12.51 ± 22.64 mm^2 for the vertical thin sections, and 10.42 ± 12.20 mm^2 for the horizontal thin sections (Figs. 9A-9B). Foliated sediment inclusions are also found in the ice (Fig. 9C).

The $\delta^{18}O$ values of Moose Lake wedge ice gave a mean value of –25‰ (Fig. 7), which is within the range of winter precipitation recorded at Inuvik (NWT) and other Holocene-age ice wedges in the Old Crow area (–27 to –23‰; Lauriol *et al.*, 1995). In a δD-$\delta^{18}O$ diagram (Fig. 7), the Moose Lake ice wedges results do not show a clear linear relationship.

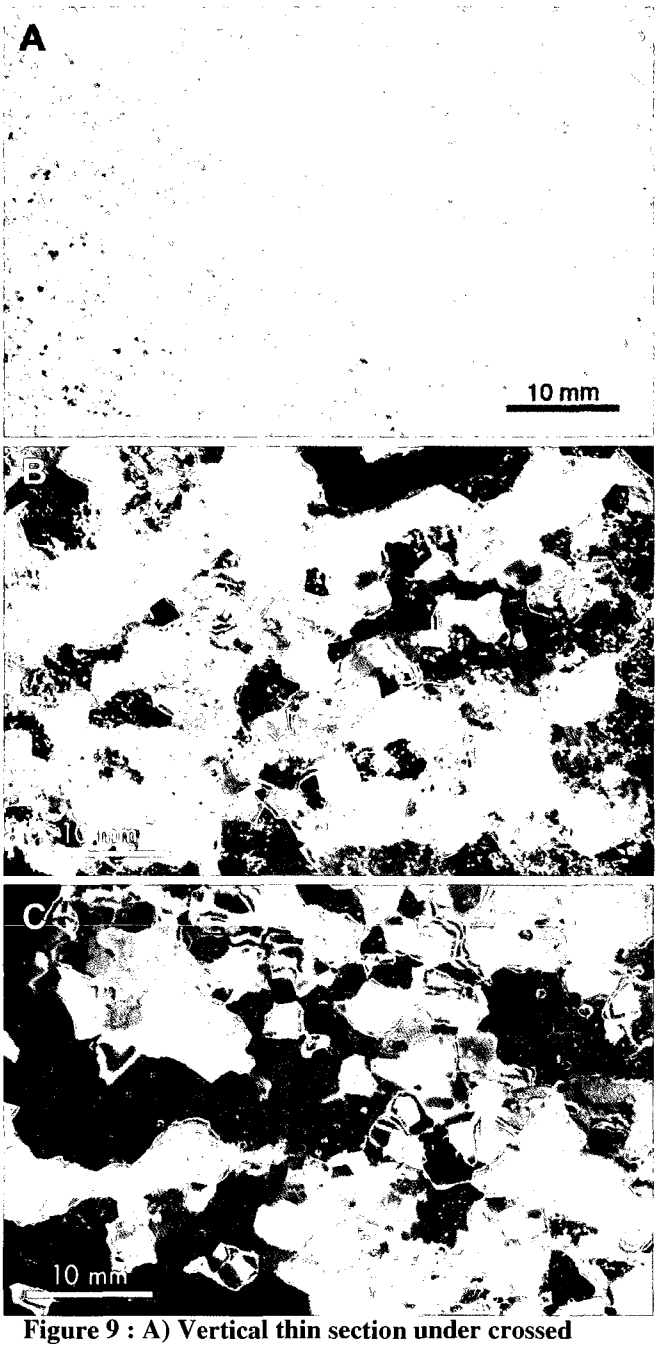

Figure 9 : A) Vertical thin section under crossed polarizing filters; B) Horizontal thin section under crossed polaroids; and C) Vertical Thin section under plain light showing ice bubbles of wedge ice from the Moose Lake area.

The gases entrapped in the Moose Lake wedge ice provided average O_2/Ar and N_2/Ar ratios of –30.1 ± 13.2% and –1.0 ± 1.0%, respectively (Fig. 8A). These ratios are close to the

atmospheric ratios, albeit with slightly lower O_2/Ar values. The $\delta^{18}O_{O2}$, and $\delta^{15}N_{N2}$ values of the occluded gases in the Moose Lake samples average 2.8 ± 2.2‰ and –0.6 ± 0.3‰, respectively. The $\delta^{18}O_{O2}$ values are slightly higher than the atmospheric value, whereas the $\delta^{15}N_{N2}$ values are close to the atmospheric composition.

Vault Creek tunnel, central Alaska

Gas inclusions in the wedge ice collected from the Vault Creek tunnel consist of small spherical bubbles (1-2 mm in diameter), more or less organized and dispersed throughout the ice (Fig. 10A). Foliated sediment inclusions are also found in the ice. However, since the thin section is cut on the vertical axis parallel to the ice veinlets, is does not show the true foliation of bubbles and sediments. Crystallographic analyses showed small subhedral to euhedral ice crystals with area averaging 14.68 ± 17.10 mm^2 for the vertical thin sections (Fig. 10B).

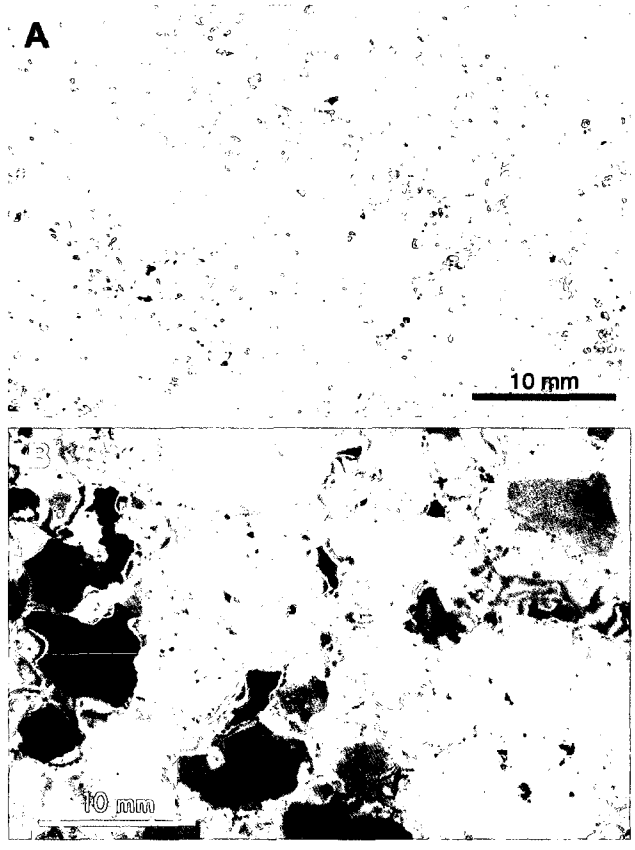

Figure 10 : A) Vertical thin section under plain light showing ice bubbles; and B) Vertical thin section under crossed polarizing filters of wedge ice from the Vault Creek tunnel, central Alaska.

Although the stable O-H isotope composition of ice wedge in the Vault Creek tunnel were not analyzed in this study, Meyer *et al.* (2008) reported $\delta^{18}O$ values between –29.3 and –23.6‰. Seven ice wedges collected in the Vault Creek tunnel plot along individual regression slopes ranging between 5.6 and 9.4 (Meyer, personal communication). Samples from these ice wedges plot along a regression slope of 7.8 ($\delta D = 7.8\ \delta^{18}O - 1.8$; $r^2 = 0.98$), similar to the Global Meteoric Water Line (GMWL).

The air occluded in the ice wedges collected in the Vault Creek tunnel provided average O_2/Ar and N_2/Ar ratios of –30.0 ± 9.9% and 2.4 ± 1.3%, respectively (Fig. 8A). These ratios are

close to the atmospheric ratio, although the O_2/Ar value is slightly lower. The $\delta^{18}O_{O2}$ and $\delta^{15}N_{N2}$ values of the occluded gases in the Vault Creek samples average –0.2 ± 0.8‰ and –0.9 ± 0.2‰, respectively, similar to those in the atmosphere.

DISCUSSION

Ice crystallography

French (2007) observed that wedge ice formed by the freezing of liquid water tend to contain elongated bubbles distributed vertically, whereas wedge ice derived by snow (or hoar) infilling, the bubbles are more spherical. Corte (1963) and Shumski (1964) found that crystals in ice wedges are limited horizontally by the width of the cracks. The smaller grains are those formed recently in a thermal contraction crack, while those at each side are older grains formed by recrystallization from small ones (Corte, 1963).

The Vault Creek and Old Crow samples agree with French's observations: the Vault Creek ice wedges contain small spherical bubbles and the gas ratios close to atmospheric values, while the Old Crow ice wedges contain elongated and spherical bubbles with mixed signal gas ratios. However, Moose Lake ice wedges contain elongated bubbles and the gas ratios show an atmospheric signature. Smaller crystals may indicate recent cracking compared to larger crystals, which are older and experienced recrystallization. On the other hand, crystal size may also relate to different crack widths, with the larger crystals indicating greater crack widths. However, Mackay and Burn (2002) showed that larger cracks occur during initial cracking so larger crystals, if relating to different crack widths, may not relate to colder temperatures.

Stable O-H isotopes in ice

The stable isotopes of O and H in wedge ice may provide clues about the source and mechanism of infill. The source of infill can be determined from the $\delta^{18}O$ of ice, because of the temperature and rainout effects on isotope fractionation in meteoric precipitation (Dansgaard, 1964); colder temperatures generally resulting in lower $\delta^{18}O$ values. Ice formed by snow (or hoar) densification should have a $\delta^{18}O$-δD relation close the local meteoric water line (LMWL; Craig, 1961). However, wedge ice formed by the sequential melting-refreezing of liquid water in a closed system (i.e., no replenishment) will have a significantly lower $\delta^{18}O$-δD regression slope, as is observed in regelation ice underneath glaciers (Jouzel and Souchez, 1982; Souchez and

Jouzel, 1984). Theory predicts that the slope of the $\delta^{18}O$-δD relation in regelation ice evolves during freezing following a Rayleigh-type equilibrium process, such that the most ^{18}O- and D-depleted water fractions, which are last to freeze, form ice with the lowest $\delta^{18}O$-δD slope values. In the theoretical situation of a surface crack filled by the sequential freezing of surface water (rain, runoff or snow meltwater), one should expect that ice that was last to form will display the lowest $\delta^{18}O$-δD slope relative to the LMWL. A similar result should be obtained if there was partial melting and refreezing of the ice in the wedge. The situation becomes more complex if there is an addition or loss of water during freezing (open-system situation). In either case, the $\delta^{18}O$-δD relationship in the ice wedge infill also depends on the initial isotopic composition of the water source. However, if freezing occurs very rapidly, fractionation will be minimal and the ice samples will plot along a $\delta^{18}O$-δD regression line similar to that of the LMWL.

The measurement of the deuterium excess ($d = \delta D - 8\ \delta^{18}O$; Dansgaard, 1964) can provide further information on the origin and conditions of formation of the ice. Under equilibrium freezing conditions, the first ice that forms has a greater δD (and $\delta^{18}O$) value due to the preferential enrichment of the heavier isotopes in the ice (i.e., with an associated depletion of these isotopes in the residual water), but as freezing progresses, the δD values of the ice becomes progressively lower. This is accompanied by a concurrent increase in d values because the freezing equilibrium slope has a value lower than that of the water source. As a result, a negative relationship is expected between d and δD during equilibrium freezing, whereas kinetic fractionation effect will obscur such relationships (Souchez *et al.*, 2000).

Figure 7 shows that the $\delta^{18}O$ and δD values measured in the Holocene-age ice wedges from the Old Crow and Moose Lake areas are close to values measured in modern winter precipitation collected at Inuvik (NWT), Mayo (YT) and Barrow (Alaska). The Pleistocene-age ice wedges obtained from the Vault Creek tunnel have comparatively lower $\delta^{18}O$ and δD values, presumably reflecting the colder temperatures during that period. The majority of the ice wedges samples from Old Crow and Moose Lake also plot along regression slopes that are lower than the LMWL measured at Inuvik (NWT) and Mayo (YT), indicating that the ice infill was not the result of dry snow (or hoar) compaction, but involved the freezing of liquid water, as was proposed previously

by Lauriol et al. (1995). In contrast, ice wedge samples from the Pleistocene-age Vault Creek tunnel have a $\delta^{18}O$-δD regression slope that is near the LMWL measured at Barrow, Alaska (Meyer, pers. comm.), suggesting that they were derived from unfractionned precipitation.

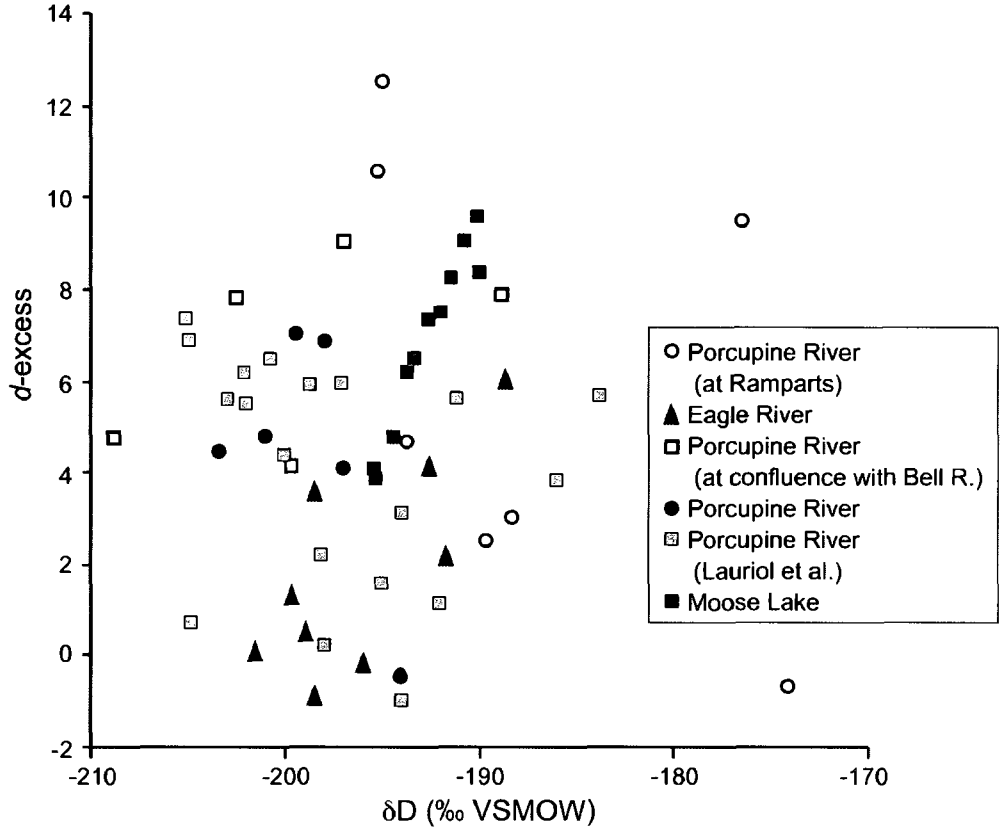

Figure 11: Deuterium excess and deuterium in the wedge ice samples collected from the Old Crow region in northern Yukon, near Moose Lake in central Yukon

When plotted on a *d*-δD diagram (Fig. 11), most Holocene-age ice wedge samples show no obvious linear relationships, which could be explained by kinetic fractionation effects due, for example, to variable freezing rates (Souchez *et al.*, 2000). A positive linear *d*-δD relationship is apparent for the Moose Lake samples. However, its significance is questionable because some instrumental drifting was observed while measuring δD of these samples, which would account for the apparent relationship. By contrast, the stable O-H isotope composition of the Pleistocene-age wedge ice samples from Vault Creek tunnel suggest that they are formed by the condensation of water vapor or infilling of snow in the thermal cracks followed by densification (e.g., Meyer et al., 2002).

Gas composition

The gas composition of air entrapped in wedge ice can provide supporting evidence regarding the mechanism and source of infill. Ice wedges formed by the freezing of infiltrating liquid water in the thermal cracks should preserve molar gas ratios similar to the theoretical dissolved gas ratios, whereas ice wedges formed by dry compaction of snow or hoar inside the thermal cracks should preserve molar gas ratios more similar to atmospheric values.

The molar ratios of gases entrapped in the wedge ice examined in this study show two separate groupings (Fig. 8). The first group, which is composed of wedge ice samples from Vault Creek tunnel and Moose Lake, has N_2/Ar values close to atmospheric composition but O_2/Ar values lower than both the atmospheric and theoretical dissolved gas ratios. The second group is composed of the ice wedges collected in the Old Crow region. Gas ratios results correlate with the crystal areas. The first group had larger crystals (over 10 mm^2 on average) than the second group, which has smaller crystals (from 1 to 6 mm^2 on average). For the second groupe of ice wedges, the N_2/Ar values fall between the atmospheric and theoretical dissolved values, whereas the O_2/Ar values are much lower than these two end-members. The N_2/Ar ratios suggest that the Vault Creek tunnel and Moose Lake ice wedges formed primarly by dry compaction of snow or hoar. In contrast, the N_2/Ar ratios in the Old Crow ice wedges may have formed by a mixture of snow compaction and the freezing of infiltrated water. The low O_2/Ar ratios in the ice suggest that they were modified by syngenetic or epigenetic processes affecting the [O_2]. A higher [Ar] would have resulted in lower N_2/Ar ratios that those observed. The low O_2/Ar ratios are more suggestive of a selective loss (or consumption) of O_2. Shumski (1964) also observed a near absence of O_2 in a few ice wedges. The consumption of O_2 could be accomplished by respiration activity ($CH_2O + O_2 \Leftrightarrow CO_2 + H_2O$) of autotroph or heterotroph microorganisms living within the ice bubbles or interstitial water at the grain boundaries (e.g., Amato et al., 2007; Stewart-Johnson et al., 2007; Hodson et al., 2008).

Most ice wedge samples from Old Crow and Moose Lake have entrapped oxygen with $\delta^{18}O_{O2}$ far above atmospheric values (16.32 ‰; Fig. 8B), which also suggest that respiration did occur. Under closed (or semi-closed) system conditions where there is limited gas exchange with the atmosphere, the metabolic respiration pathway of microorganisms would preferentially consume the light ^{16}O through enzymatic process (leading to decreased [O_2]), resulting in an enrichment in ^{18}O in the residual O_2 pool. Although ^{18}O isotope fractionation also takes place as

gases dissolve into water, the enrichment is only ca. +0.7 ‰ in the water (Benson and Krause, 1984). The degree of ^{18}O enrichment during respiration is expected to be much greater and would depend on the initial [O_2], and a fractionation factor during oxidation of organic matter, which is specific to the metabolic pathway of the microbial communities present.

INFILLING PROCESS IN WEDGE ICE

Based on the results, it appears that the climatic and environmental conditions may be affecting the source and mechanism of infill of wedge ice. The ice wedges in the Vault Creek tunnel, dated to the late Pleistocene, a cold and dry period, preserved bubble shape, stable O-H isotope and gas compositions similar to that expected for ice formed by snow densification or hoar-frost accretion. During the cold Pleistocene period, the strong temperature and humidity gradient along an ice wedge crack may have cause condensation of water vapour along the walls of the crack in early spring, thus resulting in hoar-frost accretion. This type of infilling was suggested by Tomirdiaro (1996) and Meyer *et al.* (2002) to explain the formation of Pleistocene-age ice wedge in Siberia. Alternatively, it is possible that during thermal cracking of the ground, loose snow could infiltrate the fissure. During the summer, the relaxation of the ground would cause the transformation of hoar or snow into ice. Consequently, the results presented in this study, combined with other examples in the literature (e.g., French and Guglielmin, 2000; Meyer *et al.*, 2002; Schirrmeister *et al.*, 2002; Popp *et al.*, 2006) suggest that the cold and dry climate prevailing during the Pleistocene period and in Antarctica favored the infiltration of snow or hoar-frost accretion in the crack.

The ice wedges from the Old Crow region, dated to the late Holocene, a cold and wet period, preserved bubble shape and isotopic and gas compositions more similar to what is expected for ice formed by the freezing of liquid water. Following a rapid and sustained drop in air temperature during the cold winter months, frost cracks will form in the ground (i.e., Lachenbruch, 1966; Mackay, 1974; 1992; Allard and Kasper, 1998; Christiansen, 2005; Fortier and Allard, 2005). In the spring, snow meltwater can infiltrate the thermal contraction cracks, and given that the ground's temperature is below 0°C, the snow meltwater will freeze in the crack as an ice vein (Washburn, 1980; Lauriol *et al.* 1995). This repeated process will create multiple veins ice wedges, the youngest ice being near the center. To account for the molar

ratios of gases that ranges between the atmospheric signal and the concentration of the gas dissolved in water, it is possible that thermal contraction cracks may act as capillary channels and annual water infill would favour entrapment and downward transport of small air bubbles into the cracks. In this case, ratios in between theoretical values could still be an indication of a water filling process in ice wedges. Another explanation is that depth-hoar crystals or snow may act as centers of crystallization for the water, which fills the cracks in the event of incomplete remelting, making random crystal orientation and ratios in between theoretical values.

The Moose Lake ice wedges on the other hand preserved a mixed signal, giving ratios close to the atmospheric signal and bubble shape indicating that the ice formed by the freezing of liquid water. The combination of the gas ratio and bubble shape results may be explained by a liquid water infill, which would have experienced addition of excess air through capillary, as described for the Old Crow ice wedges. It is also possible that during the summer, the relaxation of the ground could causes cracking of the ice and the gases trapped in the ice subsequently exchanged with the atmosphere, leading to the gas ratios being more similar to atmospheric values, rather than theoretical dissolved values. However, more sampling should be done at this site, since there is a lack of evidence to clearly identify the source of infill.

CONCLUSION

The results presented above infer that the climatic conditions may influence the source of infilling during the ice wedge growth. Wet and dry environments may result in two different signatures in ice wedges. For example, the Vault Creek tunnel ice wedges, dated to the late Pleistocene, a cold and dry period, preserved bubble shape, stable O-H isotope and gas compositions similar to that expected for ice formed by snow densification. On the other hand, the ice wedges from the Old Crow region, dated to the late Holocene, preserved bubble shape, and isotopic and gas compositions more similar to what is expected for ice formed by the freezing of liquid water. The Moose Lake ice wedges preserved an atmospheric signal in the gas composition, with ice bubbles resulting from the freezing of liquid water.

The O_2/Ar ratios appeared to be much lower than usual in Old Crow ice wedges, and could be explained by respiration activities of microorganisms living within the ice bubbles or

interstitial water at the grain boundaries. The results from the occluded gases (O_2, N_2 and Ar) failed to give a clear differentiation between sources of infill, since the ratios were modified by biological and chemical processes such as microbial respiration. Consequently, additional gases that could be used in the identification of ground ice type and that would provide a better discrimination in case where biological processes affect the molar gas ratios are the noble gases Kr and Xe. These gases have very large solubility differences, and together with Ar, are not modified by chemical or biological reactions, and would therefore be very useful in situations where such reactions would produce a similar signature. However, extracting and measuring these noble gases with high precision and reproducibility is currently a technical challenge.

In the North American literature, the commonly accepted process for the formation of ice wedge involves freezing of the snow meltwater that infiltrates the thermal contraction cracks (Washburn, 1980; Lauriol *et al.* 1995). The fact that none of the wedges sampled gave true dissolved ratios is important, but without further sampling it will not be clear whether the entire range of possibilities is shown in this study or whether the sample sites are all close to one end of the spectrum. Nonetheless, these results are providing new clues to the understanding of ice wedge formation and filling process, and should be significant to palaeoclimatic interpretation of ground ice in permafrost areas.

ACKNOWLEDGMENTS

This project was supported by Natural Science and Engineering Research Council of Canada Grant # (NSERC) discovery grants to I.D. Clark and B. Lauriol (RGPIN 007995-2005) and by Northern Scientific Training Program (NSTP) grant to M. St-Jean. We wish to thank W. Abdi, G. St-Jean (G.G Hatch Isotope Laboratory, University of Ottawa) for their technical assistance in the improvement of the gas extraction wet-line and the mass spectrometry method. Special thanks to Ruth Gothardt, for logistical support in Whitehorse, to Kenji Yoshikawa, for logistical support in Fairbanks, and to Hanno Meyer, for the exchange of ideas and data. Valuable field assistance was provided by J. Clark, J.-F. Dion, and I. Clark.

References

Allard M, Kasper J. 1998. Temperature conditions for ice wedge cracking: field measurements from Salluit, northern Québec. *In* Proceedings of the 7th International Permafrost Conference, Yellowknife, N.W.T, June 1998. Edited by A.G. Lewkowicz and M. Allard. Collection Nordicanada, No. 57, Centre d'études Nordiques, Université Laval, Québec, Que., pp 5-11.

Benson BB, Krause DJr. 1984. The concentration and isotopic fractionation of oxygen dissolved in freshwater and seawater in equilibrium with the atmosphere. *Limnology and Oceanography* **29**: 632-662.

Cardyn R., Clark ID, Lacelle D, Lauriol B, Zdanowicz C, Calmels F. 2007. Molar gas ratios of air entrapped in ice: A new tool to determine the nature and origin of relict massive ground ice bodies in permafrost. *Quaternary Research* **68**(2): 239-248.

Christiansen HH. 2005. Thermal Regime of Ice-wedge Cracking in Adventdalen, Svalbard, *Permafrost and Periglacial Processes* **16**: 87-98.

Clark ID, Fritz P. 1997. *Environmental Isotopes in Hydrogeology*, Lewis Publisher: Boca Raton; 328 pp.

Craig H. 1961. Isotopic variations in meteoric waters. *Science* **133**: 1702-1703.

Corte AE. 1963. Relationship between four ground patterns, structure of the active layer, and type and distribution of ice in the permafrost. *Biuletyn Peryglacialny* **12**: 7-90.

Dansgaard W. 1964. Stable isotopes in precipitation. *Tellus* **16**: 436-468.

Environment Canada. 2009. Canadian Climate Normals 1971-2001. Canada Atmospheric Environment Service, Minister of Supply and Services Canada, Ottawa, ON, Canada.

French HM and Guglielmin M. 2000. Frozen ground phenomena in the vicinity of Terra Nova Bay, Northern Victoria Land, Antarctica : A preliminary report. *Geografiska Annaler* **82A**(4): 513-526.

French HM, Harry DG. 1990. Observations on buried glacier ice and massive segregated ice, western Arctic coast, Canada. *Permafrost and Periglacial Processes* **1**:31-43.

French HM, Pollard WH. 1986. Ground-ice investigations, Klondike District, Yukon Territory. *Canadian Journal of Earth Sciences* **23**(4): 550-560.

French HM. 2007. *The Periglacial Environment,* Third Edition, Addison Wesley Longman Limited, 478 pages.

French HM. 1998. An Appraisal of Cryostratigraphy in North-West Arctic Canada. *Permafrost and Periglacial Processes* **9**: 297-312.

Fortier D, Allard M. 2005. Frost-cracking Conditions, Bylot Island, Eastern Canadian Arctic Archipelago. *Permafrost and Periglacial Processes* **16**: 145-161.

Fortier D, Allard M, Shur Y. 2007. Observation of rapid drainage system development by thermal erosion of ice wedges on Bylot Island, Canadian Arctic Archipelago. *Permafrost and Periglacial Processes* **18** (3): 229-243.

Guthrie, R.D. 1990. *Frozen Fauna of the Mammoth Steppe*, The University of Chicago Press: Chicago; 323 pp.

Heaton THE, Vogel JC. 1981. "Excess air" in groundwater. *Journal of Hydrology* **50**: 2011-216.

IAEA/WMO. 2004. Global Network of Isotopes in Precipitation. The GNIP Database. Accessible at: http://isohis.iaea.org

Jouzel J, Souchez RA. 1982. Melting-Refreezing at the glacier sole and isotopic composition of the ice. *Journal of Glaciology* **28** (98): 35-41.

Kasper JN, Allard M. 2001. Late-Holocene climatic changes as detected by the growth and decay of ice wedges on the southern shore of Hudson Strait, northern Quebec, Canada. *The Holocene* **11***(5):* 563-577.

Lachenbruch AH. 1962. Mechanics of thermal contraction cracks and ice-wedge polygons in permafrost. Geological Society of America, Special Paper 70.

Lacelle D. 2002. *Ground ice investigation in the far northwest of Canada*, Thesis (M.Sc.), University of Ottawa, 101 pp.

Lacelle D, Bjornson J, Lauriol. B, Clark ID, Troutet Y. 2004. Segregated-intrusive ice of subglacial meltwater origin in retrogressive thaw flow headwalls, Richardson Mountains, NWT, Canada. *Quaternary Science Reviews* **23** (5-6): 681-696.

Lacelle D, Lauriol B., Clark ID, Cardyn R, Zdanowicz C. 2007. Nature and origin of a Pleistocene-age massive ground ice body exposed in the Chapman Lake moraine complex, central Yukon Territory, Canada. *Quaternary Research* **68**: 249-260.

Langway CC. 1958. *Ice fabrics and the universal stage.* US Army Snow Ice and Permafrost Research Establishment. Technical Report 62, 16 pp.

Lauriol B, Duchesne C, Clark ID. 1995. Systématique du remplissage en eau des fentes de gel: les résultats d'une étude oxygène-18 et deutérium. *Permafrost and Periglacial Processes* **16**: 47-55.

Lorrain RD, Demeur P. 1985. Isotopic evidence for relic Pleistocene glacier ice on Victoria Island, Canadian Arctic Archipelago. *Arctic and Alpine Research* **17**: 89-98.

Mackay JR. 1974. Ice-wedges cracks, Garry Island, Northwest Territories, *Canadian Journal of Earth Sciences* **11**:1366-1383.

Mackay JR. 1989. Massive ice: some field criteria for the identification of ice types; In *Current Research*, Part G, Geological Survey of Canada, Paper 89-1G, p.5-11.

Mackay JR. 1990. Some observations on the growth and deformation of epigenetic, syngenetic and anti-syngenetic ice wedges. *Permafrost and Periglacial Processes* **1**: 15-29.

Mackay JR. 1992. The frequency of ice-wedge cracking (1967-1987) at Garry Island, western Arctic coast, Canada. *Canadian Journal of Earth Sciences,* **29***:* 236-248.

Mackay JR. 2000. Thermally induced movements in ice-wedge polygons, western Arctic Coast: A long-term study, *Géographie physique et Quaternaire* **54**(1): 41-68.

Mackay JR, Burn CR. 2002. The first 20 years (1978-1979 to 1998-1999) of ice-wedge growth at the Illisarvik experimental drained lake site, western Arctic coast, Canada. *Canadian Journal of Earth Sciences* **39**: 95-111.

Mackay JR, Dallimore RS. 1992. Massive ice of the Tuktoyaktuk area, western Arctic coast, Canada. *Canadian Journal of Earth Sciences* **29**: 1235-1249

Meyer H, Dereviagin A, Siegert C, Schirrmeister, L. and Hubberten, H.W. 2002. Palaeoclimate Reconstruction on Big Lyakhovsky Island, North Siberia – Hydrogen and Oxygen Isotopes in Ice Wedges. *Permafrost and Periglacial Processes* **13**: 91-105.

Meyer H, Yoshikawa K, Scirrmester L, Andreev A. 2008. The Vault Creek Tunnel (Fairbanks Region, Alaska): A Late Quaternary Palaeoenvironmental Permafrost Record, *In:* Proceedings of the 9th International Conference on Permafrost, Fairbanks, Alaska, 29 June - 3 July 2009, Edited by Douglas L. Kane and Kenneth M. Hinkel, Volume 2, pp.1191-1196.

Michel, FA. 1990. Isotopic composition of ice-wedge ice in the northwestern Canada, In *Proceedings, Fifth Canadian Permafrost Conference*, Université Laval, Centre d'études nordiques: Québec; and national Research Council of Canada: Ottawa; *Collection Nordicana 54:* 5-9

Michel FA, Fritz P. 1982. Significance of isotope variations in permafrost waters at Illisarvik, N.W.T. Proceedings, 4th Canadian Permafrost Conference, Calgary, Alberta, p.173-181.

Murton JB, French HM. 1994. Cryostructures in permafrost, Tuktoyaktuk coastlands, western arctic Canada, *Canadian Journal of Earth Sciences* **31:** 737-747.

Pollard WH. 1983. *A study of seasonal frost mounds, North Fork Pass, Northern Interior Yukon Territory,* Thesis (Ph.D.), University of Ottawa, 236 pages.

Popp S, Diekmann B, Meyer H, Siegert C. 2006. Palaeoclimate Signals as Inferred from Stable-isotope Composition of Ground Ice in the Verkhoyansk Foreland, Central Yakutia. *Permafrost and Periglacial Processes* **17**: 119-132. DOI: 10.1002/ppp.556

Ricker KE. 1968. *Quaternary geology of the southern Ogilvie Ranges, Yukon Territory.* M.Sc. thesis. University of British Columbia, Vancouver, British Columbia.

Shumskii PA. 1964. *Principles of Structural Glaciology,* Dover Publications, Inc. New York, 497 pp.

Souchez RA, Jouzel J. 1984. On the isotopic composition in δD and $\delta^{18}O$ of water and ice during freezing, *Journal of Glaciology* **30** (106): 369-372.

Souchez RA, Jouzel J, Lorrain S. Sleewaegen S, Stiévenard M, Verbeke V. 2000. A kinetic isotope effect during ice formation by water freezing, *Geophysical Research Letters* **27** (13): 1923-1926.

Tomirdiaro SV. 1996. Palaeogeography of Beringia and Arctida, In *American Beginning: the prehistory and palaecology of Beringia*. West FW (ed.). University of Chicago Press: Chicago; 58-69.

Washburn AL. 1980. *Geocryology: a survey of periglacial processes and environments*, Wiley: New York; 406 pp.

Chapter 6: Conclusion

The main goal of this study was to investigate the filling process in ice wedges of various ages (modern to Pleistocene) preserved in Yukon and Alaska, using a variety of parameters, including ice crystallography, the determination of $\delta^{18}O_{ice}$ and δD_{ice}, the molar ratios of occluded gases (O_2/Ar and N_2/Ar), and the stable isotope composition of O_2 ($\delta^{18}O_{O2}$) and N_2 ($\delta^{15}N_{N2}$) gases.

To measure the gas composition (O_2, N_2 and Ar) in ice wedges, a few modifications had to be made to the original extraction technique implemented by Cardyn et al. (2007), and they were presented in Chapter 4. The first modification involved the replacement of the stainless steel tube by a glass tube containing 5A molecular sieve, with a Vacutainer red cap, which is connected to the line through a needle that is coming out of the line. The second modification involves the elimination of the transfer loop step, which was replaced by an ultrapure helium source directly connected to the extraction line. The third modification involved the removal of the peak jump during the analysis on the mass spectrometer, which was replaced by doing two separate runs, one analyzing O_2 and Ar and the other one analyzing N_2. The fourth modification involved the creation of a special software who can get real Amperage based data, removing major data corrections that were required before. These modifications improved the precision of the technique: 46 air standards yielded average O_2/Ar and N_2/Ar ratios of 22.43±0.13 and 83.58±0.64, standard deviation for the N_2/Ar ratios, which was 7.87 before, decreased to less than 1, with a value of 0.64.

Chapter 5 presents a manuscript that investigates the filling process in ice wedges. The study results indicate that climatic conditions may influence the source of infilling during the ice

wedge growth. Therefore, wet and dry environments may result in two different signatures in ice wedges. For example, the Vault Creek tunnel ice wedges, dated to the late Pleistocene, a cold and dry period, preserved stable O-H isotope and gas compositions similar to that expected for ice formed by snow densification. On the other end, the ice wedges from the Old Crow region, dated to the late Holocene, preserved isotopic and gas compositions more similar to what is expected for ice formed by the freezing of liquid water. However, the Moose Lake ice wedges preserved an atmospheric signal in the gas composition, with ice bubbles resulting from the freezing of liquid water.

In some cases, the results from the occluded gases (O_2, N_2 and Ar) were modified by biological and chemical processes such as microbial respiration. Consequently, in future cases where biological processes affect the molar gas ratios, additional gases, such as Kr, Xe and Ar, should be used in the identification of ground ice type or filling process. These gases have very large solubility differences, and are not modified by chemical or biological reactions. However, extracting and measuring these noble gases with high precision and reproducibility is currently a technical challenge.

In the North American literature, the commonly accepted process for the formation of ice wedge involves freezing of the snow meltwater that infiltrates the thermal contraction cracks. The fact that none of the wedges sampled gave true dissolved ratios is important, but without further sampling it will not be clear whether the entire range of possibilities is shown in this study or whether the sample sites are all close to one end of the spectrum. Gas composition analyses should be done on more ice wedges of different age, type and location to support the findings of this study. Nonetheless, these results are providing new clues to the understanding of ice wedge

formation and filling process, and are significant to palaeoclimatic interpretation of ground ice in permafrost areas.

References

ACGR (associated Committee on Geotechnical Research). 1988. Glossary of permafrost and related ground ice terms, Permafrost Subcommittee, National Research Council of Canada Technical Memorandum 142, 156 pages.

Alexeev, S.V. and Alexeeva, L.P. 2002. Ground Ice in the Sedimentary Rocks and Kimberlites of Yakutia, Russia. *Permafrost and Periglacial Processes* 13: 53-59.

Allard, M. and Kasper, J. 1998. Temperature conditions for ice wedge cracking: field measurements from Salluit, northern Québec. *In* Proceedings of the 7th International Permafrost Conference, Yellowknife, N.W.T, June 1998. Edited by A.G. Lewkowicz and M. Allard. Collection Nordicanada, No. 57, Centre d'études Nordiques, Université Laval, Québec, Que., pp 5-11.

Andrews, J.N. 1992. Mechanisms for noble gas dissolution by groundwater, *Isotopes of Noble Gases as Traces in Environmental Studies*, International Atomic Energy Agency, Vienna, pp.87-109.

Ansimova, NP; Kritsuk, LN. 1983. Usinf cryochemical data in the study of massive ice bodies, In *Problems of Geocryology*, Nauka, Moscow; 230-239. (in Russian).

Arnaud, L., Barnola, J.-M., Duval, P., 2000. Physical modeling of the densification of snow/firn and ice in the upper part of polar ice sheets. In: Hondoh, T. (Ed.), *Physics of Ice Core Records.* Sapporo, pp. 285–305.

Astakhov, VI; Kaplyanskaya, FA; Tarnogradsky, VD. 1996. Pleistocene permafrost of West Siberia as a deformable glacier bed. *Permafrost and Periglacial Processes* 7:165-191.

Barnola, J.M., Pimienta, P., Raynaud, D., Korotkevich, Y.S., 1991. CO2 climate Relationship as deduces from the Vostok ice core: A reexamination based on new measurements and on reevaluation of the air dating, *Tellus* 43 (B): 83-90.

Bender, M., Sowers, T., Dickson, M.L., Orchardon, J., Grootes, P., Mayewski, P.A., Meese, D.A., 1994. Climate correlations between Greenland and Antarctica during the past 100,000 years, Nature 372: 663-666.

Benson, B.B., Krause, D.Jr., 1980. The concentration and isotopic fractionation of oxygen dissolved in freshwater and seawater in equilibrium with the atmosphere, *Limnology and Oceanography 25: 662-671.*

Benson, B.B., Krause, D.Jr., 1984. The concentration and isotopic fractionation of oxygen dissolved in freshwater and seawater in equilibrium with the atmosphere, *Limnology and Oceanography 29: 632-662.*

Berg, T.E. and Black, R.F. 1966. Preliminary measurements of growth of nonsorted polygons, Victoria Land, Antarctica, American Geophysical Union, *Antarctic Research Series 8:* 61-108.
Black, R.F. 1974. Ice-wedge polygons of northern Alaska. *In* Glacial geomorphology. Edited by D.R. Coates. State University of New York, Binghamton, N.Y. Publications in Geomorphology, pp.247-275.

Brouchkov, A. and Fukuda, F. 2002. Preliminary measurements on methane content in permafrost, Central Yakutia, and some experimental data. Permafrost and Periglacial Processes 13(3): 187-197.

Caillon, N., Severinghaus, J.P., Jouzel, J., Barnola, J., Kang, J., Lipenkow, V.Y. 2003. Timing of atmospheric CO2 and Antarctic temperature changes across termination III, *Science 299:* 1728-1731.

Cardyn, R., Clark, I.D., Lacelle, D., Lauriol, B., Zdanowicz, C., and Calmels, F. 2007. Molar gas ratios of air entrapped in ice: A new tool to determine the nature and origin of relict massive ground ice bodies in permafrost, *Quaternary Research 68 (2):* 239-248.

Christiansen, H.H. 2005. Thermal Regime of Ice-wedge Cracking in Adventdalen, Svalbard, Permafrost and Periglacial Processes, 16: 87-98.

Clark, I.D. and Fritz, P. 1997. Environmental isotopes in Hydrogeology, CRC Press LLC, 328 pages.

Clark, I.D., Henderson, L., Chappellaz, J., Fisher, D., Koerner, R., Worthy, D.E.J., Kotzer, T., Norman, A.-L., Barnola, J.-M., 2007. CO_2 isotopes as tracers of firn air diffusion and age in an Arctic ice cap with summer melting, Devon Island, Canada. *Journal of Geophysical Research* 112, doi:10.1029/ 2006JDS007471.

Coplen, T.B., A.L. Herczeg, and C. Barnes, Isotope engineering: using stable isotopes of the water molecule to solve practical problems, in *Environmental Tracers in Subsurface Hydrology,* ed. by P.G. Cook and A.L. Herczeg, Kluwer Academic Publishers, Boston, 2000

Corte, A.E. 1963. Relationship between four ground patterns, structure of the active layer, and type and distribution of ice in the permafrost, Biuletyn Peryglacialny 12: 7-90.

Craig, H., Horibe, Y., Sower, T., 1988. Gravitational Separation of gases and isotopes in polar ice caps, *Science 242:* 1675-1678.

Craig, H. 1961. Isotopic variations in meteoric waters. *Science 133*: 1702-1703.

CRC handbook of chemistry and physics, 1988. Weast, R.C. (Ed.), The chemical rubber Co., Boca Raton.

Dansgaard, W. 1964. Stable isotopes in precipitation, *Tellus 16:* 436-468.

Dredge, L.A. Kerr, D.E., Wolfe, S.A. 1999. Surficial materials an related ground ice conditions, Slave Province, N.W.T. Canada. *Canadian Journal of Earth Sciences 36*: 1227-1238.

Dubikov, GI, 1983. Geochemical investigations of ground ice and frozen ground (study at Nej-To Lake), In *Regional and Engineering Geochryology Topics*, Stroyizdat, Moscow, 52-73 (in Russian).

Dubikov, GI; Ivanova, NV. 1988. Pore solutions content in saline frozen deposits of West Siberia, In *Problems of Geocryology*, Nedra, Moscow, p. 92-101 (in Russian).

Dyke, A.S, Savelle, J.M. 2000. Major end moraines of Younger Dryas age on Wollaston Peninsula, Victoria Island, Canadian Arctic: implications for paleoclimate and for formation of hummocky moraine. *Canadian Journal of Earth Sciences 37*: 601-619.

Figurin, A.E 1823. Gosudarstvennyi Admiral'teistvennyi Departamant, Russia, Zapiski 5: 275.

Fortier D, and Allard M. 2005. Frost-cracking Conditions, Bylot Island, Eastern Canadian Arctic Archipelago, *Permafrost and Periglacial Processes 16:* 145-161.
Fraser, T.A. and C.R. Burn, 1997. On the nature and origin of "muck" deposits in the Klondike area, Yukon Territory, *Canadian Journal of Earth Sciences 34*: 1333-1344.

Fortier D, Allard M, Shur Y. 2007. Observation of rapid drainage system development by thermal erosion of ice wedges on Bylot Island, Canadian Arctic Archipelago. *Permafrost and Periglacial Processes* **18** (3): 229-243.

French, H.M. 2007. The Periglacial Environment, Third Edition, Addison Wesley Longman Limited, 478 pages.

French, H.M. 1998. An Appraisal of Cryostratigraphy in North-West Arctic Canada. *Permafrost and Periglacial Processes* 9: 297-312.

French, H.M. and Guglielmin, M., 2000. Frozen ground phenomena in the vicinity of Terra Nova Bay, Northern Victoria Land, Antarctica: A preliminary report, *Geografiska Annaler 82A(4):* 513-526.

French, H.M. and Harry, D.G. 1990. Observations on buried glacier ice and massive segregated ice, western Arctic coast, Canada. *Permafrost and Periglacial Processes* 1, 31-43.

French, H.M. and Pollard, W.H. 1986. Ground-ice investigations, Klondike District, Yukon Territory, *Canadian Journal of Earth Sciences 23(4)*: 550-560.

Friedman, I. and O'Neill, J.R. 1977. Compilation of stable isotope fractionation factors of geochemical interest. In : M.Fleisher (Ed.), Data of Geochemistry, USGS Professional Paper 440-KK :1-12 (6th ed.).

Harry, D.G., Frenchm H.M., Pollard, W.H. Massive ground ice and ice-cored terrain near Sabine Point, Yukon Coastal Plain, Canadian Journal of Earth Sciences 25 (11) : 1846-1856.

Hattori, A. 1983. Denitrification and dissimilatory nitrate reduction, *In*: Carpenter, E.J., Capone, D.G. (Eds.), Nitrogen in the marine environment, Academic Press, San Diego, pp. 191-141.
Hoefs, J., *Stable Isotope Geochemistry,* 4th ed., Springer-Verlag, Berlin, 1997

Hughes, O.L. 1969, Distribution of open-system pingos in central Yukon Territory with respect to glacial limits. Geological Survey of Canada, Paper 69-34. 8p.

Jouzel, J. and Souchez, R.A. 1982. Melting-Refreezing at the glacier sole and isotopic composition of the ice, *Journal of Glaciology 28 (98):* 35-41.

Kasper, J.N. and Allard, M. 2001. Late-Holocene climatic changes as detected by the growth and decay of ice wedges on the southern shore of Hudson Strait, northern Quebec, Canada. *The Holocene 11(5):* 563-577.

Kendall, C., and Aravena, R. 2000. Nitrate isotopes in groundwater systems, *In:* Cook, P., and Herczeg, A.L. (eds.), Environmental tracers in subsurface hydrology, pp. 261-297.

Kotler, E. and C.R. Burn, 2000. Cryostratigraphy of the Klondike "muck" deposits, west-central Yukon Territory, *Canadian Journal of Earth Sciences 37*: 849-861.

Kritsuk, LN; Ansimova, NP. 1985. Chemical content of massive ice and its relation to ground water. *Cryohydrogeological Investigations*, Permafrost Institute, Yakutsk, p.94-108 (in Russian).

Kritsuk, LN; Chervova, EI. 1985. Cryohydrochemical characteristics of surface water and ground ice of central Yamal Peninsula. *Cryohydrogeological Investigations*, Permafrost Institute, Yakutsk, p.117-126 (in Russian).

Lacelle, D. 2002. Ground ice investigation in the far northwest of Canada, Thesis (M.Sc.), University of Ottawa, 101 pages.

Lacelle , D., Bjornson, J., Lauriol,. B., Clark, I.D., Troutet, Y. 2004. Segregated-intrusive ice of subglacial meltwater origin in retrogressive thaw flow headwalls, Richardson Mountains, NWT, Canada, *Quaternary Science Reviews 23 (5-6):* 681-696.

Lacelle, D., Fisher, D., Clark, I.D., Berinstain, A. 2008. Distinguishing between vapor- and liquid-formed ground ice in the northern martian regolith and potential for biosignatures preserved in ice bodies, *Icarus* 197: 458-469.

Lacelle, D., Lauriol, B., Clark, I.D., Cardyn, R., Zdanovicz, C. 2007. Middle Pleistocene-age glacier ice exposed in the headwall of a retrogressive thaw flow near Chapman Lake, central Yukon Territory, Canada. *Quaternary Research 68(2):*249-260.

Lachenbruch, A.H. 1962. Mechanics of thermal contraction cracks and ice-wedge polygons in permafrost. Geological Society of America, Special Paper 70.

Lazukov, GI, 1972. Anthropogene of the northern half of West Siberia (Paleogeography). Moscow University Press, Moscow, (in Russian).

Landais, A., Barnola, J.M., Kawamura, K., Caillon, N., Delmotte, M., Van Ommen, T., Dreyfus, G., Jouzel, J., Masson-Delmotte, V., Minster, B., Freitag, J., Leuenberger, M., Schwander, J., Huber, C., Etheridge, D., Morgan, V., 2006. Firn-air $\delta^{15}N$ in modern polar sites and glacial-interglacial ice: a model-data mismatch during glacial periods in Antarctica? *Quaternary Science Reviews 25*: 49-62.

Langway, Jr., C.C. 1958. Ice fabrics and the universal stage. US Army Snow Ice and Permafrost Research Establishment. Technical Report 62, 16 pages.

Lauriol, B., Duchesne, C. and Clark, I.D. 1995. Systématique du remplissage en eau des fentes de gel: les résultats d'une étude oxygène-18 et deutérium. *Permafrost and Periglacial Processes* 16: 47-55.

Lauriol, B., Cabana, Y., Cinq-Mars, J., Geurts, M., Grimm, F.W., 2002b. Cliff-top eolian deposits and associated molluscan assemblages as indicators of Late Pleistocene and Holocene environments in Beringia. Quaternary International, 87: 59–79.

Leibman, MO, 1996. Results of chemical testing for various types of water and ice, Yamal Peninsula, Russia. *Permafrost and Periglacial Processes* 7: 287-296

Leibman, MO, Vasiliev AA, Rogov VV, Ingólfsson, Ó. 2000. Massive ground ice studies on Yugorskiy peninsula, using crystallographic methods. Kriosfera Zemli 4(2): 31-40 (in Russian).
Lemmen, D.S., Duk-Rodkin, A. and Bednarski, J.M. 1994. Late glacial drainage systems along the northwestern margin of the Laurentide ice sheet. *Quaternary Science Reviews 13*: 805-828

Lis, G., Wassenaar, L.I., Hendry, M.J. 2008. High-precision laser spectroscopy D/H and $^{18}O/^{16}O$ measurements of microliter natural water samples. *Analytical Chemistry* 80, 287-293.

Lliboutry, L. 1964. Traité de glaciologie, Tome 1 : Glace – Neige, Hydrologie nivale, Masson et Cie, Paris, 427 pages.

Lorrain, R.D. Demeur, P. 1985. Isotopic evidence for relic Pleistocene glacier ice on Victoria Island, Canadian Arctic Archipelago, Artic and Alpine Research 17: 89-98.

Mackay, J.R. 1971. The origin of massive ice beds in permafrost, western Arctic coast, Canada *Canadian Journal of Earth Sciences* 8: 397-422.

Mackay, J.R. 1972. The world of underground ice. *Annals of the Association of American Geographers 62*: 1-22.

Mackay, J.R. and Black, R.F. 1973. Origin, composition, and structure of perennially frozen ground and ground ice. *Permafrost 2nd Int. Conference Yakutsk, U.S.S.R. 13-28 July, 1973: North American Contribution* . Washington, D.C., NAS (USA) 185-192.

Mackay, J.R. 1974. Ice wedge cracks, Garry Island, NWT. *Canadian Journal of Earth Sciences* 11: 1366-1383.

Mackay, J.R. 1989. Massive ice: some field criteria for the identification of ice types; In *Current Research*, Part G, Geological Survey of Canada, Paper 89-1G, p.5-11.

Mackay, J.R. 1990. Some observations on the growth and deformation of epigenetic, syngenetic and antisyngenetic ice wedges. *Permafrost and Periglacial Processes* 1: 15-29

Mackay, J.R. 1992. The frequency of ice-wedge cracking (1967-1987) at Garry Island, western Arctic coast, Canada. *Canadian Journal of Earth Sciences* 29(2): 236-248.

Mackay, J.R., Dallimore, R.S. 1992. Massive ice of the Tuktoyaktuk area, western Arctic coast, Canada, *Canadian Journal of Earth Sciences 29*: 1235-1249.
Mackay and Burn, 2002. The first 20 years (1978-1979 to 1998-1999) of ice-wedge growth at the Illisarvik experimental drained lake site, western Arctic coast, Canada, *Canadian Journal of Earth Sciences 39:* 95-111.

Mariotti, A. 1983. Atmospheric nitrogen is a reliable standard for natural ^{15}N abundance measurements, *Nature 303:* 685-687.

Michel, F.A. 1990. Isotopic composition of ice-wedge ice in the northwestern Canada, *Nordicana* 54: 5-9

Michel, FA, 1998. The relationship of massive ground ice and the Late Pleistocene history of northwest Siberia. *Quaternary International* 45/46:43-48

Michel, FA, and Fritz, P. 1982. Signification of isotope variations in permafrost waters at Illisarvik, NWT. Proceedings, 4th Canadian Permafrost Conference, Calgary, p. 173-181.

Moorman, B.J., F.A. Michel and A. Wilson, 1996. ^{14}C dating of trapped gases in massive ground ice, Western Canadian Arctic. *Permafrost and Periglacial Processes* 7 :257-266.

Moorman, B.J., Michel, F.A., Wilson, A.T., 1998. The development of tabular massive ground ice at Peninsula Points, N.W.T., Canada, *In* Proceedings of 7th International Conference on Permafrost, Yellowknife, Canada, *Collection Nordicana 55*: 757-762.

Murton, J.B. 2005. Ground-ice stratigraphy and formation at North Head, Tuktoyaktuk Coastlands, western Arctic Canada: a product of glacier-permafrost interactions, *Permafrost and Periglacial Processes 16:* 31-50.

Murton, J.B. and French, H.M. 1994. Cryostructures in permafrost, Tuktoyaktuk coastlands, western arctic Canada, *Canadian Journal of Earth Sciences 31*: 737-747.

Murton, J.B., Whiteman, C.A., Waller, R.I., Pollard, W.H., Clark, I.D., Dallimore, S.R. 2005. Basal ice facies and supraglacial melt-out till of the Laurentide Ice Sheet, Tuktoyaktuk Coastlands, western Arctic Canada, *Quaternary Science Reviews 24*: 681-708.
Norris, D.K. 1984. Geology of the Northern Yukon and Northwest district of Mackenzie, 1:500,000, Ottawa: Geological Survey of Canada, map 1581A.

Östrem, G. 1963. Comparative crystallographic studies on ice from ice-cored moraines, snow-banks and glacier, *Geografiska Annaler* XLV: 210-233.

Petrenki, V., Severinghaus, J.P., Brook, E.J., Reeh, N., Schaefer, H. 2006. Gas records from the West Greenland ice margin covering the last glacial termination: a horizontal ice core, *Quaternary Science Reviews 25*: 865-875.

Pissart, A. 1987. Géomorphologie périglaciaire, Edition Laboratoire de Géomorphologie et de Géologie du Quaternaire, Université de Liège, Liège, 135 pages.

Pollard, W.H 1990. The Nature and Origin of Ground Ice in the Hershel Island Area, Yukon Territory, In *Permafrost-Canada, Proceedings, Fifth Canadian Permafrost Conference*, Université Laval, Centre d'études nordiques: Québec; and national Research Council of Canada: Ottawa; *Collection Nordicana 54:* 23-30.

Pollard, W.H. and Dallimore, S.R. 1988. Petrographic characteristics of massive ground ice, Yukon Coastal Plain, Canada, *In* Proceedings, Fifth International Conference on Permafrost, August 1988 Trondheim, Norway. Tapir Press, Trondheim, Norway, 224-229.

Pollard, W.H. and French, H.M. 1984. The groundwater hydraulics of seasonal frost mounds, Northern Yukon, *Canadian Journal of Earth Sciences 21 (10):* 1073-1081.

Pollard, W.H. and French, H.M. 1985. The internal structure and ice crystallography of seasonal frost mounds, *Journal of Glaciology 31 (108):* 157-162.

Schwander, J. 1996. Gas diffusion in firn. *In* Wolfe, E.W., Bales, R.C (Eds.), Chemical exchange between the atmosphere and polar snow, NATO ASI SERIES 1, pp. 528-540.

Shumskii, P.A. 1964. Principles of Structural Glaciology, Dover Publications, Inc. New York, 497 pages.

Sowers, T., Bender, M. 1989. Elemental and isotopic composition of occluded O_2 and N_2 in polar ice, *Journal of Geophysical Research 94*: 5137-5150.

Sowers, Bender, M., Raynaud, D., Korotkevich, Y.S. 1992. $\delta^{15}N$ of N_2 in air trapped in polar ice: a tracer of gas transport in the firn and a possible constraint on ice-age gas differences, *Journal of Geophysical Research 97*: 15,683-15,697.

Sowers, T., Brook, E., Etheridge, D., Blunier, T., Fuchs, A., Leuenberger, M., Chappellaz, J., Barnola, J.M., Wahlen, M., Deck, B., Weyhenmeyer, C. 1997. An interlaboratory comparison of techniques for extracting and analyzing trapped gases in ice cores. *Journal of Geophysical Research 102:* 26,527-26,538.

St-Onge, D.A. MacMartin, I. 1995. The Bluenose Lake Moraine, a moraine with a glacier core. *Géographie Physique et Quaternaire 53*: 287-295.

Tomirdiaro, S.V. 1996. Palaeogeography of Beringia and Arctida, *In* American Beginning: the prehistory and palaecologie of Beringia. Editor: F.W. West, Chicago, University of Chicago Press, p.58-69.

van de Wal, R.S.W., Meijer, H.A.J., de Rooij, M., van der Veen, C. 2007. Radiocarbon analyses along the EDML ice core in Antarctica. *Tellus* 59B(1) : 157-164.

Vardy, S.R. Warnerm B.G. and Aravena, R. 1998. Holocene climate and the development of a subarctic peatland near Inuvik, Northwest Territories, Canada. *Climate Change 40:* 285-313.

Washburn, A.L. 1980. Geocryology: a survey of periglacial processes and environments, Wiler, New York, 406 p.

Wilson, R.C., Drury, S.A, Chapman, J.L. 2000. The Great Ice Age: Climate Change and Life, The Open University, p.72-74.

Appendix 1

Extraction technique step-by-step procedures

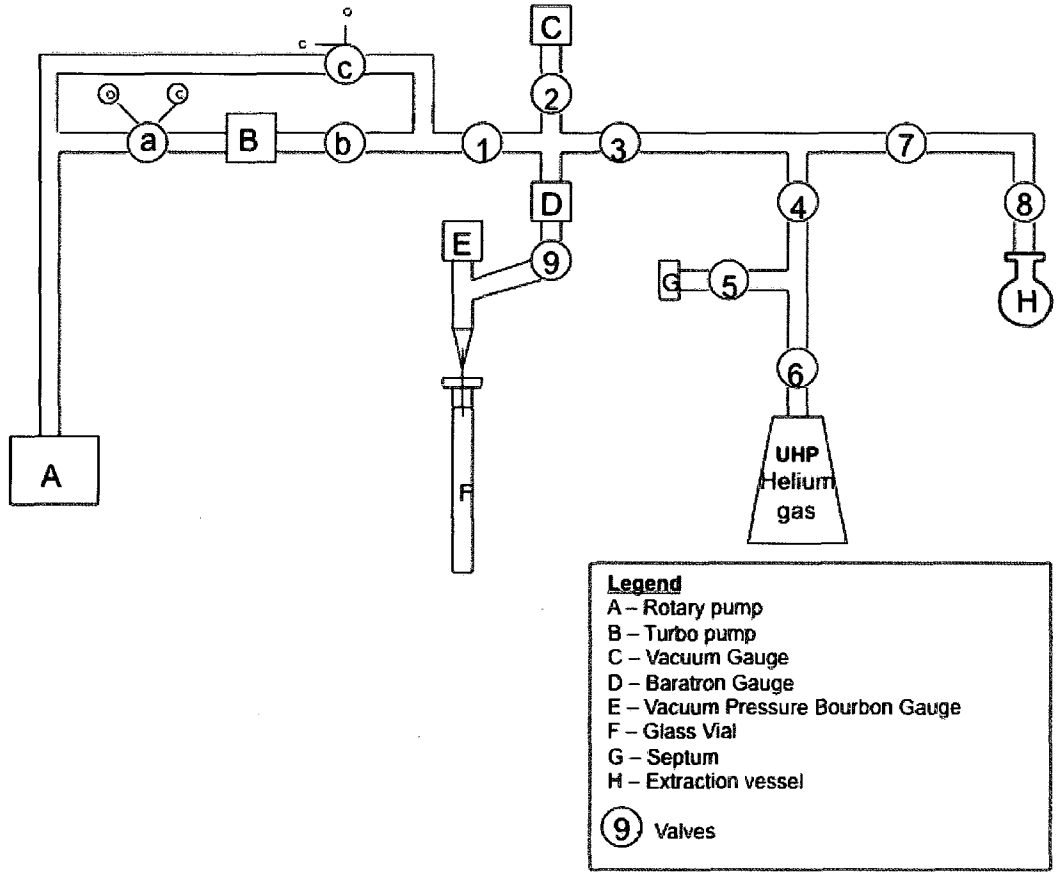

Figure 1: Wet extraction line

Mass spectrometry preparation:

1. Attach the proper reference gas to the mass spectrometer (MS) (Ref 1= N_2, Ref 2 = 5%Ar-95%He, Ref 3 = O_2)
2. Switch to or install GC 5A molecular sieve capillary column (25m) held at room temperature.
3. Flush the reference lines and column for 6 hours or overnight
4. Perform linearity checks on the 3 gases.
5. Set reference gases to 12 nano amp, 3.5 nano amp, and 12 nano amp, respectively.
6. Run a bypass (Exetainer with air from the lab) to "warm up" the mass spectrometer

Standard air measurement:

1. Perform leak test on the extracting line by closing the valve (1) connecting the turbo pump to the extraction line. The reading on the pressure gauge (C) should stay low. Reopen the valve.
2. Insert the needle into the septum and wait until the pressure drops again to close valve (5), (1), (9) and (7). Valve 6 and 8 should already be closed.
3. Inject an aliquot of the standard through the septum just before valve (5), and take the syringe out slowly to prevent air entering the septum.
4. Open valve (5) and allow the standard to expand is the line for approximately 1 minutes. Write the pressure measurement on gauge (C).
5. Insert the glass tube (F) into liquid nitrogen. Make sure the molecular sieves at the bottom of the vial are covered by liquid nitrogen.
6. Open valve (9). Let the air transfer for 5 minutes.
7. After 5 minutes, close valve (4), open valve (6), and insert an exit needle into the septum. Verify the Helium flow, should be around 70 ml/min. Let the Helium flush for 2 minutes.
8. Close valve 5, open valve 4, wait until pressure is at 1 atm on the gauge (E), then take the glass vial off the line.
9. Analyze the glass vial on mass spectrometer.
10. Isotopic values should be similar to other standard results. If not, investigate before continuing with an ice sample.
11. Close valve (9) and (6). Put another glass vial (with a new rubber cap) on the line. Then, open valve (5), (4), (3), (9), (7) and (2), but keep valve (1), (6) and (8) closed.
12. Close valve (a) and (b), open valve (c). Open the valve (1) and pump until pressure gauge (C) reading is under 0.1. Then, open valve (a) and (b), close valve (c). Heat the glass vessel for 5 minutes with the becher containing heating tape, to release all residual air contained by the molecular sieves.

N.B.

- Change the red rubber cap at every use (one use include being once on the line and being analyze once at the mass spectrometer – 2 holes)
- Change the 2 septum on the extraction line after each extraction, and several times during the day when you are doing linearity and stability of injected standards.
- For linearity, take 0.3, 0.6 and 0.9 ml aliquots of air. For the standard you do each day, take the 0.6 ml aliquot.

Blank:

1. Close valve (1), (8), (2) and (4). Valve (6) should already be closed.
2. Insert the glass tube (F) into liquid nitrogen. Make sure the molecular sieves at the bottom of the vial are covered by liquid nitrogen.
3. Open valve (6), and insert an exit needle into the septum. Verify the Helium flow, should be around 70 ml/min. Let the Helium flush for 15 minutes.
4. After 15 minutes, close valve (5), open valve (4), wait until pressure is at 1 atm on the gauge (E), then take the glass vial off the line.

5. Close valve (9) and (6). Put another glass vial (with a new rubber cap) on the line. Then, open valve (5), (4), (3), (9), and (2), but keep valve (1), (6) and (8) closed.
6. Close valve (a) and (b), open valve (c). Open the valve (1) and pump until pressure gauge (C) reading is under 0.1. Then, open valve (a) and (b), close valve (c). Heat the glass vessel for 5 minutes with the becher containing heating tape, to release all residual air contained by the molecular sieves.

Extraction preparation:

1. Rinse the extraction vessel (H) with distilled water
2. Clean the extraction vessel (H) with acetone
3. Dry in the oven (approx. 50°C) for at least 15 minutes
4. Cool the vessel at room temperature for approximately 15 minutes
5. Suspend the vessel in hemispherical dewar containing chilled ethanol for at least 20 minutes (ethanol bath should be at -20°C or lower)
6. Transfer ice sample into the vessel using metal tweezers without dropping the ice in the vessel.
7. Attach the vessel to the line. Raise the ethanol bath (~ -20 °C) so that the part of the vessel where the ice stands is completely covered.
8. At this point, the valve (9), (2) and (4) connecting the glass tube to the extraction line should be close. Close valve (a) and (b), open valve (c). Open valve (8) connecting the vessel to the extraction line. Pump for 30 minutes and ensure that the bath temperature stays at at -20°C or colder. When the pressure is under 0.500 on the pressure gauge (C), open valve (b), so nothing is going to accumulate in the turbo pump.
9. After 30 minutes, close the valve (8) connecting the vessel to the line.
10. Close valve (a). Open the valve (9), (2) and (4). When the pressure in under 0.1, open valve (a) and (b), and close valve (c).
11. Remove the ethanol bath

Extraction:

1. Slowly immerse the vessel in lukewarm water to initiate melting of the ice (2 minutes)
2. Immerse the vessel in warm tap water until the ice is completely melted. If your sample is big, stir your water or change your water for new warm tap water can accelerate the melting.
3. Chill the ethanol bath to -75 °C
4. Raise the lab jack until the bottom of the vessel touches the ethanol bath
5. When ice is frozen all the way to the top, cool the ethanol to -100 °C and raise the dewar until the part containing the ice is completely immersed
6. Freeze for at least 15 minutes and keep the temperature of the ethanol bath at -100 °C
7. Close valve (9), (1), (2) and (4). Insert the glass tube (F) into liquid nitrogen. Make sure the molecular sieves at the bottom of the vial are covered by liquid nitrogen.
8. Open valve (8) and allow the sample to expand is the line for approximately 1 minutes. Write the pressure measurement on gauge (C).
9. Open valve (9) and let the sample transfer to the glass tube (F) for 15 minutes. Keep the bath cooled (between -90 °C and -100 °C).

10. Close valve (8), wait until pressure on gauge (C) is under 0.1, and then close valve (9). Open valve 1 and 4. Remove the liquid nitrogen bath from the glass vial. If the pressure is higher than VAC on gauge (E), take it into consideration when you will fill the vial with Helium at the end (take the vial off the line sooner, when pressure on gauge (E) is lower than 1 atm).
11. Repeat steps 1-6. In the 15 minutes of freezing, close valve (4) and open valve (6) and (5), and insert an exit needle into the septum. Verify the Helium flow, should be around 70 ml/min. Let the Helium flush until you will use it to fill the glass tube.
12. Repeat steps 7-9.
13. Close valve (8), wait until pressure on gauge (C) is under 0.1, close valve (5), open valve (4), wait until pressure is at 1 atm on the gauge (E), then take the glass vial off the line. Warm the vial under your armpit or insert it into lukewarm water or just wait until equilibrium with room temperature.
14. When the vial is at room temperature, it is ready for analysis on the GC-MS.
15. Close valve (9) and (3). Open valve (8) to had helium into the extraction vessel until it is easy to take it off the line. When you take the vessel off the line, close valve 8 and 6. Valve 5 should be closed from earlier steps. Replace the septum rubbers (G) after each extraction. Put another glass vial (with a new rubber cap) on the line. Then, open valve (5), (4), (7), (3), (9), and (2), but keep valve (1), (6) and 8 closed.
16. Close valve (a) and (b), open valve (c). Open the valve (1) and pump until pressure gauge (C) reading is under 0.1. Then, open valve (a) and (b), close valve (c). Heat the glass vessel for 5 minutes with the becher containing heating tape, to release all residual air contained by the molecular sieves.
17. Heat the small part of the line that is over the extraction vessel, between valve (7) and (8), for 1-2 minutes, to remove all possible water vapor that could form in the line through the repeated freezing and thawing of the extraction vessel.

Appendix 2:
Gas ratios results

#sample	O_2/Ar	N_2/Ar	$\delta^{18}O$	δN	#sample	O_2/Ar	N_2/Ar	$\delta^{18}O$	δN
OC-143-1	1,95	69,12	-1,08	-1,68	**ER-1-1**	21,57	85,55	-2,20	-1,43
OC-143-2	0,90	66,21	9,01	0,38	**ER-1-2**	21,20	85,40	-3,05	-1,91
OC-143-3	1,06	65,54	4,62	-1,04	**ER-2-1**	1,40	76,61	3,11	-0,89
OC-INC-1	4,01	76,92	8,69	-0,55	**ER-2-2**	N/A	N/A	13,49	N/A
OC-INC-2	3,37	76,34	16,32	-0,59	**ER-2-3**	1,73	77,26	5,95	-0,63
OC-INC-3	4,71	73,79	12,56	-0,41	**ER-2-5**	2,67	76,98	0,67	-0,66
OC-144-1	5,34	67,89	3,91	-0,12	**ER-3-1**	2,66	68,10	2,56	0,14
					ER-3-2	0,97	65,85	7,60	-0,78
ML-1	13,57	82,82	4,34	-1,04	**ER-3-4**	3,21	68,78	1,59	-0,18
ML-2	12,83	81,84	6,19	-0,91					
ML-3	14,13	82,86	4,57	-0,61	**RC-1-1**	1,93	85,34	8,53	-1,56
ML-2008-1	17,61	83,28	1,20	-0,42	**RC-1-2**	6,79	84,68	1,68	-0,82
ML-2008-3	17,62	83,05	0,95	-0,47	**RC-1-3**	0,62	85,18	15,42	-0,02
ML-2008-4	13,32	81,64	2,37	-0,67	**RC-2-1**	2,94	85,47	0,17	-0,31
					RC-2-2	1,51	85,20	2,23	-0,71
VC-1-1	19,42	85,60	0,60	-0,56	**RC-2-3**	5,53	84,45	0,27	-0,42
VC-1-2	16,07	87,07	-0,51	-1,11	**RC-2-4**	3,18	85,37	-0,79	-0,52
VC-1-3	14,10	86,03	0,70	-0,94					
VC-2-1	14,13	85,19	-0,78	-0,99	**ET-TM-1**	22,58	89,21	-0,43	-0,45
VC-2-2	14,83	84,13	-1,19	-0,77	**ET-TM-2**	22,69	90,88	-1,54	-1,21
					ET-TM-3	22,48	87,20	-0,85	-0,70
CL-1	14,05	92,06	5,06	-0,94					
CL-2	14,23	91,67	3,93	-1,35	**ET-SA-1**	23,22	99,47	-0,94	-0,30
CL-3	15,03	91,88	4,05	-1,00	**ET-SA-2**	24,36	113,20	-3,41	-1,51
					ET-SA-3	24,00	112,67	-3,03	-1,50
CA-PL-1	17,48	49,79	-1,60	-1,31	**POW-1**	22,52	83,02	-0,44	-0,42
Air	**22,43**	**83,60**	**0,00**	**0,00**					
Water	**20,83**	**35,50**	-	-					

Legend			
OC	Old Crow	**ER**	Eagle River
ML	Moose Lake	**RC**	Red Creek
VC	Vault Creek (Fairbanks)	**ET-TM**	Etziza-Terminal moraine
CL	Chapman Lake	**ET-SA**	Etziza-Sandur
CA-PL	Glace provenant du plancher d'une caverne	**POW**	Prince of Whales

Appendix 3: Crystallographic Analyses

Vault Creek ice wedges (VC):

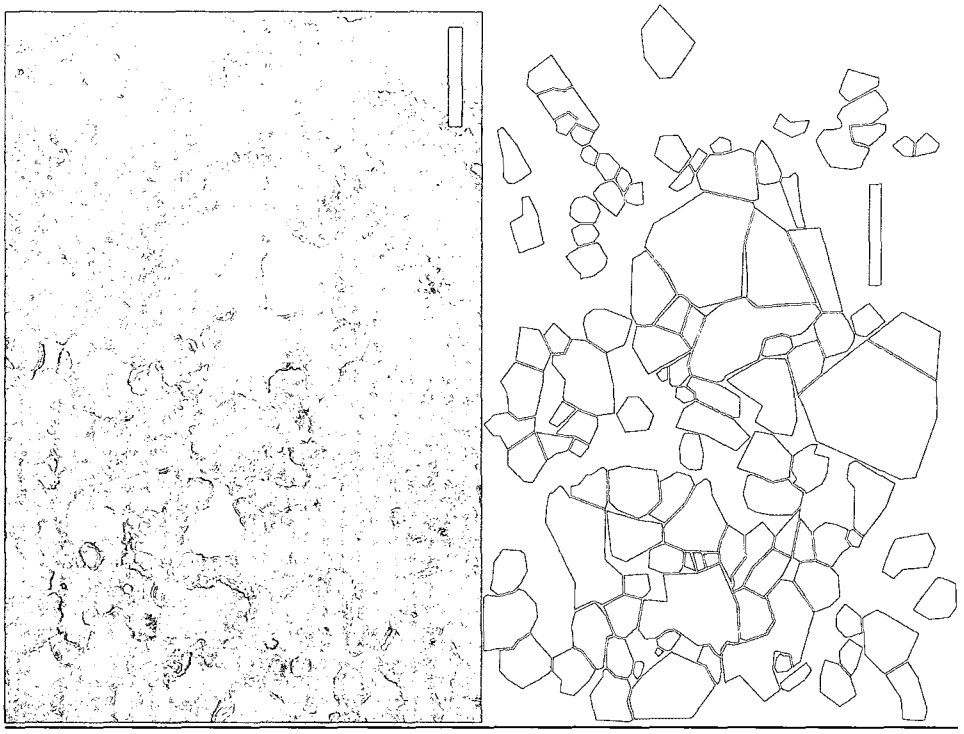

98-VC-1-B	Area (mm^2)	Circular Diameter (mm)	Aspect Ratio
Mean	14.36	3.81	1.54
Maximum	122.73	12.50	3.06
Minimum	0.48	0.78	1.08
Standard deviation	17.09	1.95	0.37
Count	109.00	109.00	109.00

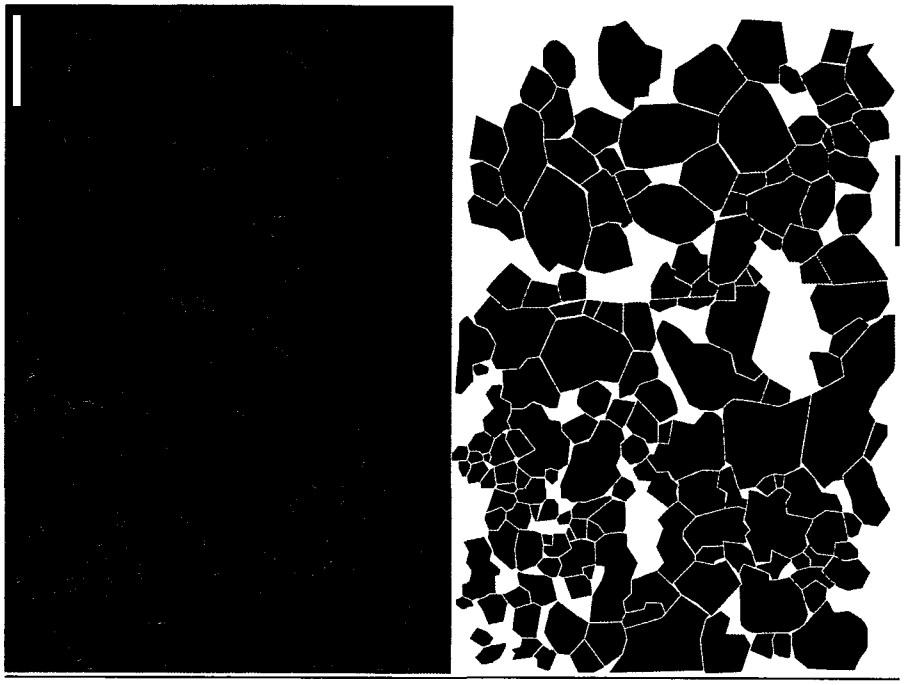

101-VC-1-B	Area (mm^2)	Circicular Diameter (mm)	Aspect Ratio
Mean	15.22	3.90	1.51
Maximum	101.17	11.35	2.79
Minimum	0.57	0.86	1.08
Standard deviation	16.52	2.06	0.31
Count	162.00	162.00	162.00

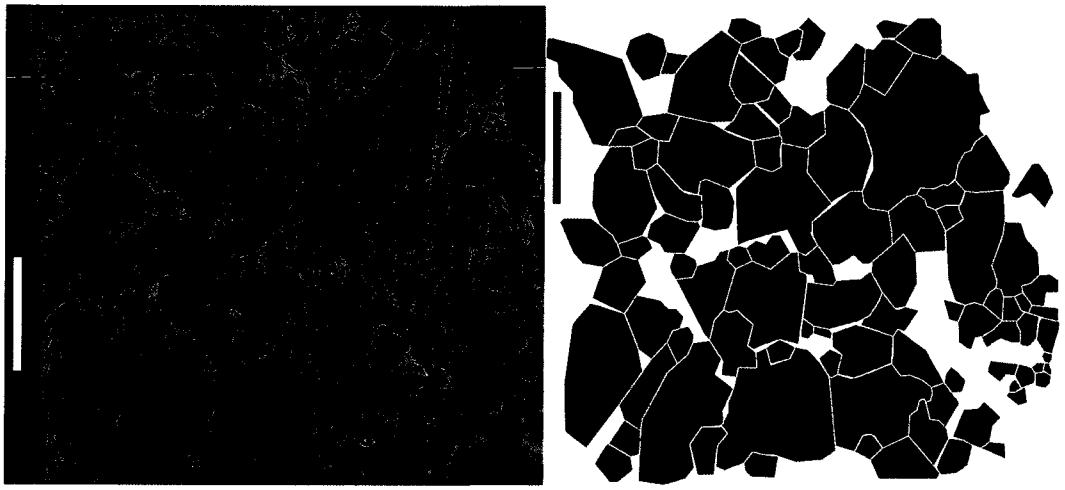

103-VC-1-B	Area (mm^2)	Circular Diameter (mm)	Aspect Ratio
Mean	14.08	3.64	1.50
Maximum	107.92	11.72	2.47
Minimum	0.45	0.76	1.14
Standard deviation	18.25	2.18	0.27
Count	92.00	92.00	92.00

Old Crow ice wedges (OC):

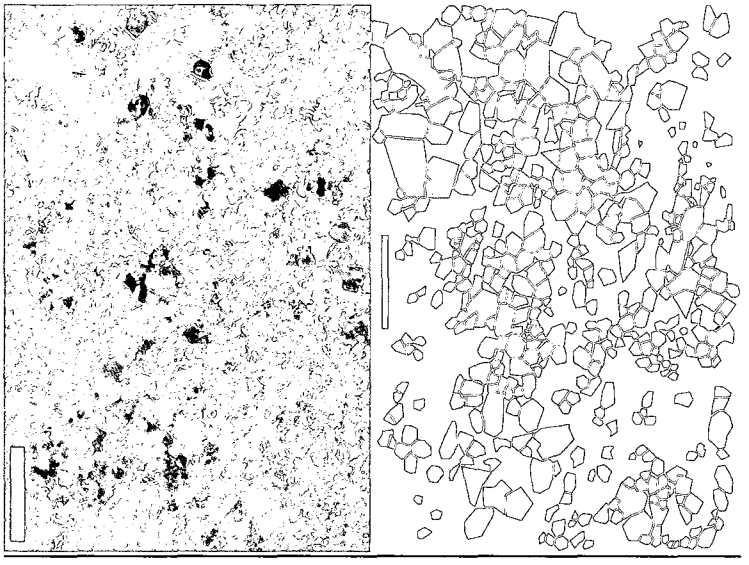

110-OC-INC-A	Area (mm^2)	Circular Diameter (mm)	Aspect Ratio
Mean	2.17	1.52	1.52
Maximum	25.83	5.73	3.44
Minimum	0.14	0.42	1.07
Standard deviation	2.39	0.68	0.34
Count	499.00	499.00	499.00

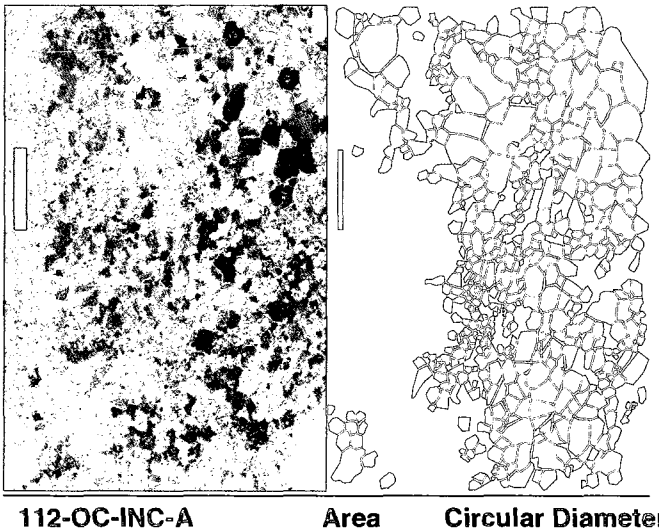

112-OC-INC-A	Area (mm^2)	Circular Diameter (mm)	Aspect Ratio
Mean	2.36	1.53	1.58
Maximum	30.53	6.23	3.70
Minimum	0.07	0.29	1.05
Standard deviation	3.22	0.83	0.36
Count	548.00	548.00	548.00

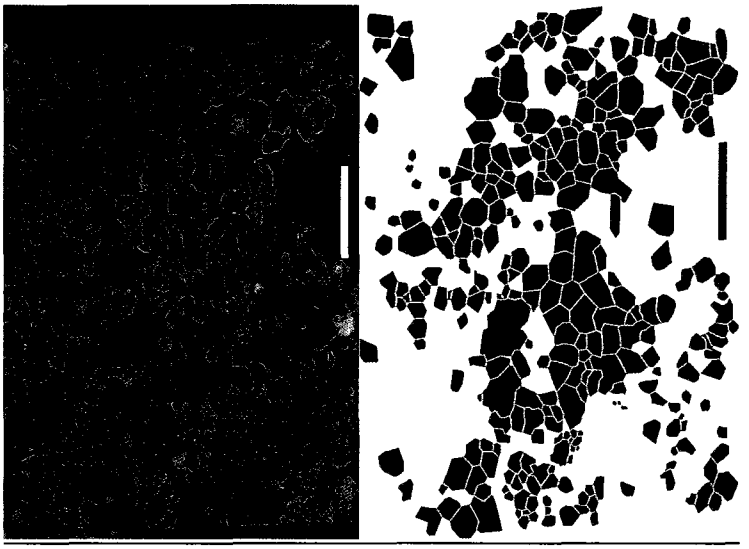

120-OC-INC-A	Area (mm^2)	Circular Diameter (mm)	Aspect Ratio
Mean	2.75	1.71	1.52
Maximum	22.86	5.40	4.18
Minimum	0.11	0.38	1.07
Standard deviation	2.53	0.75	0.32
Count	304.00	304.00	304.00

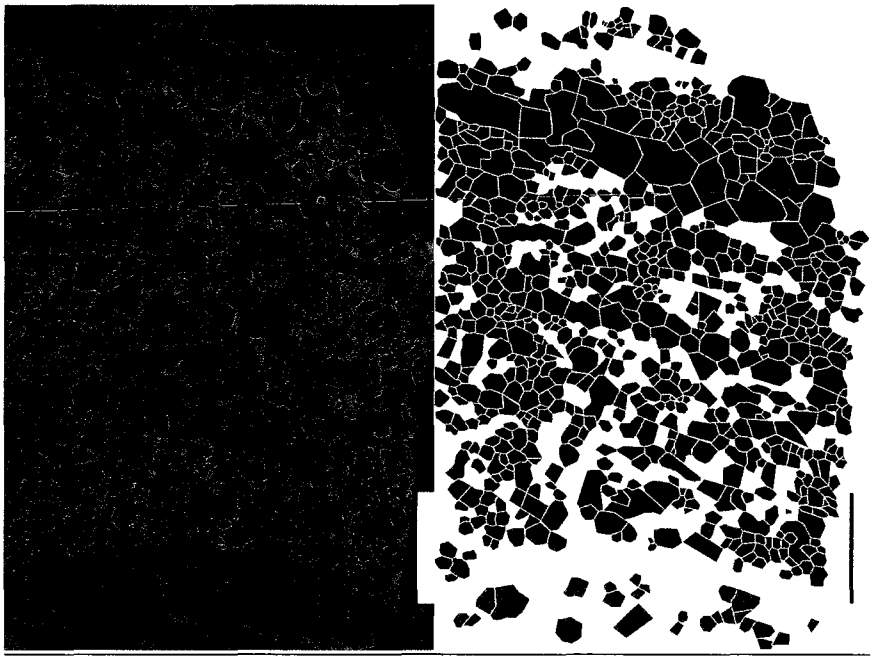

227-OC-INC-B	Area (mm^2)	Circular Diameter (mm)	Aspect Ratio
Mean	1.58	1.27	1.52
Maximum	22.46	5.35	3.97
Minimum	0.00	0.02	1.00
Standard deviation	1.94	0.63	0.31
Count	752.00	752.00	752.00

Moose Lake ice wedges:

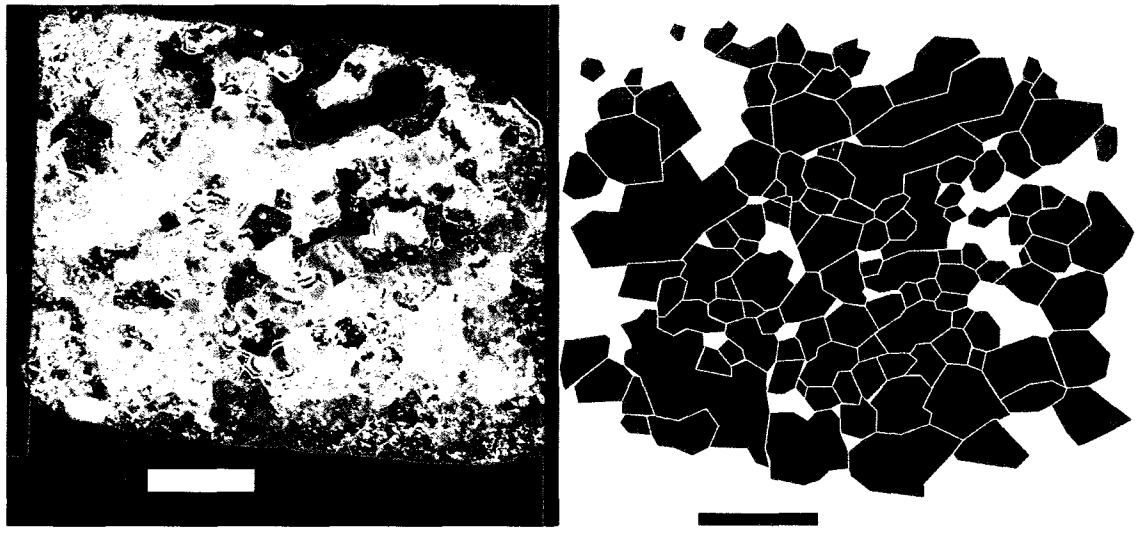

78-ML-1-B	Area (mm^2)	Circular Diameter (mm)	Aspect Ratio
Mean	10.42	3.25	1.51
Maximum	77.05	9.90	2.72
Minimum	0.66	0.92	1.07
Standard deviation	12.20	1.65	0.28
Count	118.00	118.00	118.00

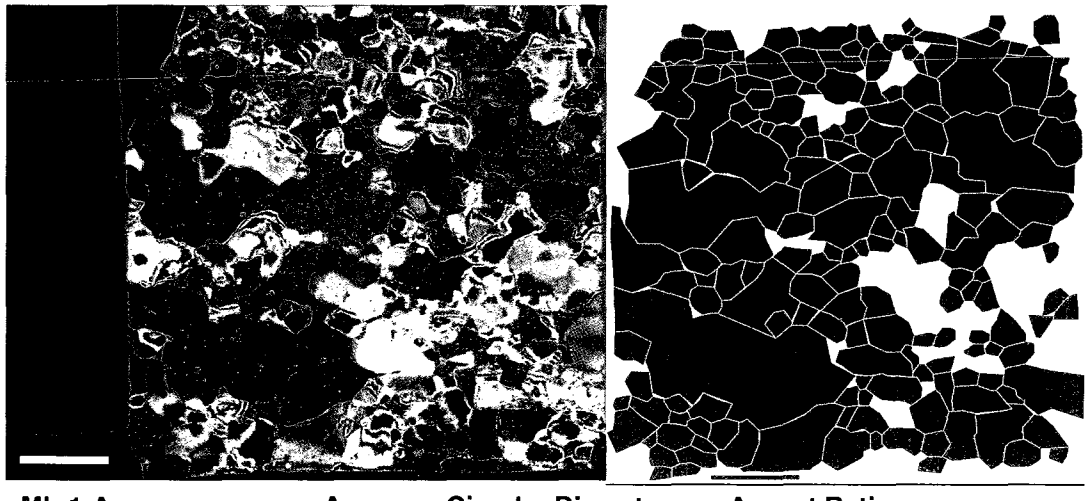

ML-1-A	Area (mm^2)	Circular Diameter (mm)	Aspect Ratio
Mean	12.51	3.44	1.57
Maximum	238.56	17.43	2.90
Minimum	0.97	1.11	1.12
Standard deviation	22.64	2.03	0.31
Count	170.00	170.00	170.00